

# University of Alberta

## Calabi-Yau Hypersurfaces and Complete Intersections in Toric Varieties

by  
Andrey Yurievich Novoseltsev

A thesis submitted to the Faculty of Graduate Studies and Research in  
partial fulfilment of the requirements for the degree of

Doctor of Philosophy  
in  
Mathematics

Department of Mathematical and Statistical Sciences

©Andrey Yurievich Novoseltsev

Fall 2011

Edmonton, Alberta

Permission is hereby granted to the University of Alberta Libraries to reproduce single copies of this thesis and to lend or sell such copies for private, scholarly or scientific research purposes only. Where the thesis is converted to, or otherwise made available in digital form, the University of Alberta will advise potential users of the thesis of these terms.

The author reserves all other publication and other rights in association with the copyright in the thesis and, except as herein before provided, neither the thesis nor any substantial portion thereof may be printed or otherwise reproduced in any material form whatsoever without the author's prior written permission.

*Памяти Игоря Борисовича Симоненко*

*To the memory of Igor Borisovich Simonenko*

# Abstract

In this thesis we report on several projects that stemmed out from an attempt to obtain an example for the last class in Doran-Morgan classification of “variations of Hodge structure which can underlie families of Calabi-Yau threefolds over the thrice-punctured sphere with  $b^3 = 4$ , or equivalently  $h^{2,1} = 1$ ” [DM06].

First, a framework for toric varieties and their Calabi-Yau subvarieties has been implemented in the free open-source mathematical software system Sage. While there are other software packages, both commercial and free, for toric geometry, Sage has the advantage of smooth integration of numerous libraries for other related objects such as graphs, symbolic expressions, fast linear algebra, arbitrary precision and exact arithmetic, etc., combined with a powerful yet simple interface. We hope that our framework will prove useful both in research and teaching.

Next, closed-form combinatorial expressions were obtained for Hodge numbers  $h^{p,1}(X)$  of Calabi-Yau nef complete intersections of two hypersurfaces in toric varieties. Such formulas were long known for anticanonical hypersurfaces, while for nef complete intersections one had to use a highly-recursive generating function, whose actual computation requires significant resources. Our result provides a more efficient way to compute Hodge numbers of given Calabi-Yau varieties and can potentially be exploited to search for complete intersections with prescribed Hodge numbers.

Finally, we have used torically induced fibrations by  $M$ -polarized K3-surfaces to construct an explicit geometric transition between an anticanonical hypersurface and a nef complete intersection through a singular subfamily of hypersurfaces. While we have concentrated on varieties inspired by the aforementioned Doran-Morgan classification, similar techniques may be used for (partial) desingularization of other singular subfamilies of generically smooth hypersurfaces.

# Acknowledgement

Many people have influenced me and this thesis.

First of all, I am infinitely grateful to my advisors Igor B. Simonenko, Ivan G. Avramidi, Charles F. Doran, for their encouragement and guidance, and my wife Rachael E. Defibaugh-Chávez for her support and patience.

I have learned a lot from my fellow students Matthew R. Ballard, Jacob M. Lewis, Robert L. Miller, Ursula Witcher, thanks to them and all other students at the University of Washington and the University of Alberta.

The graduate workshop led by David A. Cox and Hal Schenck and their book [CLS11] greatly helped me to organize my knowledge of toric geometry.

Thanks to the community of Sage developers and especially to William A. Stein for starting and leading the project, Volker Braun for collaborating with me on the toric geometry code, and Dan Drake for creating SageTeX.

I would not be able to achieve the current typesetting quality of this thesis without extensive use of The L<sup>A</sup>T<sub>E</sub>X Companion [MG04] by Frank Mittelbach and Michel Goossens.

# Contents

<b>Introduction</b>	<b>1</b>
<b>1 Toric Geometry via Sage</b>	<b>4</b>
1.1 Why Sage? . . . . .	4
1.2 Cones and Fans . . . . .	6
1.3 Fans from Polytopes . . . . .	12
1.4 Fan Morphisms . . . . .	14
1.5 Toric Varieties . . . . .	16
1.6 Homogeneous Coordinates . . . . .	19
1.7 Torus Orbits and Toric Divisors . . . . .	23
1.8 Toric Morphisms . . . . .	26
<b>2 Toric Geometry in Mirror Symmetry</b>	<b>31</b>
2.1 Reflexive Polytopes and Fano Varieties . . . . .	31
2.2 Anticanonical Hypersurfaces . . . . .	36
2.3 Nef Complete Intersections . . . . .	38
2.4 Torically Induced Fibrations . . . . .	42
<b>3 Hodge Numbers of CICY in Toric Varieties</b>	<b>44</b>
3.1 Generating Functions for Stringy Hodge Numbers . . . . .	45
3.2 The Hypersurface Case . . . . .	48
3.3 The Bipartite Complete Intersection Case . . . . .	51
3.4 Examples . . . . .	57
3.5 Relations with Other Results . . . . .	61
<b>4 Geometric Transitions Through Singular Subfamilies</b>	<b>64</b>
4.1 Complete Intersection Model . . . . .	64
4.2 Anticanonical Hypersurface Model . . . . .	71

4.3	Geometric Transitions . . . . .	74
4.4	K3 Fibrations . . . . .	76
4.5	Ambient Space Morphism . . . . .	79
4.6	Singular Subfamilies: Hypersurfaces . . . . .	82
4.7	Singular Subfamilies: Desingularization . . . . .	86
4.8	Involutions . . . . .	91
4.9	Open Questions . . . . .	93
	<b>Bibliography</b>	<b>95</b>

# List of Tables

3.1 Relevant terms of  $S$ - and  $B$ -polynomials . . . . . 54

# List of Figures

1	Hodge numbers of Calabi-Yau threefolds . . . . .	2
1.1	Complete 2-dimensional fan . . . . .	14
1.2	Fan subdivision . . . . .	15
1.3	Subfan inclusion . . . . .	16
1.4	Automatic fan subdivision . . . . .	16
1.5	Projective plane . . . . .	21
1.6	Product of projective lines . . . . .	23
1.7	Resolution of $\mathbb{WP}(1, 2, 3)$ . . . . .	28
2.1	Fano toric variety polar to the projective plane . . . . .	34
2.2	Resolution of the toric variety polar to the projective plane . .	34
4.1	Base $B^2$ of the fibration $\tilde{\alpha}$ . . . . .	78

# Introduction

In this brief introduction (partially based on [CdIOHS08, CK99, HKK<sup>+</sup>03, Mav00]) we highlight some of the key points in the discovery and study of the mirror symmetry phenomenon.

Calabi-Yau manifolds got a lot of attention after it was noticed [CHSW85] that they arise naturally in the context of string theory: in addition to the usual four dimensions of the space-time, six (real) extra ones have to be compactified to a Calabi-Yau (complex) threefold. It was also suggested [Dix88, LVW89] that Calabi-Yau threefolds should come in pairs  $(M, M^\circ)$ , with each threefold in a pair leading to the same physical theory. Such pairs  $(M, M^\circ)$  became known as mirror pairs.

More and more examples of Calabi-Yau manifolds were constructed, including complete intersections in products of projective spaces [CDLS88, CLS88] and orbifold quotients of hypersurfaces in projective [GP90] and weighted projective spaces [CLS90]. Some of them were explicitly constructed as mirror pairs [GP90], but the symmetry was not perfect: it was expected that Hodge numbers are reversed in a mirror pair  $(M, M^\circ)$ :  $h^{1,1}(M) = h^{2,1}(M^\circ)$ , yet in the obtained lists there were numerous threefolds without possible mirrors.

All of the examples of Calabi-Yau threefolds mentioned above were eventually gathered in the setting of toric geometry [Bat94, BB96b] with a simple combinatorial recipe for obtaining *candidate* mirror pairs realized as hypersurfaces or complete intersections in toric varieties. It was shown [BB96a] that mirror symmetry holds for the appropriately defined Hodge numbers of these candidates in arbitrary dimension. In dimension three all Hodge numbers of Calabi-Yau hypersurfaces in toric varieties were computed [KS02], giving 30,108 distinct pairs. [Figure 1 on the following page](#) shows these Hodge number pairs and, on the same scale, 264 pairs of Hodge numbers corresponding to *all complete intersections* in products of projective spaces.

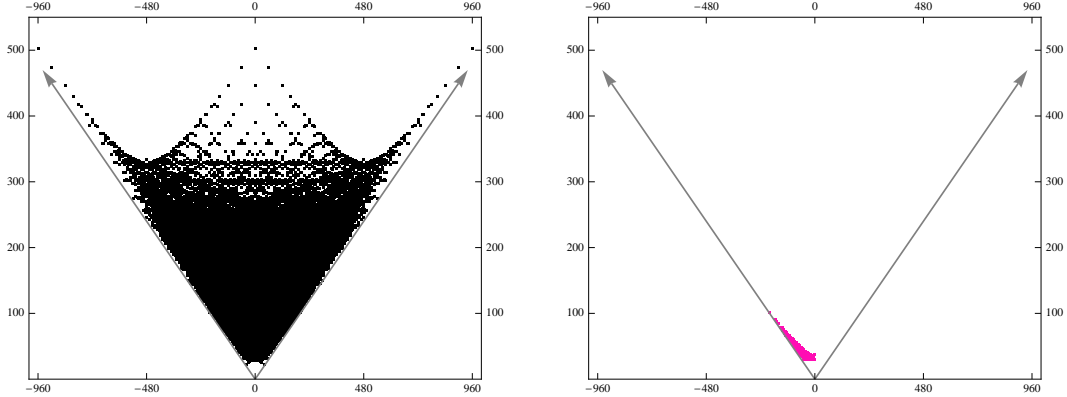


Figure 1: Hodge numbers of Calabi-Yau threefolds realized as hypersurfaces in toric varieties (left) and complete intersections in products of projective spaces (right). Horizontal axis:  $\chi(M) = 2(h^{1,1}(M) - h^{2,1}(M))$ , vertical axis:  $h^{1,1}(M) + h^{2,1}(M)$ . Mirror symmetry corresponds to  $\chi(M) = -\chi(M^\circ)$  (and is clearly absent for complete intersections). Both images are taken from [CdlOHS08].

More recently tropical geometry was combined with toric geometry in an attempt to make the construction of mirror manifolds more direct and less dependent on embedding into a suitable ambient space [GS06, GS10b]. It is expected that this approach will help us to better understand mathematical reasons of mirror duality: physics suggests much more than just exchange of the Hodge numbers in a mirror pair, yet physical arguments are based on string theory which does not yet have a complete mathematical foundation.

Mirror symmetry and geometry of Calabi-Yau manifolds remains a very active area of research involving and connecting many areas of mathematics including all flavours of geometry (algebraic, arithmetic, combinatorial, differential, symplectic, toric, tropical, ...) and homological algebra. There is a number of generalizations one can make compared to the original case of Calabi-Yau compact complex three-dimensional manifolds. Mild singularities are very natural in the context of toric and tropical approaches in mathematics and have certain interpretations in physics. It is of interest both to mathematicians and physicists to consider Calabi-Yau varieties of dimension lower (elliptic curves and K3 surfaces) or higher than three. Some models consider non-compact varieties and varieties over fields other than complex numbers. There are even proposals that drop the Calabi-Yau requirement and expect a kind of mirror symmetry to hold for varieties of other types as well!

This thesis is organized in the following way: [Chapter 1](#) introduces general foundations of toric geometry, simultaneously serving as an excuse to demonstrate the framework for toric varieties in Sage. [Chapter 2](#) explains mirror symmetry constructions in toric geometry. [Chapter 3](#) presents a new combinatorial way to compute Hodge numbers of Calabi-Yau complete intersections in toric varieties, based on the previously known generating function. [Chapter 4](#) relies on Sage to connect certain Calabi-Yau hypersurfaces and complete intersections in toric varieties via explicit geometric transitions.

# Chapter 1

## Toric Geometry via Sage

In this chapter we provide an introduction to relevant parts of toric geometry. Standard references are books by Oda [Oda88] and Fulton [Ful93], but we base our exposition mostly on a wonderful new textbook by Cox, Little and Schenck [CLS11], which reflects modern development of the area, provides vast detailed examples, and has a lot of exercises.

While all mathematical results presented in this chapter are well known (and can be found in [CLS11]), the novelty of our presentation is in illustrating all notions using code [BN11] developed for Sage [S<sup>+</sup>11] by Volker Braun and the author, whenever possible. (This code is still under active development and certain features are not implemented, but it already includes several hundred methods covering some of the major constructions.)

### 1.1 Why Sage?

When one decides to use computers for mathematical computations, there are many software options to choose from, including general-purpose programming languages such as C if one is ready to implement all necessary supporting framework. To some extent the final choice depends on personal preferences and it is likely to be impossible to convince everyone that this choice is right. Nevertheless, in this section we try to provide some hopefully convincing arguments in favour of Sage.

*Sage is a software for mathematical computations.* It covers many areas of mathematics, so it is likely that one does not have to reimplement any algorithms for basic computations (e.g. precise arithmetic, linear algebra,

polynomial rings, plots) and there is a good chance that more advanced ones will be available (e.g. symbolic operations, graphs, cohomology). So at the very least Sage deserves consideration as a platform of choice.

*Sage makes it easy to interface other software packages.* If it turns out that it is absolutely necessary to use some feature X from a package Y (but the package Y cannot do *everything* that you need), it is quite easy to do so from Sage. Interfaces to many packages are already included in Sage and there is a general framework for creating new interfaces.

*Sage is free (costs no money).* While commercial software packages may be available to students and faculty in universities “free of charge” and there are often significant discounts to students wishing to install it on their own computers, universities still have to pay for expensive site licenses, students may no longer use their copies after graduation, and even after discounts these packages are too expensive for people in many countries.

*Sage is free (has non-restrictive license) and open-source.* The usual analogy used by Sage developers is that anyone can read a proof of some theorem and then use both the theorem *and* its proof to create new results. Similarly, if a program was used to produce mathematical results, its code has to be available for anyone to study and modify, if desired.

*Sage is convenient.* It uses a general-purpose easy-to-learn interpreted programming language Python [vR<sup>+</sup>10] for its interaction and at the same time allows smooth transition to compiled code via Cython [EBB<sup>+</sup>10]. The graphical user interface of Sage works through a browser, in the same way on all supported platforms, both locally and over a network, with built-in features for collaboration.

*Sage is documented and supported.* While it is difficult to compete with commercial projects in this area, Sage strives to provide extensive documentation and automatic tests for every function (currently about 85% of functions are fully documented). Despite inclusion of multiple components, Sage automatically builds on all supported platforms without necessity of any tuning or requiring administrative rights. In fact, installing “complete Sage” can be the easiest way to get a working installation of some of its components!

*Sage development process is transparent.* All contributions to Sage are peer reviewed, author-referee communication takes place on a freely accessible site, and anyone has immediate access to code implementing new functionality

even before it gets merged into the main distribution. In particular, when you report a bug there is a chance that it will be fixed in a matter of days if not hours, which is important if this bug prevents you from continuing your work and you are not able to fix it yourself.

Quoting a recent note in Nature [Mer10], “As a general rule, researchers do not test or document their programs rigorously, and they rarely release their codes, making it almost impossible to reproduce and verify published results generated by scientific software [...]. At best, poorly written programs cause researchers [...] to waste valuable time and energy. But the coding problems can sometimes cause substantial harm, and have forced some scientists to retract papers.” We hope that future development of Sage will promote better coding practices and sharing between researchers: since code submitted to Sage must be documented, tested, and readable, and since at least one person other than the author of the code must certify that it looks correct, it is likely to be of substantially higher quality than code written “just for internal use”. Of course, writing proper documentation and tests requires extra time, but being able to reuse previously submitted code should amply compensate for it.

Due to the above arguments and personal preferences the author decided to use Sage. Perhaps, the fact that most computer-aided examples in [CLS11] are implemented either in Macaulay2 [GS<sup>+</sup>10a] or in Sage can serve as a more objective indication of a good choice of platform. Also, in the spirit of interfacing other software packages from Sage, the author has done some work on improving robustness of Sage-Macaulay2 interaction and it is anticipated that there will be support for automatic conversion of toric geometry objects between these systems allowing one not only to complement features missing in one of the implementations, but also use it as a way of correctness verification.

As an unanticipated and very pleasant side-effect of using Sage, the author was able to use SageTeX [D<sup>+</sup>10] to automatically process all code examples and create graphics for this thesis, eliminating the need for copy-pasting and formatting of command line sessions and/or inserting screenshots.

## 1.2 Cones and Fans

Let  $M$  and  $N$  be dual lattices of rank  $n$ , i.e.  $M \simeq N \simeq \mathbb{Z}^n$  as free Abelian groups and we identify  $M$  with  $\text{Hom}_{\mathbb{Z}}(N, \mathbb{Z})$  and  $N$  with  $\text{Hom}_{\mathbb{Z}}(M, \mathbb{Z})$  using

the natural pairing  $\langle \cdot, \cdot \rangle : M \times N \rightarrow \mathbb{Z}$ . We can create such lattices in Sage for any explicit rank  $n$ :

```
sage: N = ToricLattice(2)
sage: M = N.dual()
sage: M
2-d lattice M
sage: N(3,4)
N(3, 4)
sage: M(1,2) * N(3,4)
11
```

While the default names for dual toric lattices are  $M$  and  $N$  as above to match the standard notation in the literature, it is possible to use any other names as well:

```
sage: L = ToricLattice(5, "L")
sage: L, L.dual()
(5-d lattice L, 5-d lattice L*)
```

For each lattice we have the associated real vector space, which we will denote by the subscript  $\mathbb{R}$ , e.g. for the lattice  $N$  it is  $N_{\mathbb{R}} = N \otimes_{\mathbb{Z}} \mathbb{R}$ . In order to avoid excessive repetitions, below  $M$ ,  $N$ ,  $M_{\mathbb{R}}$ , and  $N_{\mathbb{R}}$  are always assumed to be as described above.

**Definition 1.2.1.** A **convex polyhedral cone**  $\sigma$  in  $N_{\mathbb{R}}$  is a set of the form

$$\sigma = \text{Cone}(S) = \left\{ \sum_{v \in S} \lambda_v v : \lambda_v \in \mathbb{R}_{\geq 0} \right\}$$

for some finite set  $S \subset N_{\mathbb{R}}$ . We say that  $\sigma$  is **strictly convex** if it contains no subspaces of  $N_{\mathbb{R}}$  except for the trivial one. We say that  $\sigma$  is **rational**, if it can be generated by a finite set  $S \subset N$ . We also let  $\text{Cone}(\emptyset) = \{0\}$ .

*Remark 1.2.2.* Note that for a strictly convex rational polyhedral cone there is a canonical choice of generators, namely the lattice points of minimal (non-zero) norm on the generating rays (or edges) of the cone.

*Remark 1.2.3.* Below we deal exclusively with rational convex polyhedral cones, so after the above definition we actually drop these adjectives and refer

to such cones as “just” cones. In most cases, but not all, our cones are also strictly convex, this condition is always stated explicitly.

In Sage, cones take into account both remarks:

```
sage: quadrant = Cone([(1/2,0), (1,2), (0,3)])
sage: quadrant.rays()
(N(1, 0), N(0, 1))
```

The `Cone` command constructs a (rational convex polyhedral) cone, normalizing generators to primitive integral vectors and discarding unnecessary generators. It does not always pick a minimal set of generators for non-strictly convex cones, since it is usually more convenient to deal with pairs of opposite generators:

```
sage: plane = Cone([(1,0), (0,1), (-1,-1)])
sage: plane.rays()
(N(1, 0), N(-1, 0), N(0, 1), N(0, -1))
sage: plane.ray_matrix()
[ 1 -1  0  0]
[ 0  0  1 -1]
```

However, you can force Sage to use the rays provided by you, if necessary:

```
sage: plane = Cone([(1,0), (0,1), (-1,-1)], check=False)
sage: plane.ray_matrix()
[ 1  0 -1]
[ 0  1 -1]
```

In these examples we have used `rays` and `ray_matrix` methods to output rays either as a list or as columns of a matrix. There are also several other representations described in the documentation.

**Definition 1.2.4.** Let  $\sigma \subset N_{\mathbb{R}}$  be a cone. Its **dual cone**  $\sigma^{\vee}$  is

$$\sigma^{\vee} = \{u \in M_{\mathbb{R}} : \langle u, v \rangle \geq 0 \text{ for all } v \in \sigma\}.$$

For the two cones constructed above the dual ones are the first quadrant and the trivial cone in  $M_{\mathbb{R}}$ :

```
sage: quadrant.dual()
2-d cone in 2-d lattice M
```

```

sage: quadrant.dual().rays()
(M(1, 0), M(0, 1))
sage: plane.dual()
0-d cone in 2-d lattice M
sage: plane.dual().rays()
()
sage: plane.dual().is_trivial()
True
sage: plane.dual().dual() is plane
True

```

**Definition 1.2.5.** A **face**  $\tau$  of a cone  $\sigma \subset N_{\mathbb{R}}$  is any set of the form  $\tau = \sigma \cap u^{\perp}$  for  $u \in \sigma^{\vee}$ , where  $u^{\perp} = \{v \in N_{\mathbb{R}} : \langle u, v \rangle = 0\}$  (for  $u \neq 0$  it is called a **supporting hyperplane** of  $\sigma$ ). A **proper face**  $\tau$  is any face  $\tau \neq \sigma$ .

Faces of a strictly convex cone  $\sigma$  (including the origin and  $\sigma$  itself) form an *atomistic and coatomistic Eulerian lattice* with respect to the inclusion relation and grading by dimension.

**Definition 1.2.6.** Let  $\mathcal{P}$  be a poset. It is a **lattice** if any two elements of  $\mathcal{P}$  have a unique infimum (called their **meet**) and a unique supremum (called their **join**).

For cones the intersection of any two faces is a face and for any two faces there is a unique smallest face containing them.

*Remark 1.2.7.* If  $\mathcal{P}$  is a lattice, then, of course, any finite collection of its elements has both meet and join. In particular, if  $\mathcal{P}$  is finite, then it has the minimum and maximum elements which we will denote as  $\hat{0}$  and  $\hat{1}$  respectively.

**Definition 1.2.8.** Let  $\mathcal{P}$  be a lattice with the minimum element  $\hat{0}$ . An element  $a \in \mathcal{P}$  is an **atom** if it covers  $\hat{0}$ , i.e. there is no element  $x \in \mathcal{P}$  such that  $\hat{0} < x < a$ . Lattice  $\mathcal{P}$  is **atomic** if for any element  $x \in \mathcal{P}$  there exists an atom  $a \in \mathcal{P}$  such that  $a \leq x$ . Lattice  $\mathcal{P}$  is **atomistic** if any element  $x \in \mathcal{P}$  is a join of atoms of  $\mathcal{P}$ . **Coatom**, **coatomic**, and **coatomistic** are dual notions.

For cones any face can be specified by either rays generating it or facets (faces of codimension one) containing it.

**Definition 1.2.9.** A graded poset  $\mathcal{P}$  is an **Eulerian poset** if any non-trivial interval in  $\mathcal{P}$ , i.e. the set  $[x, y] = \{z \in \mathcal{P} : x \leq z \leq y\}$  for any  $x, y \in \mathcal{P}$  such that  $x < y$ , has the same number of elements of even and odd rank.

Sage provides a number of methods for working with faces and “walking along” the face lattice, to illustrate some of these methods we first construct a slightly more complicated cone than before:

```
sage: cone = Cone([(0,0,1), (1,0,1), (1,1,1), (0,1,1)])
sage: cone.face_lattice()
Finite poset containing 10 elements
sage: [len(cone.faces(d)) for d in [0..3]]
[1, 4, 4, 1]
sage: ray = cone.embed(Cone([(1,0,1)]))
```

The last command constructed a 1-dimensional cone `ray` in the direction  $(1,0,1)$ , which “knows” that it is considered as a face of `cone`. This is important if we want to look at neighbours of `ray` in the face lattice of `cone`:

```
sage: ray.facets()
(0-d face of 3-d cone in 3-d lattice N,)
sage: ray.facet_of()
(2-d face of 3-d cone in 3-d lattice N, 2-d face of 3-d cone in 3-d lattice N)
sage: ray.adjacent()
(1-d face of 3-d cone in 3-d lattice N, 1-d face of 3-d cone in 3-d lattice N)
```

For non-strictly convex cones the situation is similar, but all faces share the largest contained linear subspace and the minimal set of generating rays is defined only modulo this subspace. Note also that cone duality induces an inclusion-reversing bijection between the faces of a cone  $\sigma \subset N_{\mathbb{R}}$  and the faces of its dual cone  $\sigma^{\vee} \subset M_{\mathbb{R}}$ .

**Definition 1.2.10.** A **fan**  $\Sigma$  in  $N_{\mathbb{R}}$  is a finite collection of *strictly convex* rational polyhedral cones in  $N_{\mathbb{R}}$  such that

- 1) if  $\sigma \in \Sigma$  and  $\tau$  is a face of  $\sigma$ , then  $\tau \in \Sigma$ ,
- 2) if  $\sigma_1, \sigma_2 \in \Sigma$ , then  $\tau = \sigma_1 \cap \sigma_2$  is a face of each.

The set of all  $k$ -dimensional cones of  $\Sigma$  will be denoted by  $\Sigma(k)$  and the set of maximal cones (not contained in any other cone of  $\Sigma$ ) by  $\Sigma_{\max}$ .

Note that because of the face containment requirement fans are likely to contain “a lot” of cones, but to define a fan it is sufficient to provide only its maximal cones. Sage allows fan construction from any collection of (compatible) cones, but it may warn you about “redundant” ones.

```
sage: cone0 = Cone([(1,0), (0,1)])
sage: cone1 = Cone([(0,1), (-1,-1)])
sage: cone2 = Cone([(-1,-1), (1,0)])
sage: fan = Fan([cone0, cone1, cone2])
sage: fan
Rational polyhedral fan in 2-d lattice N
sage: fan.ngenerating_cones()
3
sage: fan(1)
(1-d cone of Rational polyhedral fan in 2-d lattice N, 1-d cone of Rational polyhedral fan in 2-d lattice N, 1-d cone of Rational polyhedral fan in 2-d lattice N)
sage: fan.ray_matrix()
[ 0  1 -1]
[ 1  0 -1]
```

Similar to the face lattice of a cone, cones of a fan form a lattice with the fan itself as its maximal element. These lattices are particularly similar for an important special case of complete fans.

**Definition 1.2.11.** Let  $\Sigma$  be a fan in  $N_{\mathbb{R}}$ . Its **support** is

$$|\Sigma| = \bigcup_{\sigma \in \Sigma} \sigma \subset N_{\mathbb{R}}.$$

If  $|\Sigma| = N_{\mathbb{R}}$ ,  $\Sigma$  is called **complete**.

For complete fans every cone can be described either by rays (1-dimensional cones) generating it, or by maximal-dimensional cones (analogs of facets) containing it:

```
sage: ray = fan(1)[0]
sage: ray.rays()
(N(0, 1),)
sage: ray.ambient_ray_indices()
```

```

(0,)
sage: fan.rays(ray.ambient_ray_indices())
(N(0, 1),)
sage: ray.star_generator_indices()
(0, 1)
sage: fan.generating_cone(0).intersection(
fan.generating_cone(1)).rays()
(N(0, 1),)

```

### 1.3 Fans from Polytopes

A natural source of fans is provided by lattice polytopes.

**Definition 1.3.1.** A **lattice polytope**  $\Delta$  in  $M_{\mathbb{R}}$  is the convex hull of finitely many lattice points of  $M$ . We call  $\Delta$  **full-dimensional** if the affine subspace spanned by it is  $M_{\mathbb{R}}$  itself.

In Sage support for lattice polytopes is provided via `lattice_polytope` module written mostly by the author [Nov11], while more general polyhedra can be handled by `polyhedra` module written mostly by Volker Braun and Marshall Hampton [BH11]. Both modules were written before the rest of the toric geometry framework and sometimes it leads to (small) interface inconsistencies, e.g. lattice polytopes in Sage are not actually aware of any lattices except for  $\mathbb{Z}^n$ . We plan to improve intermodule integration in the near future.

```

sage: simplex = LatticePolytope([(0,0), (1,0), (0,1)])
sage: simplex
A lattice polytope: 2-dimensional, 3 vertices.
sage: simplex.vertices()
[0 1 0]
[0 0 1]
sage: Delta = LatticePolytope([(-1,-1), (-1,2), (2,-1)])
sage: Delta.vertices()
[-1 -1  2]
[-1  2 -1]
sage: Delta.points()
[-1 -1  2 -1 -1  0  0  0  1  1]
[-1  2 -1  0  1 -1  0  1 -1  0]

```

In Sage `LatticePolytope`'s methods `vertices` and `points` behave similar to `ray_matrix` for `Cone`'s and `Fan`'s: they return matrices whose columns are vertices or all lattice points of the polytope.

**Definition 1.3.2.** Let  $\Delta \subset M_{\mathbb{R}}$  be a full-dimensional lattice polytope. Its **normal fan**  $\Sigma_{\Delta}$  in  $N_{\mathbb{R}}$  is generated by cones  $C_v$  for all vertices  $v$  of  $\Delta$ . Each  $C_v$  is generated by inner normals of facets of  $\Delta$  containing  $v$ .

Note that the normal fan is insensitive to shifts and scaling of the original polytope, in particular `simplex` and `Delta` constructed above should produce the same normal fans:

```
sage: Sigma_simplex = NormalFan(simplex)
sage: Sigma_simplex.is_complete()
True
sage: Sigma_simplex.ray_matrix()
[ 1  0 -1]
[ 0  1 -1]
sage: Sigma_Delta = NormalFan(Delta)
sage: Sigma_Delta.ray_matrix()
[ 1  0 -1]
[ 0  1 -1]
sage: Sigma_simplex == Sigma_Delta
False
```

This may seem wrong, but this is due to the fact that equality of fans in Sage is understood as having the same rays and cones in the same order. To check mathematical equality we may use `is_equivalent` method:

```
sage: Sigma_simplex.is_equivalent(Sigma_Delta)
True
```

**Definition 1.3.3.** Let  $\Delta \subset N_{\mathbb{R}}$  be a lattice polytope *containing the origin*. Its **face fan**, as the name suggests, consists of cones generated by faces of  $\Delta$ .

We construct the same fan as above one more time, now as a face fan:

```
sage: Delta_p = LatticePolytope([(1,0), (0,1), (-1,-1)])
sage: fan = FaceFan(Delta_p)
sage: fan.ray_matrix()
```

```
[ 1  0 -1]
```

```
[ 0  1 -1]
```

```
sage: fan.plot()
```

**Graphics object consisting of 16 graphics primitives**

If you execute the last command in Sage, you are actually more likely to get the plot showed in [Figure 1.1](#) either opened in a graphics viewer or embedded into a notebook worksheet, rather than its text description. Dots are lattice points, coloured sectors are 2-dimensional cones, and lines between them are 1-dimensional cones with primitive integral generators marked via arrows. Label indices correspond to the internal order of rays and cones of the fan, we often hide them if there is no need to reference particular cones on diagrams.

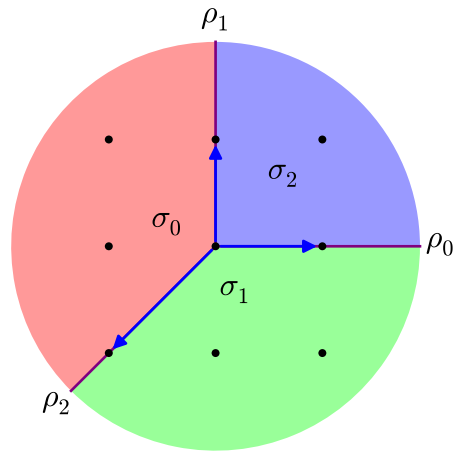


Figure 1.1: Complete 2-dimensional fan

## 1.4 Fan Morphisms

Recall that toric lattices are groups isomorphic to  $\mathbb{Z}^n$ , so while one is free to pick a basis, the origin is fixed, and a morphism between toric lattices is a group homomorphism sending the origin to the origin. If such a morphism behaves well with respect to other cones of two fixed fans, we get a fan morphism.

**Definition 1.4.1.** Let  $N$  and  $N'$  be lattices,  $\Sigma$  be a fan in  $N_{\mathbb{R}}$ , and  $\Sigma'$  be a fan in  $N'_{\mathbb{R}}$ . A **fan morphism**  $\varphi$  from  $\Sigma$  to  $\Sigma'$  is a lattice homomorphism  $\varphi : N \rightarrow N'$  such that for any cone  $\sigma \in \Sigma$  its image (under the linear extension  $\varphi_{\mathbb{R}} : N_{\mathbb{R}} \rightarrow N'_{\mathbb{R}}$  of  $\varphi$ ) is completely contained in some cone  $\sigma' \in \Sigma'$ .

Note that  $\varphi$  also induces a map between  $\Sigma$  and  $\Sigma'$  as finite sets of cones:  $\sigma \in \Sigma$  is mapped to the smallest  $\sigma' \in \Sigma'$  containing  $\varphi_{\mathbb{R}}(\sigma)$  or, alternatively,  $\sigma \mapsto \sigma'$  if the image of the relative interior of  $\sigma$  under  $\varphi_{\mathbb{R}}$  lies in the relative interior of  $\sigma'$ . We will denote this map of cones by  $\varphi$  as well, so  $\varphi(\sigma) = \sigma'$  if  $\varphi_{\mathbb{R}}(\text{RelInt}(\sigma)) \subset \text{RelInt}(\sigma')$ .

**Definition 1.4.2.** Let  $\varphi : \Sigma \rightarrow \Sigma'$  be a fan morphism, let  $\sigma \in \Sigma$ , and let  $\sigma' = \varphi(\sigma)$ . Then  $\sigma$  is a **primitive cone** corresponding to  $\sigma'$  if there is no proper face  $\tau$  of  $\sigma$  such that  $\varphi(\tau) = \sigma'$ .

Two special cases of fan morphisms are fan subdivisions and inclusions of subfans (e.g. generated by a single cone), in both cases lattices  $N$  and  $N'$  coincide and  $\varphi : N \rightarrow N'$  is the identity map. The following code creates two such fan morphisms in Sage, with the relevant fans shown in [Figure 1.2](#) and [Figure 1.3](#) on the following page.

```
sage: quadrant = Fan([Cone([(1,0), (0,1)])])
sage: subdivided_quadrant = quadrant.subdivide([(1,1)])
sage: phi = FanMorphism(identity_matrix(2), subdivided_quadrant,
quadrant)
sage: half_quadrant = Fan([subdivided_quadrant.generating_cone(0)])
sage: psi = FanMorphism(identity_matrix(2), half_quadrant,
subdivided_quadrant)
```

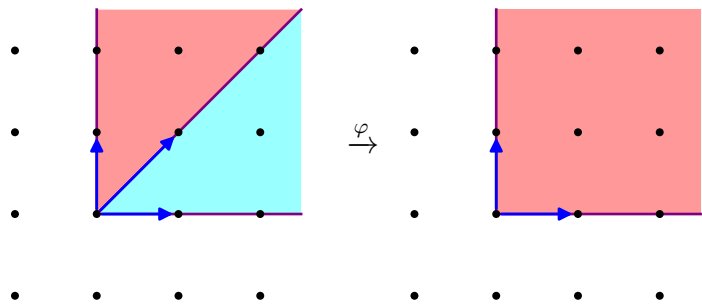


Figure 1.2: Fan subdivision

In the above example we have used `subdivide` method of fans to produce `subdivided_quadrant` by specifying new rays that had to be present in the new fan. It is also possible to automatically perform subdivisions necessary for obtaining fan morphisms between “incompatible fans.” We demonstrate it

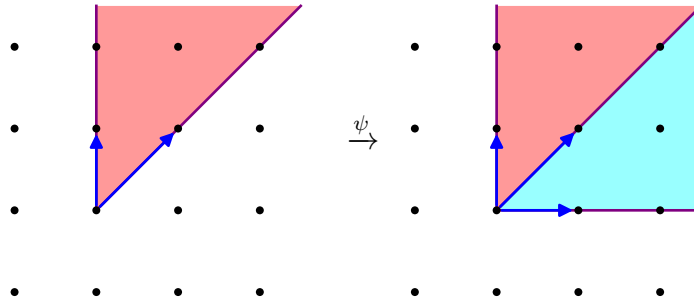


Figure 1.3: Subfan inclusion

using previously constructed complete fan (shown in Figure 1.1 on page 14) projected onto the vertical axis:

```
sage: v_fan = Fan([Cone([(0,1)]), Cone([(0,-1)])])
sage: xi = FanMorphism(matrix(2, 2, [0,0,0,1]), fan, v_fan,
subdivide=True)
sage: xi.domain_fan().ngenerating_cones()
4
```

In this case it was necessary to split one of the cones (the “top-left” one) into two, since otherwise the image of this cone was not contained in a single cone of the codomain fan, in fact, its image was not even strictly convex! The resulting fans are shown in Figure 1.4.

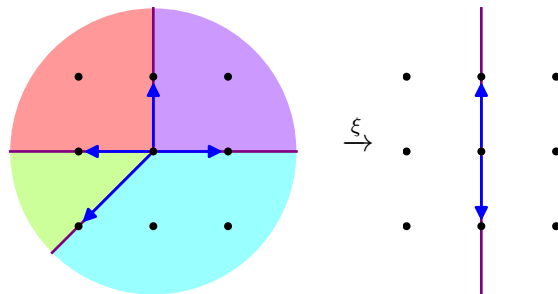


Figure 1.4: Automatic fan subdivision

## 1.5 Toric Varieties

In the context of toric geometry tori are different from the usual definitions such as products of circles.

**Definition 1.5.1.** A **torus**  $T$  is an affine variety isomorphic to  $(\mathbb{C}^*)^n$  with the group structure corresponding to componentwise multiplication in  $(\mathbb{C}^*)^n$ .

Every  $n$ -dimensional torus  $T$  has two dual lattices of rank  $n$  associated to it: its character lattice  $M$  and the lattice of one-parameter subgroups  $N$ . Fixing an isomorphism  $T \simeq (\mathbb{C}^*)^n$  also fixes isomorphisms  $M \simeq \mathbb{Z}^n$  and  $N \simeq \mathbb{Z}^n$ . Under these isomorphisms, an element  $m = (a_1, \dots, a_n) \in M$  corresponds to the character  $\chi^m : T \rightarrow \mathbb{C}^*$  defined by  $\chi^m(t) = \chi^m(t_1, \dots, t_n) = t_1^{a_1} \dots t_n^{a_n}$ , while an element  $n = (b_1, \dots, b_n) \in N$  corresponds to the one-parameter subgroup  $\lambda^n : \mathbb{C}^* \rightarrow T$  defined by  $\lambda^n(t) = (t^{b_1}, \dots, t^{b_n})$ . The natural pairing between  $M$  and  $N$  corresponds to the usual dot product  $\langle m, n \rangle = \sum_{i=1}^n a_i b_i$  or, equivalently,  $\langle m, n \rangle = \ell$ , where  $\ell \in \mathbb{Z}$  is such that  $\chi^m \circ \lambda^n(t) = t^\ell$ . There is also a canonical isomorphism  $N \otimes_{\mathbb{Z}} \mathbb{C}^* \simeq T$ , given by  $n \otimes t \mapsto \lambda^n(t)$ , so we can start with an arbitrary lattice  $N$  and obtain a torus denoted by  $T_N$ , such that  $N$  is the lattice of one-parameter subgroups of  $T_N$ .

**Definition 1.5.2.** A **toric variety** is an irreducible variety  $X$  containing a torus  $T$  as a Zariski open subset such that the action of  $T$  on itself extends to an algebraic action of  $T$  on  $X$ .

There are different ways to construct toric varieties, but in this work we are primarily interested in toric varieties corresponding to cones and fans.

**Theorem 1.5.3.** *Let  $\sigma \subset N_{\mathbb{R}}$  be a strictly convex cone. Then*

$$U_\sigma = \text{Spec}(\mathbb{C}[\sigma^\vee \cap M]),$$

where  $\mathbb{C}[\sigma^\vee \cap M]$  is the semigroup algebra of  $\sigma^\vee \cap M$ , is a normal affine toric variety of dimension  $n = \text{rk } N$  with torus  $T_N \subset U_\sigma$ .

*If  $X$  is a normal affine toric variety with torus  $T_N$ , then  $X = U_\sigma$  for some  $\sigma$  as above.*

*Proof.* See Theorems 1.2.18 and 1.3.5 in [CLS11]. □

For example, if  $\sigma = \{0\}$  is the trivial cone in  $N_{\mathbb{R}}$ , then  $\sigma^\vee \cap M = M$  and

$$U_\sigma = \text{Spec}(\mathbb{C}[M]) \simeq \text{Spec}(\mathbb{C}[t_1^{\pm 1}, \dots, t_n^{\pm 1}]) = (\mathbb{C}^*)^n \simeq T_N.$$

**Proposition 1.5.4.** *Let  $\sigma \subset N_{\mathbb{R}}$  be a strictly convex cone and  $\tau$  be its face. Then there is a natural inclusion  $U_\tau \hookrightarrow U_\sigma$ .*

*Proof.* See Proposition 1.3.16 in [CLS11] and comments thereafter.  $\square$

In particular, the inclusion  $T_N \hookrightarrow U_\sigma$  corresponds to the origin being a face of any strictly convex cone  $\sigma \subset N_{\mathbb{R}}$ . It is also possible for two strictly convex cones  $\sigma_1$  and  $\sigma_2$  in the same space  $N_{\mathbb{R}}$  to have a bigger common face  $\tau$  than the origin. In this case we get natural inclusions  $U_{\sigma_1} \hookrightarrow U_\tau \hookrightarrow U_{\sigma_2}$ , that allow us to glue  $U_{\sigma_1}$  and  $U_{\sigma_2}$  along a common open subset. Of course, this works best if  $\sigma_1$  and  $\sigma_2$  have particularly agreeable face structures.

**Theorem 1.5.5.** *Let  $\Sigma$  be a fan in  $N_{\mathbb{R}}$ . Let  $X_\Sigma$  be a variety obtained by gluing affine toric varieties  $U_\sigma$  for all  $\sigma \in \Sigma$  along their maximal common subsets, i.e.  $U_{\sigma_1}$  and  $U_{\sigma_2}$  are glued along  $U_{\sigma_1 \cap \sigma_2}$ . Then  $X_\Sigma$  is a separated normal toric variety with torus  $T_N$ .*

*If  $X$  is a separated normal toric variety with torus  $T_N$ , then  $X = X_\Sigma$  for some  $\Sigma$  as above.*

*Proof.* See Theorems 3.1.5, 3.1.7, and Corollary 3.1.8 in [CLS11].  $\square$

Below we use notation  $X_\Sigma$  for the normal toric variety associated to a fan  $\Sigma$  and, to avoid towers of subscripts,  $X_\Delta$  for the toric variety associated to the normal fan  $\Sigma_\Delta$  of a lattice polytope  $\Delta$ .

In Sage we can construct toric varieties of the form  $U_\sigma$  and  $X_\Sigma$  as follows (as  $\Sigma$  we use `fan` constructed earlier):

```
sage: sigma = Cone([(1,0), (1,2)])
sage: U_sigma = AffineToricVariety(sigma)
sage: U_sigma
2-d affine toric variety
sage: U_sigma.is_smooth()
False
sage: U_sigma.is_orbifold()
True
sage: X_Sigma = ToricVariety(fan)
sage: X_Sigma
2-d toric variety covered by 3 affine patches
sage: X_Sigma.is_smooth()
True
sage: X_Sigma.is_complete()
True
```

Note that  $X_\Sigma$  in the above example is “covered by 3 affine patches.” While there are definitely more affine open subsets of  $X_\Sigma$ , three special ones corresponding to maximal cones of  $\Sigma$  are *sufficient* to cover  $X_\Sigma$ . Smoothness and completeness of  $X_\Sigma$  in this example easily follow from the structure of  $\Sigma$ .

**Definition 1.5.6.** A cone  $\sigma \subset N_{\mathbb{R}}$  is called a **smooth cone** if it can be generated by a subset of an integral basis, i.e. a basis of the underlying lattice  $N$ . A fan is called a **smooth fan** if all of its cones are smooth.

**Definition 1.5.7.** A cone  $\sigma \subset N_{\mathbb{R}}$  is called a **simplicial cone** if it can be generated by a linearly independent set. A fan is called a **simplicial fan** if all of its cones are simplicial.

**Theorem 1.5.8.** *Let  $\Sigma$  be a fan in  $N_{\mathbb{R}}$ . Then*

- 1)  $X_\Sigma$  is smooth if and only if  $\Sigma$  is smooth,
- 2)  $X_\Sigma$  is an orbifold (has only finite quotient singularities) if and only if  $\Sigma$  is simplicial,
- 3)  $X_\Sigma$  is complete (and compact in the Euclidean topology) if and only if  $\Sigma$  is complete.

*Proof.* See Theorem 3.1.19 in [CLS11]. □

## 1.6 Homogeneous Coordinates

While the usual definition of toric varieties corresponding to fans involves gluing affine toric varieties corresponding to cones, just as we have done in Theorem 1.5.5, it is often more convenient to work with homogeneous coordinates “covering” the whole variety at once, rather than chart by chart. This description works best for orbifolds without torus factors, so we often state results for such varieties only, although most of them have variations without this assumption.

**Definition 1.6.1.** A toric variety  $X$  with torus  $T$  has a **torus factor** if it is equivariantly isomorphic to the product  $X' \times T''$  of a non-trivial torus  $T''$  and a toric variety of smaller dimension  $X'$  with torus  $T'$ , i.e.  $X \simeq X' \times T''$  and  $T \simeq T' \times T''$ .

**Proposition 1.6.2.** *Let  $\Sigma$  be a fan in  $N_{\mathbb{R}}$ . Then  $X_\Sigma$  has a torus factor if and only if rays of  $\Sigma$  do not span  $N_{\mathbb{R}}$ .*

*Proof.* See Proposition 3.3.9 in [CLS11]. □

**Definition 1.6.3.** Let  $X_\Sigma$  be a toric variety without torus factors associated to a fan  $\Sigma$  in  $N_{\mathbb{R}}$ . The **total coordinate ring** (a.k.a. **homogeneous coordinate ring** or **Cox's ring**) of  $X_\Sigma$  is the polynomial ring  $S(\Sigma) = \mathbb{C}[z_\rho : \rho \in \Sigma(1)]$  with one variable for each ray of  $\Sigma$ . The **irrelevant ideal** is  $B(\Sigma) = \langle z^{\hat{\sigma}} : \sigma \in \Sigma \rangle$ , where  $z^{\hat{\sigma}} = \prod_{\rho \notin \sigma} z_\rho$ . The zero set of this ideal is the **exceptional set**  $Z(\Sigma) = V(B(\Sigma)) \subset \mathbb{C}^{\Sigma(1)}$ , where  $\mathbb{C}^{\Sigma(1)} = \text{Spec}(S(\Sigma))$  is the usual Cartesian product of copies of  $\mathbb{C}$  indexed by rays  $\rho \in \Sigma(1)$ .

**Theorem 1.6.4.** *Let  $X_\Sigma$  be an orbifold toric variety without torus factors corresponding to a fan  $\Sigma$  in  $N_{\mathbb{R}}$ . Let  $G \subset (\mathbb{C}^*)^{\Sigma(1)}$  be the kernel of the map  $(\mathbb{C}^*)^{\Sigma(1)} \rightarrow T_N$  sending the ray in  $(\mathbb{C}^*)^{\Sigma(1)}$  corresponding to  $\rho \in \Sigma(1)$  to the one-parameter subgroup of  $T_N$  corresponding to the primitive generator of  $\rho$ . Then  $X_\Sigma \simeq (\mathbb{C}^{\Sigma(1)} \setminus Z(\Sigma)) / G$ , where the action of  $G$  is given by component-wise multiplication.*

*Proof.* See Theorem 5.1.11 in [CLS11]. □

*Remark 1.6.5.* Homogeneous coordinates can be used for more general toric varieties as well, however if there is a torus factor, the choice of coordinates corresponding to it is not canonical, while allowing worse than orbifold singularities leads to only *almost geometric quotient*, see Chapter 5 in [CLS11] for further details.

**Example 1.6.6** (The Projective Plane). Let's take a look at the quotient representation of  $X_\Sigma$  corresponding to the complete fan we have already encountered many times. Let  $\Sigma$  contain the trivial cone, rays generated by  $v_0 = (1, 0)$ ,  $v_1 = (0, 1)$ ,  $v_2 = (-1, -1)$ , and 2-dimensional cones  $\sigma_0 = \text{Cone}(\{v_1, v_2\})$ ,  $\sigma_1 = \text{Cone}(\{v_0, v_2\})$ ,  $\sigma_2 = \text{Cone}(\{v_0, v_1\})$  (see [Figure 1.1 on page 14](#)).

Since we have 3 rays, the total coordinate ring is  $S = \mathbb{C}[z_0, z_1, z_2]$  and  $\mathbb{C}^{\Sigma(1)} = \mathbb{C}^3$ . The irrelevant ideal is generated by 7 monomials (one for each cone of the fan):

$$B(\Sigma) = \langle z_0 z_1 z_2, z_1 z_2, z_0 z_2, z_0 z_1, z_2, z_1, z_0 \rangle = \langle z_0, z_1, z_2 \rangle.$$

The exceptional set is just the origin,  $Z(\Sigma) = V(z_0, z_1, z_2) = \{(0, 0, 0)\}$ .

It remains to determine  $G$ , which is the kernel of the map  $(\mathbb{C}^*)^3 \rightarrow (\mathbb{C}^*)^2$  given by  $(\lambda_0, \lambda_1, \lambda_2) \mapsto (\lambda_0 \lambda_2^{-1}, \lambda_1 \lambda_2^{-1})$ . Since  $(\lambda_0 \lambda_2^{-1}, \lambda_1 \lambda_2^{-1}) = (1, 1)$  if and

only if  $\lambda_0 = \lambda_1 = \lambda_2$ , we see that  $G \simeq \mathbb{C}^*$  with action on  $\mathbb{C}^3$  given by  $\lambda \cdot (z_0, z_1, z_2) = (\lambda z_0, \lambda z_1, \lambda z_2)$ .

Combining all pieces together, we get  $X_\Sigma = (\mathbb{C}^3 \setminus \{(0, 0, 0)\})/G$ , which is the usual quotient description of the projective plane,  $X_\Sigma \simeq \mathbb{P}^2$ !

Now that we know that our  $X_\Sigma$  is the projective plane, we can access it in Sage much quicker, avoiding explicit fan and variety construction:

```
sage: P2 = toric_varieties.P(2)
sage: P2
2-d CPR-Fano toric variety covered by 3 affine patches
sage: P2.plot()
Graphics object consisting of 16 graphics primitives
```

We explain the meaning of “CPR-Fano” in the description of P2 in [Section 2.1](#), meanwhile, note that it is possible to plot P2: Sage actually plots the underlying fan with rays labelled by corresponding coordinates, as shown in [Figure 1.5](#).

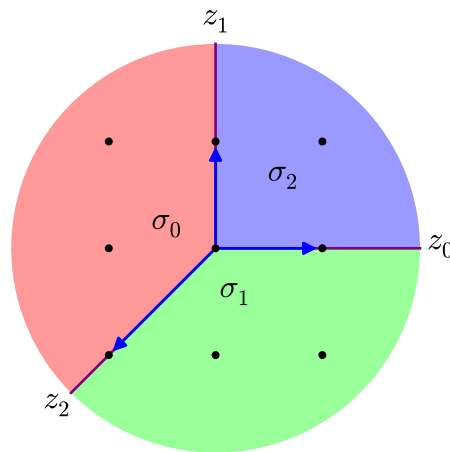


Figure 1.5: Projective plane

When working with toric varieties in Sage, beware of the following convention:

```
sage: P2.coordinate_ring()
Multivariate Polynomial Ring in z0, z1, z2 over Rational Field
```

As you see, the coordinate ring of P2 turned out to be over rational rather than complex numbers. This is done for the sake of fast *and precise* arithmetic, we

still treat toric varieties as defined over complex numbers. If you wish, you can drop this implicit assumption and work with “honest” complex varieties:

```
sage: P2_over_CC = P2.base_extend(CC)
sage: P2_over_CC.coordinate_ring()
Multivariate Polynomial Ring in z0, z1, z2 over Complex Field with
53 bits of precision
```

The projective plane example suggests that the original description of the irrelevant ideal in Definition 1.6.3 is not the most efficient one. Indeed, it is enough to take only monomials  $z^{\hat{\sigma}}$  corresponding to all  $\sigma \in \Sigma_{\max}$ , since all other cones will give multiples of these monomials. It is also possible to describe irreducible components of the exceptional set.

**Definition 1.6.7.** Let  $\Sigma$  be a fan. A **primitive collection** of  $\Sigma$  is any subset  $C$  of rays of  $\Sigma$  such that

- 1)  $C$  is not contained in any cone  $\sigma \in \Sigma$ ;
- 2) any proper subset of  $C$  is contained in some cone  $\sigma \in \Sigma$ .

**Proposition 1.6.8.** *Let  $\Sigma$  be a fan. The decomposition of the exceptional set  $Z(\Sigma)$  into its irreducible components is given by  $Z(\Sigma) = \cup_C V(z_\rho : \rho \in C)$  with  $C$  running over all primitive collections of  $\Sigma$ .*

*Proof.* See Proposition 5.1.6 in [CLS11]. □

In addition to the projective plane, let us also mention toric realizations of other standard spaces. In the 1-dimensional case there are only three possible fans: the origin corresponding to the torus  $\mathbb{C}^*$ , the ray corresponding to the affine line  $\mathbb{A}^1$ , and the complete fan corresponding to the projective line  $\mathbb{P}^1$ . In any dimension  $n$  the fan generated by the cone on standard basis vectors of the lattice corresponds to  $\mathbb{A}^n$ . If we add one more ray opposite to the sum of basis vectors and take all cones generated by all-but-one rays from this collection, we get the fan corresponding to  $\mathbb{P}^n$ . In Sage one can quickly construct these varieties using `toric_varieties.A(n)` and `toric_varieties.P(n)`. Finally, the product of fans corresponds to the product of varieties, for example [Figure 1.6 on the next page](#) shows the fan of  $\mathbb{P}^1 \times \mathbb{P}^1$ , accessible in Sage via `toric_varieties.P1xP1()`.

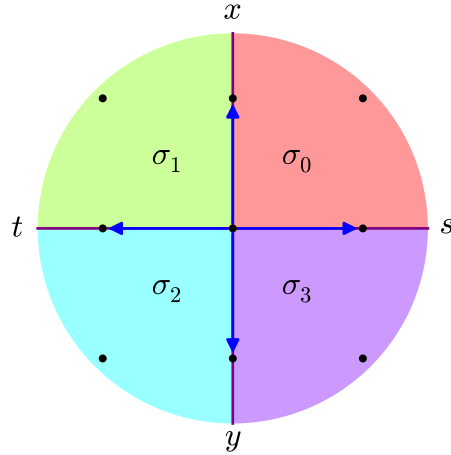


Figure 1.6: Product of projective lines

## 1.7 Torus Orbits and Toric Divisors

Since any toric variety  $X$  comes equipped with a torus action by definition, it has a stratification into orbits of this action. One of them is the torus itself and, by definition, its closure is the whole variety. Closures of other orbits correspond to subvarieties of smaller dimension and it turns out that they are numerous enough to generate both the class group  $\text{Cl}(X)$  and the Chow group of  $X$ .

**Theorem 1.7.1.** *Let  $\Sigma$  be a fan in  $N_{\mathbb{R}}$ ,  $\dim N_{\mathbb{R}} = n$ . Then:*

- 1) *There is a bijective correspondence between cones  $\sigma \in \Sigma$  and  $T_N$ -orbits  $O(\sigma) \subset X_{\Sigma}$ , with  $\dim O(\sigma) = n - \dim \sigma$ .*
- 2) *Affine subsets  $U_{\sigma}$  are unions of orbits,  $U_{\sigma} = \bigcup_{\tau \text{ face of } \sigma} O(\tau)$ .*
- 3) *The closure of  $O(\sigma)$  is  $\overline{O(\sigma)} = \bigcup_{\sigma \text{ face of } \tau \in \Sigma} O(\tau)$  in both Zariski and Euclidean topologies.*

*Proof.* See Theorem 3.2.6 in [CLS11]. □

**Definition 1.7.2.** Let  $\Sigma$  be a fan in  $N_{\mathbb{R}}$ . For any  $\rho \in \Sigma(1)$  a **prime toric divisor**  $D_{\rho}$  of  $X_{\Sigma}$  is the torus-invariant Weil divisor  $D_{\rho} = \overline{O(\rho)}$ . The **group of toric divisors** is  $\text{Div}_{T_N}(X_{\Sigma}) = \bigoplus_{\rho \in \Sigma(1)} \mathbb{Z}D_{\rho} \subset \text{Div}(X_{\Sigma})$ .

Characters correspond to principal toric divisors, so we get a natural map  $M \rightarrow \text{Div}_{T_N}(X_{\Sigma})$  and its cokernel is the class group.

**Proposition 1.7.3.** *Let  $\Sigma$  be a fan in  $N_{\mathbb{R}}$ . Let  $m \in M$ . Then the divisor on  $X_{\Sigma}$  corresponding to  $\chi^m$  is  $\operatorname{div}(\chi^m) = \sum_{\rho \in \Sigma(1)} \langle m, v_{\rho} \rangle D_{\rho}$ , where  $v_{\rho}$  is the primitive integral generator of  $\rho$ .*

*Proof.* See Proposition 4.1.2 in [CLS11]. □

**Theorem 1.7.4.** *Let  $X_{\Sigma}$  be the toric variety without torus factors corresponding to a fan  $\Sigma$  in  $N_{\mathbb{R}}$ . Then*

$$0 \rightarrow M \rightarrow \operatorname{Div}_{T_N}(X_{\Sigma}) \rightarrow \operatorname{Cl}(X_{\Sigma}) \rightarrow 0$$

*is a short exact sequence.*

*Proof.* See Theorem 4.1.3 in [CLS11]. □

The exact sequence of the above theorem gives a  $\operatorname{Cl}(X_{\Sigma})$ -grading on the total coordinate ring of  $X_{\Sigma}$ : for a monomial  $z^a \in S(\Sigma)$  with  $a \in \mathbb{Z}^{\Sigma(1)}$  we define its degree  $\deg(z^a)$  to be the class of the divisor  $\sum_{\rho} a_{\rho} D_{\rho}$ . This grading strengthens the similarity between projective spaces and more general toric varieties.

**Theorem 1.7.5.** *Let  $\Sigma$  be a simplicial fan. Then there is a bijective correspondence between closed subvarieties of  $X_{\Sigma}$  and radical homogeneous ideals  $I \subset B(\Sigma) \subset S(\Sigma)$ .*

*Proof.* See Proposition 5.2.7 in [CLS11]. □

While it is necessary to require inclusion into the irrelevant ideal to get a bijective correspondence between ideals and subvarieties, it is sometimes more convenient to work with simpler ideals that fail to satisfy this condition. In particular, a prime toric divisor  $D_{\rho}$  can be described by the equation  $z_{\rho} = 0$ , while the ideal corresponding to it according to the theorem is  $I(D_{\rho}) = \langle z_{\rho} \rangle \cap B(\Sigma)$ . This does not imply that these divisors are always Cartier, since homogeneous coordinate functions may often fail to be valid functions on the toric variety due to incompatibility with the quotient map.

Here is an example of creating a Weil toric divisor in Sage, checking that it is in fact Cartier, mapping it to the (rational) class group and lifting back to the toric divisor group.

```
sage: P1xP1 = toric_varieties.P1xP1()
```

```

sage: D1 = P1xP1.divisor(1)
sage: D1
V(t)
sage: D1.is_Cartier()
True
sage: D1_class = D1.divisor_class()
sage: D1_class
Divisor class [1, 0]
sage: P1xP1.rational_class_group().rank()
2
sage: D1_class.lift()
V(s)
sage: D1_class.lift() == D1
False

```

Next we give a combinatorial description of global sections of toric divisors.

**Definition 1.7.6.** Let  $\Sigma$  be a fan in  $N_{\mathbb{R}}$ , let  $D = \sum_{\rho} a_{\rho} D_{\rho}$  be a toric divisor on  $X_{\Sigma}$ . The **polyhedron of the divisor**  $D$  is

$$P_D = \{u \in M_{\mathbb{R}} : \langle u, v_{\rho} \rangle \geq -a_{\rho} \text{ for all } \rho \in \Sigma(1)\},$$

where  $v_{\rho}$  are primitive integral generators of the rays  $\rho$ . Given a character  $\chi^m$  with  $m \in P_D \cap M$ , its  **$D$ -homogenization** is the monomial

$$z^{\langle m, D \rangle} = \prod_{\rho} z_{\rho}^{\langle m, v_{\rho} \rangle + a_{\rho}} \in S(\Sigma).$$

Polyhedra of divisors are not lattice polytopes in general: they may be unbounded and may have non-integral vertices. Clearly, it is possible to reconstruct the divisor  $D$  from the inequalities used in the definition of  $P_D$ , however some of these inequalities may be redundant or non-unique for specifying  $P_D$  (e.g. if it is the empty polytope, it can be described by any pair of incompatible inequalities), so we don't get a bijective correspondence here.

**Proposition 1.7.7.** *Let  $\Sigma$  be a fan in  $N_{\mathbb{R}}$ , let  $D$  be a toric divisor on  $X_{\Sigma}$ . Then  $\Gamma(X_{\Sigma}, \mathcal{O}_{X_{\Sigma}}(D)) = \bigoplus_{m \in P_D \cap M} \mathbb{C}\chi^m$ .*

*Proof.* See Proposition 4.3.3 in [CLS11]. □

Of particular interest to us are the canonical divisor  $K_X$  of a toric variety  $X$  and global sections of the anticanonical divisor  $-K_X$ .

**Theorem 1.7.8.** *Let  $\Sigma$  be a fan. Then a toric canonical divisor on  $X_\Sigma$  is  $K_{X_\Sigma} = -\sum_\rho D_\rho$ .*

*Proof.* See Theorem 8.2.3 in [CLS11]. □

The anticanonical divisor of  $\mathbb{P}^1 \times \mathbb{P}^1$  has 9 sections:

```
sage: P1xP1.K()
-V(s) - V(t) - V(x) - V(y)
sage: aK = - P1xP1.K()
sage: aK
V(s) + V(t) + V(x) + V(y)
sage: P_aK = aK.polyhedron()
sage: P_aK
A 2-dimensional polyhedron in QQ^2 defined as the convex hull of 4
vertices.
sage: P_aK.vertices()
[[1, -1], [1, 1], [-1, 1], [-1, -1]]
sage: aK.sections()
(M(1, -1), M(1, 1), M(-1, 1), M(-1, -1), M(-1, 0), M(0, -1), M(0,
0), M(0, 1), M(1, 0))
sage: aK.sections_monomials()
(s^2*y^2, s^2*x^2, t^2*x^2, t^2*y^2, t^2*x*y, s*t*y^2, s*t*x*y,
s*t*x^2, s^2*x*y)
```

## 1.8 Toric Morphisms

Given a morphism between two toric varieties, it is natural to require its compatibility with the torus action.

**Definition 1.8.1.** Let  $N$  and  $N'$  be lattices,  $\Sigma$  be a fan in  $N_\mathbb{R}$ , and  $\Sigma'$  be a fan in  $N'_\mathbb{R}$ . A morphism  $\varphi : X_\Sigma \rightarrow X_{\Sigma'}$  between toric varieties is a **toric morphism** if  $\varphi$  maps the torus  $T_N \subset X_\Sigma$  into the torus  $T_{N'} \subset X_{\Sigma'}$  as a group homomorphism.

**Theorem 1.8.2.** *Let  $N$  and  $N'$  be lattices,  $\Sigma$  be a fan in  $N_{\mathbb{R}}$ , and  $\Sigma'$  be a fan in  $N'_{\mathbb{R}}$ . There is a bijection between toric morphisms from  $X_{\Sigma}$  to  $X'_{\Sigma'}$  and fan morphisms from  $\Sigma$  to  $\Sigma'$ . For a fan morphism  $\varphi : \Sigma \rightarrow \Sigma'$  the associated toric morphism  $\tilde{\varphi} : X_{\Sigma} \rightarrow X_{\Sigma'}$  is given on the torus  $T_N$  by*

$$T_N \simeq N \otimes_{\mathbb{Z}} \mathbb{C}^* \xrightarrow{\varphi \otimes 1} N' \otimes_{\mathbb{Z}} \mathbb{C}^* \simeq T_{N'}$$

and extended to  $X_{\Sigma}$  by continuity.

*Proof.* See Theorem 3.3.4 in [CLS11]. □

Now we turn our attention to a description of toric morphisms in terms of homogeneous coordinates. Recall that these coordinates work best for orbifolds without torus factors, so let's assume that we are in such a situation, i.e. both the domain fan  $\Sigma$  and the codomain fan  $\Sigma'$  are full-dimensional and simplicial.

Let  $v$  be the primitive generator of a ray  $\rho \in \Sigma$ . Let  $\sigma' \in \Sigma'$  be the minimal cone containing  $\varphi(v)$ . Let  $v'_1, \dots, v'_k$  be the primitive generators of rays  $\rho'_1, \dots, \rho'_k$  of  $\sigma'$ . Then  $\varphi(v) = a_1 v'_1 + \dots + a_k v'_k$  for a unique choice of  $a_1, \dots, a_k \in \mathbb{Q}_{>0}$ , since  $\sigma'$  is simplicial and  $\varphi(v)$  is its interior point. (We could replace  $\mathbb{Q}$  with  $\mathbb{Z}$  if  $\sigma'$  was smooth.) Now a point  $p \in X_{\Sigma}$  with all homogeneous coordinates but  $z_{\rho}$  equal to 1 is sent to a point  $p' \in X_{\Sigma'}$  with homogeneous coordinates  $z_{\rho'_1} = z_{\rho}^{a_1}, \dots, z_{\rho'_k} = z_{\rho}^{a_k}$  and all others equal to 1. This is sufficient to define the image of any point  $p \in X_{\Sigma}$  without zero homogeneous coordinates, but the resulting expression for the map makes sense globally due to the compatibility of  $\varphi$  with fans  $\Sigma$  and  $\Sigma'$ .

A subtle point of the above description is a possibility of fractional powers. While this does mean that the induced map between total coordinate rings  $S(\Sigma') \rightarrow S(\Sigma)$  is not polynomial, the ambiguity of a branch choice merely reflects the presence of a finite group action identifying them. As long as the made choice is consistent, it is still possible to use this map to pullback functions from  $X_{\Sigma'}$  to  $X_{\Sigma}$ . We illustrate this via the following example.

**Example 1.8.3** (Resolution of  $\mathbb{WP}(1, 2, 3)$ ). Let  $X_{\Sigma'}$  be a toric realization of the weighted projective space  $\mathbb{WP}(1, 2, 3)$  (`x_p` in the code below) and  $X_{\Sigma}$  be its desingularization (`x` in the code). We use coordinates  $z$  on the original space and  $y$  on the desingularization, the fans are shown on [Figure 1.7 on the following page](#).

```

sage: Delta_polar = LatticePolytope([(1,0), (0,1), (-2,-3)])
sage: X_p = ToricVariety(FaceFan(Delta_polar))
sage: X_p.is_smooth()
False
sage: X = X_p.resolve(new_rays=[(-1,-1), (-1,-2), (0,-1)],
    coordinate_names="y+")
sage: X.is_smooth()
True

```

Since it is a subdivision, an acceptable point with homogeneous coordinates

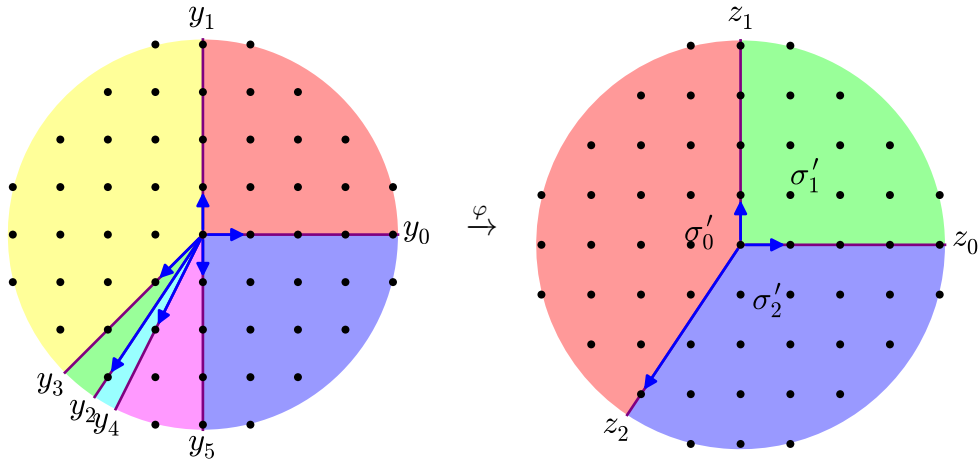


Figure 1.7: Resolution of  $\mathbb{WP}(1, 2, 3)$

$[y_0 : y_1 : y_2 : 1 : 1 : 1]$  is sent to  $[y_0 : y_1 : y_2]$ . To determine images of other points, we need to decompose the generator corresponding to  $y_3$  using ray generators of  $\sigma'_0$  and generators corresponding to  $y_4$  and  $y_5$  using ray generators of  $\sigma'_2$ . We have:

$$\begin{aligned}
 y_3 : \quad & (-1, -1) = \frac{1}{2} \cdot (0, 1) + \frac{1}{2} \cdot (-2, -3), \\
 y_4 : \quad & (-1, -2) = \frac{1}{3} \cdot (1, 0) + \frac{2}{3} \cdot (-2, -3), \\
 y_5 : \quad & (0, -1) = \frac{2}{3} \cdot (1, 0) + \frac{1}{3} \cdot (-2, -3),
 \end{aligned}$$

so the map is

$$[y_0 : y_1 : y_2 : y_3 : y_4 : y_5] \mapsto \left[ y_0 y_4^{1/3} y_5^{2/3} : y_1 y_3^{1/2} : y_2 y_3^{1/2} y_4^{2/3} y_5^{1/3} \right].$$

Sage does not (yet) provide built-in support for such maps, but we can emulate them using “positive” symbolic variables to allow simplification of fractional powers:

```
sage: [var(v, domain="positive") for v in
      X_p.coordinate_ring().variable_names()]
[z0, z1, z2]
sage: [var(v, domain="positive") for v in
      X.coordinate_ring().variable_names()]
[y0, y1, y2, y3, y4, y5]
sage: sd = {z0: y0*y4^(1/3)*y5^(2/3), z1: y1*y3^(1/2), z2:
           y2*y3^(1/2)*y4^(2/3)*y5^(1/3)}
```

Substituting this dictionary into functions on the original variety, we will get pullbacks to the resolved one. For example, let’s pullback the sum of all monomial sections of the divisor corresponding to  $z_0$ :

```
sage: D = X_p.divisor(0)
sage: D
V(z0)
sage: sum(D.sections_monomials())
z2^2 + z0
sage: SR(sum(D.sections_monomials())).subs(sd)
y2^2*y3*y4^(4/3)*y5^(2/3) + y0*y4^(1/3)*y5^(2/3)
```

Here is a typeset and factored version of the pullback:

$$(y_2^2 y_3 y_4 + y_0) y_4^{\frac{1}{3}} y_5^{\frac{2}{3}}.$$

Obviously, this is not a rational function, but we could expect something like this since we were pulling back only a  $\mathbb{Q}$ -Cartier divisor:

```
sage: D.is_Cartier()
False
sage: D.is_QQ_Cartier()
True
sage: threeD = 3*D
sage: threeD
3*V(z0)
```

```
sage: threeD.is_Cartier()
```

```
True
```

Performing the above steps for `threeD` instead of `D` shows that the pullback of its section

$$z_2^6 + z_0 z_2^4 + z_0^2 z_2^2 + z_1 z_2^3 + z_0^3 + z_0 z_1 z_2 + z_1^2$$

is

$$y_2^6 y_3^3 y_4^4 y_5^2 + y_0 y_2^4 y_3^2 y_4^3 y_5^2 + y_0^2 y_2^2 y_3 y_4^2 y_5^2 + y_1 y_2^3 y_3^2 y_4^2 y_5 + y_0^3 y_4 y_5^2 + y_0 y_1 y_2 y_3 y_4 y_5 + y_1^2 y_3.$$

These two polynomials are actually sections of the anticanonical line bundles and, as we will see in the next chapter, they define one-dimensional Calabi-Yau varieties, i.e. elliptic curves.

# Chapter 2

## Toric Geometry in Mirror Symmetry

In this chapter we describe Batyrev's construction of mirror families of Calabi-Yau anticanonical hypersurfaces in toric varieties [Bat94] and its generalization to nef complete intersections by Batyrev and Borisov [BB96b]. As before, we provide Sage examples whenever possible.

### 2.1 Reflexive Polytopes and Fano Varieties

We have already seen in Section 1.3 how fans and, therefore, toric varieties can be associated to lattice polytopes. Now we concentrate on a special class of such varieties.

**Definition 2.1.1.** A **Gorenstein Fano variety** is a complete normal variety whose anticanonical divisor is Cartier and ample.

**Definition 2.1.2.** Let  $\Delta \subset M_{\mathbb{R}}$  be a full-dimensional lattice polytope. Its **polar polytope** is  $\Delta^{\circ} = \{v \in N_{\mathbb{R}} : \langle u, v \rangle \geq -1 \text{ for all } u \in \Delta\} \subset N_{\mathbb{R}}$ .

**Definition 2.1.3.** A **reflexive polytope** is a full-dimensional lattice polytope  $\Delta \subset M_{\mathbb{R}}$  such that its polar  $\Delta^{\circ} \subset N_{\mathbb{R}}$  is also a (full-dimensional) lattice polytope.

Alternatively, a lattice polytope  $\Delta \subset M_{\mathbb{R}}$  is reflexive if it contains the origin in its interior and the lattice distance from every facet to the origin is 1, i.e.

if  $v$  is a primitive integral inner normal to a facet of  $\Delta$ , then the equation of the supporting hyperplane of this facet is  $\langle u, v \rangle + 1 = 0$ .

Note that  $(\Delta^\circ)^\circ = \Delta$ , so we get polar duality between reflexive polytopes in  $M_{\mathbb{R}}$  and reflexive polytopes in  $N_{\mathbb{R}}$ . Similar to duality of cones, faces of  $\Delta$  and  $\Delta^\circ$  are in an inclusion-reversing bijective correspondence.

**Theorem 2.1.4.** *Let  $\Sigma$  be a fan in  $N_{\mathbb{R}}$ . Then  $X_\Sigma$  is a projective Gorenstein Fano variety if and only if  $\Sigma$  is the normal fan of a reflexive polytope  $\Delta \subset M_{\mathbb{R}}$ , i.e.  $\Sigma = \Sigma_\Delta$ .*

*Proof.* See Theorem 8.3.4 in [CLS11]. □

We have constructed the fan of the projective plane in several ways, one of them was using the normal fan of the following polytope:

```
sage: Delta = LatticePolytope([(2,-1), (-1,2), (-1,-1)])
sage: Delta.is_reflexive()
True
sage: Delta.polar().vertices()
[ 1  0 -1]
[ 0  1 -1]
sage: NormalFan(Delta).ray_matrix()
[ 1  0 -1]
[ 0  1 -1]
```

For a reflexive polytope  $\Delta$  vertices of  $\Delta^\circ$  coincide with primitive integral generators of rays of the normal fan  $\Sigma_\Delta$ , so one can also think of  $\Sigma_\Delta$  as the face fan of  $\Delta^\circ$ . From the computational point of view, it may be more convenient to use the latter since you can pick the order of vertices of  $\Delta^\circ$  if you construct them directly (automatically constructed polar polytopes and normal fans have their vertices/rays in a fixed, but random order).

```
sage: P2_n = ToricVariety(NormalFan(Delta))
sage: P2_f = ToricVariety(FaceFan(Delta.polar()))
sage: P2_n == P2_f
True
```

Sage provides special support for working with Fano toric varieties, so instead of the above commands one can use

```

sage: P2_n = CPRFanoToricVariety(Delta)
sage: P2_f = CPRFanoToricVariety(Delta_polar=Delta.polar())
sage: P2_n == P2_f
True

```

Now let's take a look at the Fano toric variety corresponding to the *normal fan* of  $\Delta^\circ$  or, equivalently, let's switch the roles of  $\Delta$  and  $\Delta^\circ$  in our computations:

```

sage: Delta = Delta.polar()
sage: X = CPRFanoToricVariety(Delta)
sage: X
2-d CPR-Fano toric variety covered by 3 affine patches
sage: X.is_smooth()
False
sage: X.is_orbifold()
True

```

As we see,  $X$  has some finite quotient singularities, since its fan (shown in [Figure 2.1 on the next page](#)) is simplicial but not smooth. To figure out the exact nature of these singularities, we can use the quotient description of  $X$  from [Section 1.6](#). As for the projective plane,  $X = (\mathbb{C}^3 \setminus \{(0, 0, 0)\})/G$ , but the group  $G$  is a little different. It is the kernel of the map  $(\mathbb{C}^*)^3 \rightarrow (\mathbb{C}^*)^2$  given by  $(\lambda_0, \lambda_1, \lambda_2) \mapsto (\lambda_0^2 \lambda_1^{-1} \lambda_2^{-1}, \lambda_0^{-1} \lambda_1^2 \lambda_2^{-1})$ . Equating the image to  $(1, 1)$ , we get  $\lambda_0^2 = \lambda_1 \lambda_2$  and  $\lambda_0 = \lambda_1^2 \lambda_2^{-1}$ , so  $\lambda_1^4 \lambda_2^{-2} = \lambda_1 \lambda_2$  and  $\lambda_1^3 = \lambda_2^3$ . Then  $\lambda_1 = \epsilon_3 \lambda_2$ , where  $\epsilon_3$  is a primitive cube root of unity, and  $\lambda_0 = (\epsilon_3 \lambda_2)^2 \lambda_2^{-1} = \epsilon_3^2 \lambda_2$ . We see that  $G \simeq \mathbb{C}^* \times \mathbb{Z}_3$  with action on  $\mathbb{C}^3$  given by  $(\lambda, k) \cdot (z_0, z_1, z_2) = (\lambda \epsilon_3^{2k} z_0, \lambda \epsilon_3^k z_1, \lambda z_2)$ , so  $X = \mathbb{P}^2/\mathbb{Z}_3$ .

It is possible to resolve orbifold singularities of toric varieties in Sage by specifying either rays used for fan subdivision or, in the case of Fano varieties, points of  $\Delta^\circ$ . The easiest way to resolve many (but not necessarily all in higher dimensions) singularities is to use all these points:

```

sage: X_res = CPRFanoToricVariety(Delta, coordinate_points="all")
sage: X_res
2-d CPR-Fano toric variety covered by 9 affine patches
sage: X_res.is_smooth()
True

```

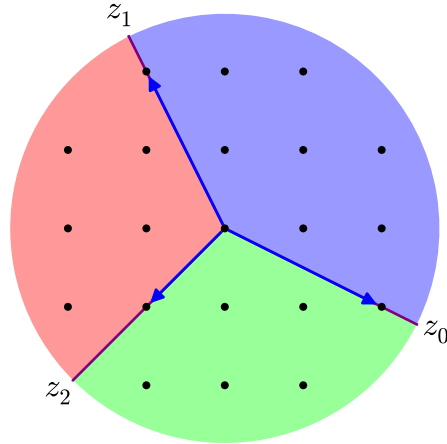


Figure 2.1: Fano toric variety polar to the projective plane

The fan of this resolved variety is shown in Figure 2.2. Since it is obtained as a subdivision of  $\Sigma_\Delta$ , it is not immediately clear if it is the normal fan of some other reflexive polytope. We will see later that it is not, so  $X_{\text{res}}$  is not Fano. On the other hand, it is closely related to one.

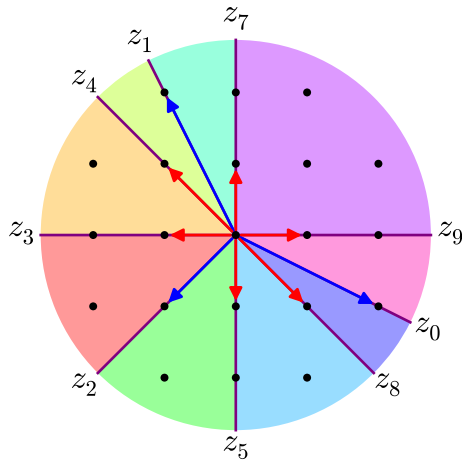


Figure 2.2: Resolution of the toric variety polar to the projective plane

**Definition 2.1.5.** Let  $\Delta \subset M_{\mathbb{R}}$  be a reflexive polytope. Let  $\Sigma$  be a subdivision of  $\Sigma_\Delta$ . If all rays of  $\Sigma$  are generated by (some of) the boundary lattice points of  $\Delta^\circ$ , it is a **crepant subdivision**. If  $\Sigma$  is also simplicial and the corresponding toric variety  $X_\Sigma$  is projective, it is a **projective crepant subdivision**. If also *all* boundary lattice points of  $\Delta^\circ$  generate rays of  $\Sigma$ , it is a **maximal**

### projective crepant subdivision.

Such subdivisions correspond to *maximal projective crepant partial desingularizations* (*MPCP-desingularizations*) introduced by Batyrev in [Bat94]. The meaning of “maximal” and “projective” is clear from the definition. “Partial” reflects the fact that such subdivisions are not always sufficient to completely resolve all singularities of the toric variety associated to the original normal fan. Finally, “crepant” means that the corresponding morphism between varieties is crepant.

**Proposition 2.1.6.** *Let  $\Delta \subset M_{\mathbb{R}}$  be a reflexive polytope. Let  $\Sigma$  be a subdivision of  $\Sigma_{\Delta}$ . Then the associated morphism  $\varphi : X_{\Sigma} \rightarrow X_{\Delta}$  is crepant (meaning that  $\varphi^*(K_{X_{\Delta}}) = K_{X_{\Sigma}}$ ) if and only if  $\Sigma$  is a crepant subdivision.*

*Proof.* See Proposition 2.2.12 in [Bat94]. □

From the computational point of view, it is not always convenient to work with maximal subdivisions since associated varieties may involve too many homogeneous variables and affine charts. Also, as it is clear from the definition, “crepant” has a simpler combinatorial interpretation than “projective.” For these reasons Sage provides support for *crepant partial resolutions* of Fano toric varieties and we refer to them as *CPR-Fano toric varieties*.

There are infinitely many reflexive polytopes, for example, all polygons

$$P_k = \text{Conv} \{(1, 0), (k, 1), (-1 - k, -1)\}, \quad k \in \mathbb{Z},$$

are reflexive with polar polygons

$$P_k^{\circ} = \text{Conv} \{(2, -2k - 1), (-1, k - 1), (-1, k + 2)\}.$$

Note that in this example we can go from any polygon  $P_{k_1}$  to any other  $P_{k_2}$  using a  $GL(2, \mathbb{Z})$ -transformation, i.e. by changing lattice coordinates:

$$P_{k_2} = \begin{pmatrix} 1 & k_2 - k_1 \\ 0 & 1 \end{pmatrix} \cdot P_{k_1}.$$

These transformations induce isomorphisms between corresponding toric varieties, so it is natural to distinguish reflexive polytopes only up to a  $GL(2, \mathbb{Z})$ -transformation. In this case it is known that there are only finitely many re-

flexive polytopes in each dimension. Obviously, there is only one 1-dimensional reflexive polytope, it is also not very difficult to obtain by hand all 16 reflexive polygons. The general construction algorithm is known [KS97] and implemented in software PALP (Package for Analyzing Lattice Polytopes) [KS04]. Using their software Kreuzer and Skarke have obtained complete lists of 4,319 reflexive polytopes in dimension 3 [KS98] and 473,800,776 reflexive polytopes in dimension 4 [KS02]. It is estimated that there are about  $10^{18}$  reflexive polytopes in dimension 5 [Kre08].

Reflexive polygons and 3-dimensional polytopes are easily accessible in Sage:

```
sage: p = ReflexivePolytope(2, 12)
sage: p
Reflexive polytope 12: 2-dimensional, 3 vertices.
sage: p.vertices()
[ 1  1 -3]
[ 0  2 -2]
sage: max(p.nfacets() for p in ReflexivePolytopes(2))
6
```

The last computation shows that there are no reflexive polygons with 9 facets, therefore, the fan in Figure 2.2 on page 34 is not the normal fan of one.

## 2.2 Anticanonical Hypersurfaces

Since we need to allow some singularities, we are using the term *Calabi-Yau variety* in the sense of Definition 1.4.1 in [CK99].

**Definition 2.2.1.** A **Calabi-Yau variety** is an irreducible normal compact variety  $V$  which satisfies the following conditions:

- 1)  $V$  has at most Gorenstein canonical singularities;
- 2)  $V$  has trivial canonical sheaf;
- 3)  $H^i(V, \mathcal{O}_V) = 0$  for  $i = 1, \dots, \dim V - 1$ .

**Theorem 2.2.2.** *Let  $\Delta$  be a reflexive polytope of dimension  $n$ . A generic anticanonical hypersurface in  $X = X_\Delta$ , i.e. a generic section  $f \in \Gamma(X, \mathcal{O}_X(-K_X))$ , is a Calabi-Yau variety of dimension  $n - 1$ . A generic anticanonical hyper-*

surface in  $X = X_\Sigma$ , where  $\Sigma$  is a projective crepant subdivision of  $\Sigma_\Delta$ , is a Calabi-Yau orbifold of dimension  $n - 1$ .

*Proof.* See Proposition 4.1.3 in [CK99]. □

For a reflexive polytope  $\Delta \subset M_{\mathbb{R}}$  projective crepant subdivisions of  $\Sigma_\Delta$  correspond to special triangulations of the boundary of  $\Delta^\circ$ . For any such subdivision the polytope of the anticanonical divisor is easily seen to be  $\Delta$  itself. This means that in equations of anticanonical Calabi-Yau hypersurfaces variables correspond to points of  $\Delta^\circ$  while (coefficients of) monomials correspond to points of  $\Delta$ . Due to polar duality of reflexive polytopes roles of  $\Delta$  and  $\Delta^\circ$  can be reversed, leading to another family of hypersurfaces in another toric variety. Batyrev showed [Bat94] that if  $\dim \Delta = 4$ , then generic anticanonical hypersurfaces in MPCP-desingularizations of  $X_\Delta$  are *smooth* Calabi-Yau threefolds and the exchange  $\Delta \rightsquigarrow \Delta^\circ$  corresponds to the exchange  $h^{1,1} \rightsquigarrow h^{2,1}$  of the Hodge numbers of anticanonical hypersurfaces of two families, making them candidates for mirror pairs.

The anticanonical “hypersurfaces” in the projective plane and its quotient discussed above are 1-dimensional Calabi-Yau varieties, i.e. elliptic curves:

```
sage: P2 = toric_varieties.P(2)
sage: P2.anticanonical_hypersurface()
Closed subscheme of 2-d CPR-Fano toric variety covered by 3 affine
patches defined by:
a0*z0^3 + a1*z1^3 + a6*z0*z1*z2 + a2*z2^3
sage: P2.anticanonical_hypersurface(
    monomial_points="all").defining_polynomials()[0]
a0*z0^3 + a9*z0^2*z1 + a7*z0*z1^2 + a1*z1^3 + a8*z0^2*z2 +
a6*z0*z1*z2 + a4*z1^2*z2 + a5*z0*z2^2 + a3*z1*z2^2 + a2*z2^3
sage: P2P = CPRFanoToricVariety(P2.Delta_polar())
sage: P2P.anticanonical_hypersurface(
    monomial_points="all").defining_polynomials()[0]
a0*z0^3 + a1*z1^3 + a3*z0*z1*z2 + a2*z2^3
```

Anticanonical hypersurfaces in  $\mathbb{P}^2$  are zero sets of cubic polynomials, which may include up to 10 monomials corresponding to 10 lattice points inside of the lattice polytope  $\Delta$  corresponding to  $\mathbb{P}^2$ . As the above example shows, only 4 of these monomials are used in Sage by default. This is due to the fact that

using automorphisms of the toric variety it is possible to set to zero coefficients of monomials corresponding to interior points of facets of  $\Delta$  (see Section 6.1.2 of [CK99]), so in most situations they can be discarded. For the quotient  $\mathbb{P}^2/\mathbb{Z}^3$ , however, there are only 4 monomials invariant under the  $\mathbb{Z}^3$ -action and it is not possible to use more.

## 2.3 Nef Complete Intersections

The construction of Calabi-Yau varieties as anticanonical hypersurfaces in toric varieties was generalized by Batyrev and Borisov to the case of complete intersections associated to nef-partitions of reflexive polytopes [Bor93, BB96b].

**Definition 2.3.1.** Let  $\Delta \subset M_{\mathbb{R}}$  be a reflexive polytope. A **nef-partition** is a decomposition of the vertex set  $V$  of  $\Delta^\circ \subset N_{\mathbb{R}}$  into a disjoint union

$$V = V_0 \sqcup V_1 \sqcup \cdots \sqcup V_{r-1}$$

such that divisors  $E_i = \sum_{v_\rho \in V_i} D_\rho$  are Cartier. Equivalently, let  $\nabla_i \subset N_{\mathbb{R}}$  be the convex hull of vertices from  $V_i$  and the origin. These polytopes form a nef-partition if their Minkowski sum  $\nabla \subset N_{\mathbb{R}}$  is a reflexive polytope. The **dual nef-partition** is formed by polytopes  $\Delta_i \subset M_{\mathbb{R}}$  of  $E_i$ , which give a decomposition of the vertex set of  $\nabla^\circ \subset M_{\mathbb{R}}$  and their Minkowski sum is  $\Delta$ .

For the remainder of this section we use the notation of the above definition without repeating it.

*Remark 2.3.2.* The term “nef-partition” may be used for any of the following decompositions:

- 1)  $V(\Delta^\circ)$  into the disjoint union of  $V_i$ ,
- 2)  $\Delta$  into the Minkowski sum of  $\Delta_i$ ,
- 3) the anticanonical divisor of  $X_\Delta$  into the sum of  $E_i$ .

Each of these decompositions can be easily translated into another and some care should be taken only to avoid mixing a nef-partition and its dual.

As it follows from the definition, the polar duality of reflexive polytopes switches convex hull and Minkowski sum for dual nef-partitions:

$$\begin{aligned} \Delta^\circ &= \text{Conv}(\nabla_0, \nabla_1, \dots, \nabla_{r-1}), \\ \nabla &= \nabla_0 + \nabla_1 + \cdots + \nabla_{r-1}, \end{aligned}$$

$$\begin{aligned}\Delta &= \Delta_0 + \Delta_1 + \cdots + \Delta_{r-1}, \\ \nabla^\circ &= \text{Conv}(\Delta_0, \Delta_1, \dots, \Delta_{r-1}).\end{aligned}$$

It is possible to give a purely combinatorial description of the nef-partition duality, which is convenient for computational purposes.

**Proposition 2.3.3.** *For the polytopes of dual nef-partitions we have*

$$\begin{aligned}\Delta_i &= \{u \in M_{\mathbb{R}} : \langle u, \nabla_j \rangle \geq -\delta_{ij} \text{ for all } j \in \{0, \dots, r-1\}\}, \\ \nabla_i &= \{v \in N_{\mathbb{R}} : \langle \Delta_j, v \rangle \geq -\delta_{ij} \text{ for all } j \in \{0, \dots, r-1\}\}.\end{aligned}$$

*Proof.* See Proposition 3.13 in [BN08]. □

One can also interpret the duality of nef-partitions as the duality of associated cones. Below  $\overline{M} = M \times \mathbb{Z}^r$  and  $\overline{N} = N \times \mathbb{Z}^r$  are dual lattices,  $\overline{M}_{\mathbb{R}}$  and  $\overline{N}_{\mathbb{R}}$  are vector spaces spanned by them.

**Definition 2.3.4.** The **Cayley polytope**  $P \subset \overline{M}_{\mathbb{R}}$  of a nef-partition is given by

$$P = \text{Conv}(\Delta_0 \times e_0, \Delta_1 \times e_1, \dots, \Delta_{r-1} \times e_{r-1}),$$

where  $\{e_i\}_{i=0}^{r-1}$  is the standard basis of  $\mathbb{Z}^r$ . The **dual Cayley polytope**  $P^* \subset \overline{N}_{\mathbb{R}}$  is the Cayley polytope of the dual nef-partition.

**Definition 2.3.5.** The **Cayley cone**  $C \subset \overline{M}_{\mathbb{R}}$  of a nef-partition is the cone spanned by its Cayley polytope.

**Proposition 2.3.6.** *The Cayley cone  $C$  is full-dimensional. The dimension of the Cayley polytope  $P$  is  $n - r + 1$ .*

*Proof.* Since  $\nabla^\circ = \text{Conv}(\Delta_0, \Delta_1, \dots, \Delta_{r-1})$  is reflexive and full-dimensional, we can pick  $n$  linearly independent vertices of it,  $v_1, \dots, v_n$ . The corresponding points of the Cayley polytope are  $(v_j, e_{i_j})$ , where  $v_j \in \Delta_{i_j}$ . The origin has  $r$  corresponding points  $(0, e_i)$ , since it is contained in every  $\Delta_i$ . These  $n + r$  points are linearly independent in  $M_{\mathbb{R}} \times \mathbb{R}^r$ : if their linear combination is equal to zero, then the first  $n$  coefficients must be equal to zero due to linear independence of  $v_1, \dots, v_n$  and the last  $r$  coefficients due to linear independence of points corresponding to the origin. Therefore,  $\dim C = n + r$ .

Since  $C$  is generated by  $P$  and  $\dim C = n + r$ , we already know that  $\dim P \geq n + r - 1$ . To see that  $\dim P < n + r$ , observe that it is contained in the hyperplane normal to  $(0, \dots, 0, 1, \dots, 1)$  ( $n$  zeros and  $r$  ones).  $\square$

**Definition 2.3.7.** A lattice polytope  $Q$  is a **Gorenstein polytope** of index  $r$  if its multiple  $r \cdot Q$  has a unique interior lattice point  $q$  and its shift  $r \cdot Q - q$  is a reflexive polytope.

In particular, all reflexive polytopes are Gorenstein polytopes of index 1.

**Definition 2.3.8.** A full-dimensional cone  $\sigma \subset \overline{M}_{\mathbb{R}}$  is a **Gorenstein cone** if it generated by finitely many lattice points which are contained in the hyperplane  $\{u \in \overline{M}_{\mathbb{R}} : \langle u, n \rangle = 1\}$  for some  $n \in \overline{N}$ . If the intersection of this hyperplane with  $\sigma$  is a Gorenstein polytope  $Q$  of index  $r$  (with respect to the sublattice of this hyperplane),  $\sigma$  is a **reflexive Gorenstein cone** of index  $r$  supported by  $Q$ .

**Proposition 2.3.9.** *The Cayley polytope  $P$  is a Gorenstein polytope of index  $r$  with respect to its spanned affine sublattice. The Cayley cone  $C$  is a reflexive Gorenstein cone of index  $r$  supported by  $P$ . Its dual cone  $C^{\vee}$  is supported by the dual Cayley polytope  $P^*$ .*

*Proof.* See Theorem 2.6, Definition 3.11, and Proposition 3.13 in [BN08].  $\square$

*Remark 2.3.10.* Note that all definitions and results above make sense for  $r = 1$ , i.e. for partitions with a single part. In this case the duality of Cayley polytopes is the polar duality of reflexive polytopes.

In order to find nef-partitions of a given reflexive polytope, one can use `nef.x` program from PALP [KS04]. Two-part nef-partitions computed by it are readily accessible in Sage:

```
sage: Delta_polar = LatticePolytope([(1,0), (0,1), (-1,0), (0,-1)])
sage: Delta_polar.nef_partitions()
[
Nef-partition {0, 2} U {1, 3} (direct product),
Nef-partition {0, 1} U {2, 3},
Nef-partition {0, 1, 2} U {3} (projection)
]
sage: np = Delta_polar.nef_partitions()[1]
```

```

sage: np.nabla().vertices()
[ 1  0  0 -1  1 -1]
[ 0  1 -1  0 -1  1]
sage: np.nabla(0).vertices()
[1 0 0]
[0 1 0]
sage: np.nabla(1).vertices()
[-1  0  0]
[ 0 -1  0]

```

Given a nef-partition of an  $n$ -dimensional reflexive polytope, consisting of  $r$ -parts, generic sections of divisors  $E_i$  determine an  $(n - r)$ -dimensional complete intersection Calabi-Yau variety. In [BB96a] Batyrev and Borisov showed that such varieties corresponding to dual nef-partitions have mirror-symmetric *stringy* Hodge numbers. We will come back to this duality in more detail in Chapter 3, for now let's just glance at the complete intersection corresponding to the nef-partition above and its dual:

```

sage: X = CPRFanoToricVariety(np.Delta())
sage: X.nef_complete_intersection(np)
Closed subscheme of 2-d CPR-Fano toric variety covered by 4 affine
patches defined by:
a3*z0*z1 + a2*z1*z2 + a1*z0*z3 + a0*z2*z3,
b1*z0*z1 + b0*z1*z2 + b2*z0*z3 + b3*z2*z3
sage: Y = CPRFanoToricVariety(np.dual().Delta())
sage: Y.nef_complete_intersection(np.dual())
Closed subscheme of 2-d CPR-Fano toric variety covered by 6 affine
patches defined by:
a2*z0*z1*z2 + a1*z2*z3*z4 + a0*z1*z4*z5,
b0*z0*z2*z3 + b1*z0*z1*z5 + b2*z3*z4*z5

```

In order to get “honest” Calabi-Yau varieties, it is necessary to exclude a special type of nef-partitions.

**Definition 2.3.11.** A nef-partition  $\Delta = \Delta_0 + \Delta_1 + \dots + \Delta_{r-1}$  is **indecomposable**, if the Minkowski sum of any proper subset of  $\{\Delta_i\}_{i=0}^{r-1}$  is *not* a reflexive polytope in the generated sublattice. It is **decomposable** otherwise.

Decomposable nef-partitions correspond to products of Calabi-Yau vari-

eties, each of which is represented as a complete intersection of a smaller number of hypersurfaces in toric varieties of smaller dimensions.

## 2.4 Torically Induced Fibrations

Let  $N$  and  $N'$  be lattices,  $\Sigma$  be a fan in  $N_{\mathbb{R}}$ , and  $\Sigma'$  be a fan in  $N'_{\mathbb{R}}$ . By Theorem 1.8.2 there is a bijection between toric morphisms  $\tilde{\varphi} : X_{\Sigma} \rightarrow X_{\Sigma'}$  and fan morphisms  $\varphi : \Sigma \rightarrow \Sigma'$ , i.e. lattice homomorphisms  $\varphi : N \rightarrow N'$  compatible with the fan structure (see Definitions 1.4.1 and 1.8.1).

Consider the special case when the lattice homomorphism is surjective, i.e. we have an exact sequence of lattices

$$0 \rightarrow N_0 \rightarrow N \xrightarrow{\varphi} N' \rightarrow 0,$$

where  $N_0 = \ker \varphi$ . Let  $\Sigma_0 = \{\sigma \in \Sigma : \sigma \subset (N_0)_{\mathbb{R}}\}$ . We can consider  $\Sigma_0$  either as a fan in  $N_{\mathbb{R}}$  or as a fan in  $(N_0)_{\mathbb{R}}$  with two corresponding toric varieties  $X_{\Sigma_0, N}$  (a dense subset of  $X_{\Sigma}$ ) and  $X_{\Sigma_0, N_0}$ .

As it is discussed in § 3.3 [CLS11], there is a clear relation between these two varieties,

$$X_{\Sigma_0, N} \simeq X_{\Sigma_0, N_0} \times T_{N'},$$

and, in fact,  $X_{\Sigma_0, N} = \tilde{\varphi}^{-1}(T_{N'})$ , so a part of  $X_{\Sigma}$  is a fiber bundle over  $T_{N'}$  with fibers being  $X_{\Sigma_0, N_0}$ . Moreover, if  $\Sigma$  is *split by  $\Sigma'$  and  $\Sigma_0$*  (see Definition 3.3.18 in [CLS11]), then the whole  $X_{\Sigma}$  is a fiber bundle over  $X_{\Sigma'}$  (see Theorem 3.3.19 in [CLS11]). However, splitting is a very strong condition on fans, so instead of imposing it we will work with more general fibrations than fiber bundles.

**Definition 2.4.1.** Let  $\varphi : X \rightarrow Y$  be a morphism between two varieties. Then  $\varphi$  is a **fibration** if it is surjective and all of its fibers have the same dimension  $\dim X - \dim Y$ .

The following result provides a combinatorial characterization of toric fibrations in terms of primitive cones (see Definition 1.4.2).

**Theorem 2.4.2.** *Let  $\tilde{\varphi} : X_{\Sigma} \rightarrow X_{\Sigma'}$  be a surjective toric morphism. Then it is a fibration if and only if  $\varphi_{\mathbb{R}}|_{\sigma} : \sigma \rightarrow \sigma'$  is a bijection for all primitive cones  $\sigma \in \Sigma$  corresponding to all  $\sigma' \in \Sigma'$ .*

*Proof.* See Corollary 2.1.13 in [HLY02]. □

In Proposition 2.1.4 [HLY02] the authors provide a detailed description of fibers of *arbitrary* toric morphisms<sup>1</sup>, but we are primarily interested in fibrations  $\varphi : X_\Sigma \rightarrow X_{\Sigma'}$  since they may induce fibrations  $\varphi|_Y : Y \rightarrow X_\Sigma$  of Calabi-Yau subvarieties  $Y$  realized as anticanonical hypersurfaces or nef complete intersections in  $X_\Sigma$ . The fibration condition may prevent  $\Sigma$  from being “too refined”, leading to singularities of  $Y$ , however it may be possible to compose  $\varphi$  with a crepant resolution of singularities in such a way that  $Y$  becomes smooth and the restriction of the composition to  $Y$  is still a fibration. See [PS97] or [Roh04] for an explicit treatment of such resolutions of elliptically fibered K3-surfaces, where it is shown how one can determine the type of (some) exceptional elliptic fibers based directly on combinatorics of the associated reflexive polytopes.

We now describe a strategy for searching for toric fibrations. Let  $\Delta \subset M_\mathbb{R}$  be a reflexive polytope and let  $\Sigma$  be a crepant subdivision of  $\Sigma_\Delta$ . Suppose that  $\varphi : \Sigma \rightarrow \Sigma'$  is a fibration (meaning that  $\tilde{\varphi} : X_\Sigma \rightarrow X_{\Sigma'}$  is a fibration in the above sense). As before, its fiber is determined by the subfan  $\Sigma_0$  of  $\Sigma$  in the sublattice  $N_0 = \ker \varphi$  of  $N$ . Since we would like fibers of Calabi-Yau subvarieties to be lower-dimensional Calabi-Yau varieties, it is natural to require that  $\Sigma_0$  is *also associated to a reflexive polytope*, i.e. that it is a crepant subdivision of  $\Sigma_\nabla$  for  $\nabla \subset (M_0)_\mathbb{R}$ , where  $M_0$  is dual lattice of  $N_0$ . Then  $\nabla^\circ$  is a “slice” of  $\Delta^\circ$  by a linear subspace, so one can search for such slices of  $\Delta^\circ$  and then take as  $\varphi$  the projection along the linear subspace of  $\nabla^\circ$ . We can also reformulate this problem in dual terms:  $M_0 = M/(N_0)^\perp$  and the condition that  $\nabla^\circ$  is inside  $\Delta^\circ$  implies that the image of  $\Delta$  in  $M_0$  is inside  $\nabla$ . So one can alternatively look for “projections” of  $\Delta$  that are reflexive. Recall that the origin is the only interior lattice point of any reflexive polytope, so all lattice points of  $\Delta$  must be projected either into the origin or into the boundary of the projection. Due to this restriction a “large”  $\Delta$  with many lattice points is less likely to have any fibrations than a “small” one.

We consider several toric (and torically induced) fibrations in detail in [Chapter 4](#).

---

<sup>1</sup>Note that while notation in [HLY02] is very similar to ours, the authors sometimes *implicitly* assume that toric varieties in question are *complete*.

# Chapter 3

## Hodge Numbers of CICY in Toric Varieties<sup>1</sup>

In this chapter we use Batyrev-Borisov’s formula for the generating function of stringy Hodge numbers of Calabi-Yau varieties realized as complete intersections in toric varieties in order to get closed form expressions for some of the Hodge numbers of complete intersections of two hypersurfaces.

In [Bat94] Batyrev obtained combinatorial formulas for the Hodge numbers  $h^{1,1}(X)$  and  $h^{n-1,1}(X)$  of an  $n$ -dimensional Calabi-Yau variety  $X$  realized as an anticanonical hypersurface in a toric variety associated to a reflexive polytope. It is immediate from these formulas that  $h^{1,1}(X) = h^{n-1,1}(X^\circ)$ , where  $X^\circ$  is Batyrev’s mirror of  $X$ , and this equality suffices to show that mirror symmetry holds on the level of Hodge numbers for Calabi-Yau 3-folds. However, it is also important to consider higher dimensional Calabi-Yau varieties including singular ones.

Batyrev and Dais, motivated by “physicists Hodge numbers”, introduced *string-theoretic Hodge numbers* [BD96] for a certain class of singular varieties. The string-theoretic Hodge numbers coincide with the “regular” ones for smooth varieties and with “regular” Hodge numbers of a crepant desingularization if it exists. Later Batyrev also introduced *stringy Hodge numbers* [Bat98] for a different class of singular varieties. While stringy and string-theoretic Hodge numbers are not the same, they do agree for the varieties we will be dealing with in this chapter, see [BM03] for further details on relations between

---

<sup>1</sup>A version of this chapter has been published [DN10].

them.

Batyrev and Borisov were able to obtain a formula for the generating function of string-theoretic Hodge numbers in the case of complete intersections in toric varieties and show that this function has properties corresponding to mirror symmetry [BB96a]. While their formula can be used in practice for computing Hodge numbers (as it is done in software PALP [KS04]), it is recursive, takes significant time even on computers, and does not provide much qualitative information on particular Hodge numbers.

Our work was motivated by the desire to obtain for the stringy Hodge numbers of complete intersections formulas similar to those for hypersurfaces. We were able to accomplish this goal in the case of two intersecting hypersurfaces, see Theorem 3.3.1 for arbitrary nef-partitions and Theorem 3.3.7 for the simplified expressions in the indecomposable case.

### 3.1 Generating Functions for Stringy Hodge Numbers

In this section we fix the notation and define the generating function for the stringy Hodge numbers of a complete intersection. The exposition is based on [BB96a, BN08], where one can also find further properties of the objects in question (the notation there is slightly different, as those authors work with faces of cones, not of supporting polytopes). Since our approach is mostly combinatorial, we will use the generating function to define the stringy Hodge numbers.

As before, let  $M$  and  $N$  be dual lattices of dimension  $n$ , let  $\Delta \subset M_{\mathbb{R}}$  be a reflexive polytope with polar  $\Delta^{\circ} \subset N_{\mathbb{R}}$ , let  $\Sigma$  be a projective crepant subdivision of  $\Sigma_{\Delta}$ , and let  $X_{\Sigma}$  be the associated toric variety. A nef-partition

$$V(\Delta^{\circ}) = V_0 \sqcup V_1 \sqcup \dots \sqcup V_{r-1}$$

determines Cayley polytope  $P$ , Cayley cone  $C$ , and dual Cayley polytope  $P^*$  as described in Section 2.3. It also determines a family of complete intersections  $Y \subset X_{\Sigma}$  (we take  $Y$  to be a generic member of this family).

As it was noted in Section 1.2, the face lattice of  $C$  is an Eulerian poset with the minimal element being the vertex at the origin and the maximal

element  $C$  itself. This poset is the same as the face lattice of  $P$ , with  $\emptyset$  and  $P$  representing the vertex of  $C$  and  $C$  itself respectively. The face lattice of  $C$  is also dual to the one of  $C^\vee$ , which in turn is the same as the face lattice of  $P^*$ . These relations allow us to define the dual face  $x^\vee$  of  $P^*$  for any face  $x$  of  $P$ .

It is more convenient for our purposes to use faces of polytopes rather than cones, but there is a dimension discrepancy between them. While for a cone it is natural to define the rank of a face in the face lattice to be its dimension, for a face  $x$  of a polytope we let  $\text{rk } x = \dim x + 1$  with the convention that  $\dim \emptyset = -1$ , so that  $\text{rk } \emptyset = 0$ .

**Definition 3.1.1.** Let  $\mathcal{P}$  be an Eulerian poset of rank  $d$  with the minimal element  $\hat{0}$  and the maximal one  $\hat{1}$ . If  $d = 0$ , let  $G_{\mathcal{P}} = H_{\mathcal{P}} = B_{\mathcal{P}} = 1$ . If  $d > 0$ , let polynomials  $G_{\mathcal{P}}, H_{\mathcal{P}}(t) \in \mathbb{Z}[t]$  and  $B_{\mathcal{P}}(u, v) \in \mathbb{Z}[u, v]$  be defined recursively by

$$H_{\mathcal{P}}(t) = \sum_{\hat{0} < x \leq \hat{1}} (t-1)^{\text{rk } x - 1} G_{[x, \hat{1}]}(t),$$

$$G_{\mathcal{P}}(t) = \tau_{< d/2}(1-t)H_{\mathcal{P}}(t),$$

where

$$\tau_{< d/2} \sum_{k=0}^{\infty} a_k t^k = \sum_{0 \leq m < d/2} a_k t^k$$

is the truncation operator, and

$$\sum_{\hat{0} \leq x \leq \hat{1}} B_{[\hat{0}, x]}(u, v) u^{d - \text{rk } x} G_{[x, \hat{1}]}(u^{-1}v) = G_{\mathcal{P}}(uv).$$

**Proposition 3.1.2.** *Let  $\mathcal{P}$  be an Eulerian poset of rank  $d$ . The polynomial  $B_{\mathcal{P}}$  has the following properties.*

- 1) *The degree of  $B_{\mathcal{P}}(u, v)$  in  $v$  is (strictly) less than  $d/2$ .*
- 2) *If  $d \leq 2$ , then  $B_{\mathcal{P}}(u, v) = (1-u)^d$ .*
- 3) *If  $\mathcal{P}$  is the face lattice of a polygon with  $k$  vertices (and  $k$  edges), then  $d = 3$  and  $B_{\mathcal{P}}(u, v) = 1 + [k - (k-3)v](u^2 - u) - u^3$ .*

*Proof.* See [BB96a], Examples 2.8, 2.9, and Proposition 2.10. □

**Definition 3.1.3.** Let  $F \subset M_{\mathbb{R}}$  be a  $d$ -dimensional lattice polytope (or a  $d$ -dimensional face of a lattice polytope). Let  $\ell(F) = |F \cap M|$  be the number of lattice points inside  $F$ . Let  $\ell^*(F)$  be the number of lattice points in the relative interior of  $F$ . (If  $F$  is a single point, then  $\ell(F) = \ell^*(F) = 1$ .) Define functions  $S_F$  and  $T_F$  by

$$S_F(t) = (1-t)^{d+1} \sum_{k=0}^{\infty} \ell(k \cdot F) t^k,$$

$$T_F(t) = (1-t)^{d+1} \sum_{k=1}^{\infty} \ell^*(k \cdot F) t^k.$$

We also set  $S_{\emptyset} = 1$ .

**Proposition 3.1.4.** *Let  $F \subset M_{\mathbb{R}}$  be a  $d$ -dimensional lattice polytope. The functions  $S_F$  and  $T_F$  have the following properties:*

- 1)  $S_F(t) = t^{d+1} T_F(t^{-1})$ .
- 2)  $S_F(t) = 1 + [\ell(F) - d - 1]t + \text{higher order terms}$ .
- 3)  $T_F(t) = \ell^*(F)t + [\ell^*(2 \cdot F) - (d+1)\ell^*(F)]t^2 + \text{higher order terms}$ .
- 4)  $S_F$  is a polynomial of degree at most  $d$ .
- 5)  $T_F$  is a polynomial of degree exactly  $d+1$ .
- 6)  $S_F$  has degree  $d-r+1$  and  $S_F(t) = t^{d-r+1} S_F(t^{-1})$  if and only if  $F$  is a Gorenstein polytope of index  $r$ .

*Proof.* For 1 see [BB96a], Proposition 3.6 and references therein. The next two properties are immediate from the definition. Then 4 and 5 follow from 1–3. For 6 see [BN08], Remark 2.15 and references therein.  $\square$

**Definition 3.1.5.** The **stringy  $E$ -function** of a Gorenstein polytope  $P$  of index  $r$  is

$$E_P(u, v) = \frac{1}{(uv)^r} \sum_{\emptyset \leq x \leq y \leq P} (-1)^{1+\dim x} u^{1+\dim y} S_x\left(\frac{v}{u}\right) S_{y^\vee}(uv) B_{[x,y]}(u^{-1}, v).$$

If  $P$  is the Cayley polytope of a nef-partition, the coefficients of the stringy  $E$ -function are the **stringy Hodge numbers** of the corresponding Calabi-Yau

variety  $Y$  up to a sign:

$$E_P(u, v) = \sum_{p, q} (-1)^{p+q} h_{st}^{p, q}(Y) u^p v^q.$$

*Remark 3.1.6.* The formula above is taken from [KRS03], the original one in [BB96a] is less convenient for actual computations since it includes infinite sums. A similar formula is also given in [BN08] (line 11 on page 57), but there is a typo — the posets of  $B$ -polynomials must be dualized.

*Remark 3.1.7.* It is not obvious from the expression for  $E_P$  that it is a polynomial of degree  $2(n - r)$ , although this is the case for Cayley polytopes. On the other hand, the definition of  $E_P$  makes sense for any  $(n + r - 1)$ -dimensional Gorenstein polytope of index  $r$  and it was conjectured that it is always such a polynomial in [BN08]. This claim was later proved in [NS10].

## 3.2 The Hypersurface Case

In this section we consider the situation  $n = 4$  and  $r = 1$ , i.e.  $Y$  is actually a hypersurface in  $X_\Sigma$ . In this case it is possible to completely resolve singularities of  $Y$  using crepant subdivisions of  $\Sigma$ . If we do it, then  $h_{st}^{p, q}(Y) = h^{p, q}(Y)$ . These Hodge numbers were computed without using the stringy  $E$ -function [Bat94] and it is not obvious a priori that extracting its coefficients will lead to the same expressions. We verify that this is indeed the case and, therefore, it is reasonable to expect that extracting coefficients of the stringy  $E$ -function for other  $n$  and  $r$  gives suitable generalizations of Batyrev's formulas for hypersurfaces.

**Theorem 3.2.1.** *Let  $\Delta$  be a reflexive polytope of dimension 4. Let  $Y$  be a generic anticanonical Calabi-Yau hypersurface in an MPCP-desingularization of  $X_\Delta$ . Then*

$$h^{1, 1}(Y) = \ell(\Delta) - 5 - \sum_{\dim y=0} \ell^*(y^\vee) + \sum_{\dim y=1} \ell^*(y) \ell^*(y^\vee), \quad (3.2.1)$$

where each sum runs over the faces of  $\Delta$  of the indicated dimension.

*Proof.* If we consider  $Y$  as a complete intersection, the number of parts in the nef-partition is  $r = 1$ , the Cayley polytope  $P \simeq \Delta$ , and the dual Cayley

polytope  $P^* \simeq \Delta^\circ$ .

For  $n = 4$  and  $r = 1$  the stringy  $E$ -function is given as

$$uvE_P(u, v) = \sum_{\emptyset \leq x \leq y \leq P} (-1)^{1+\dim x} u^{1+\dim y} S_x\left(\frac{v}{u}\right) S_{y^\vee}(uv) B_{[x,y]}(u^{-1}, v)$$

and  $h^{1,1}(Y) = h^{2,2}(Y)$  is equal to the coefficient of  $u^2v^2$  or  $u^3v^3$  on the right hand side. Below, extensively using Propositions 3.1.2 and 3.1.4 without further mention, we will determine the coefficient of  $u^3v^3$  in the term corresponding to each pair  $(x, y)$  on the right hand side. The reason for concentrating on a “high  $v$ -degree” term is that it allows us to deal only with simple  $B$ -polynomials corresponding to Eulerian posets of small rank, as we will see below. Note also that for the current case  $\dim y^\vee = 3 - \dim y$  and  $\text{rk}[\emptyset, P] = 5$ .

First of all, observe that terms with  $B$  depending on  $v$  do not contribute to the coefficient of  $u^3v^3$ . Indeed, if the  $v$ -degree of  $B$  is positive, then  $\text{rk}[x, y] \geq 3$  and we must have  $\dim x \leq 1$ ,  $\dim y \geq 2$ , i.e.  $\dim y^\vee \leq 1$ , and at least one of these inequalities is strict. Then either both  $S$ -polynomials are equal to 1 or one is equal to 1 and the other is linear. On the other hand,  $B_{[x,y]}(u^{-1}, v)$  could only have the  $v$ -degree 2 or more if  $\text{rk}[x, y] \geq 5$ , which is only possible for  $[x, y] = [\emptyset, P]$ , where both  $S$ -polynomials are equal to 1. Therefore, the product of all these polynomials does not contain a  $u^3v^3$  term.

Next we are going to consider cases with  $\text{rk}[x, y] \leq 2$  and either  $x = \emptyset$  or  $y = P$ . The reason for separating these cases from the rest is that the degree of  $S_\emptyset = S_{P^\vee} = 1$  is not bounded by  $\dim \emptyset = -1$ .

**Suppose  $x = \emptyset$  and  $\dim y \leq 1$ .** Then the corresponding term of the generating function is

$$u^{1+\dim y} S_{y^\vee}(uv)(1 - u^{-1})^{1+\dim y} = S_{y^\vee}(uv)(u - 1)^{1+\dim y},$$

where  $S_{y^\vee}$  is a polynomial of degree at most  $3 - \dim y$ . We see that the only possible cases are  $\dim y = -1$  and  $\dim y = 0$  with the contribution to  $u^3v^3$ -term determined by the third degree term in  $S_{y^\vee}$ . Using the symmetry property of the  $S$ -polynomial of the reflexive polytope  $P^*$ , we obtain contributions

$$\ell(P^*) - 5, \tag{3.2.2}$$

$$- \sum_{\dim y=0} \ell^*(y^\vee). \quad (3.2.3)$$

**Suppose**  $\dim x \geq 2$  **and**  $y = P$ . Then the corresponding term of the generating function is

$$(-1)^{1+\dim x} u^5 S_x \left( \frac{v}{u} \right) (1 - u^{-1})^{4-\dim x},$$

where  $S_x$  is a polynomial of degree at most  $\dim x$ , which must be 3 or 4 in order to have any term with  $v^3$ . In these cases the contribution is determined by the third degree term in  $S_x$ , however,  $\left(\frac{v}{u}\right)^3$  must be multiplied by  $u^6$  in order to get  $u^3 v^3$ , which is not possible. We see that there are no contributions to the  $u^3 v^3$ -term.

Now we consider remaining cases  $\text{rk}[x, y] = 0, 1, 2$ , with  $x \neq \emptyset$  and  $y \neq P$ .

**Suppose**  $x \neq \emptyset$ ,  $y \neq P$ , **and**  $x = y$ . Then the corresponding term of the generating function is

$$(-u)^{1+\dim y} S_y \left( \frac{v}{u} \right) S_{y^\vee}(uv),$$

where  $S_y$  and  $S_{y^\vee}$  are polynomials of degrees at most  $\dim y$  and  $3 - \dim y$ . In order to get  $v^3$ , we need to multiply the leading terms of these polynomials. The  $u$ -degree of the  $v^3$  term in the total product will be

$$(1 + \dim y) - \dim y + (3 - \dim y) = 4 - \dim y.$$

Since we are interested in terms with  $u^3$ , we must have  $\dim y = 1$ . The corresponding contribution is

$$\sum_{\dim y=1} \ell^*(y) \ell^*(y^\vee). \quad (3.2.4)$$

**Suppose**  $x \neq \emptyset$ ,  $y \neq P$ , **and**  $\dim y = 1 + \dim x$  **or**  $\dim y = 2 + \dim x$ . Then we see that there are no contributions to the  $u^3 v^3$ -term, since the total degree of the product of the  $S$ -polynomials is at most 2.

Now combining all of the above contributions we obtain (3.2.1), which completes the proof.  $\square$

*Remark 3.2.2.* The terms of (3.2.1) have the following algebro-geometric mean-

ing. Toric divisors of the ambient space, corresponding to all lattice points of  $\Delta^\circ$  except for the origin, have 4 linear relations between them. Divisors corresponding to the interior points of facets do not intersect a generic Calabi-Yau hypersurface  $Y$ , while divisors corresponding to the interior points of faces of codimension 2 may become reducible when intersected with  $Y$  and split into the number of components determined by the dual face.

**Corollary 3.2.3.** *Let  $\Delta$  be a reflexive polytope of dimension 4. Let  $Y$  be a generic anticanonical Calabi-Yau hypersurface in an MPCP-desingularization of  $X_\Delta$ . If  $h^{1,1}(Y) = 1$ , then  $\Delta$  is a simplex.*

*Proof.* This easily follows from (3.2.1), if we split  $\ell(\Delta^\circ)$  into the sum of internal points of all of its faces:

$$\begin{aligned} h^{1,1}(Y) &= \ell^*(\Delta^\circ) + \sum_{\dim y=0,1,2,3} \ell^*(y^\vee) - 5 - \sum_{\dim y=0} \ell^*(y^\vee) + \sum_{\dim y=1} \ell^*(y)\ell^*(y^\vee) \\ &= \sum_{\dim y=1,2} \ell^*(y^\vee) + \left[ \sum_{\dim y=3} \ell^*(y^\vee) - 4 \right] + \sum_{\dim y=1} \ell^*(y)\ell^*(y^\vee), \end{aligned}$$

where all sums are over faces of  $\Delta$  of indicated dimensions. Since faces dual to faces of dimension 3 are vertices of  $\Delta^\circ$ , we see that the term in brackets is positive while all others are non-negative, and if  $h^{1,1}(Y) = 1$ , then  $\Delta^\circ$  must have exactly 5 vertices, i.e. be a simplex. Then its polar  $\Delta$  also must be a simplex.  $\square$

As it was noted in Section 2.1, the number of reflexive polytopes of any fixed dimension is finite (up to  $GL(n, \mathbb{Z})$ -action) and there is an algorithm allowing one to construct all of them, but this number for dimension 5 and higher is so big, that it is practically impossible. Results similar to the above corollary may lead to algorithms for construction of all reflexive polytopes corresponding to Calabi-Yau varieties with small Hodge numbers.

### 3.3 The Bipartite Complete Intersection Case

In this section we derive closed form expressions for the stringy Hodge numbers  $h_{st}^{p,q}(Y)$ , where  $0 \leq p \leq n - 2$  and  $0 \leq q \leq 1$ , of an  $(n - 2)$ -dimensional Calabi-Yau complete intersection  $Y$  corresponding to a two-part nef-partition

of an  $n$ -dimensional reflexive polytope. (We actually look for  $h_{st}^{n-2-p, n-2-q}(Y)$ , since it is technically easier, but stringy Hodge numbers satisfy the Poincare duality, see Corollary 6.13 in [BD96].) While for irreducible nef-partitions  $h_{st}^{0,0}(Y) = h_{st}^{n-2,0}(Y) = 1$  and  $h_{st}^{p,0}(Y) = 0$  for  $1 \leq p \leq n-3$ , these expressions are still of interest for general Gorenstein polytopes. In addition, they may provide non-trivial relations between lattice point counts of faces of Cayley polytopes which do come from irreducible nef-partitions.

**Theorem 3.3.1.** *Let  $\Delta$  be a reflexive polytope of dimension  $n \geq 5$ . Let  $Y$  be a generic Calabi-Yau complete intersection in an MPCP-desingularization of  $X_\Delta$ , corresponding to a two-part nef-partition with Cayley polytope  $P$ . Then*

$$\begin{aligned}
h_{st}^{1,1}(Y) &= \ell(P^*) - n - 2 && - \sum_{\dim y=0} [\ell^*(2 \cdot y^\vee) - (n+1)\ell^*(y^\vee)] \\
&+ \sum_{\dim y=1} \ell^*(y^\vee) && + \sum_{\dim y=1} \ell^*(y) [\ell^*(2 \cdot y^\vee) - n\ell^*(y^\vee)] \\
&- \sum_{\dim y=2} [\ell(y) - \ell^*(y) - 3] \ell^*(y^\vee) && + \sum_{\dim y=3} [\ell^*(2 \cdot y) - 4\ell^*(y)] \ell^*(y^\vee) \\
&- \sum_{\substack{\dim x=2 \\ \dim y=3 \\ x < y}} \ell^*(x) \ell^*(y^\vee)
\end{aligned}$$

and for  $2 \leq p \leq n-4$  we have

$$\begin{aligned}
h_{st}^{p,1}(Y) &= \sum_{\dim y=p} \ell^*(y) [\ell^*(2 \cdot y^\vee) - (n-p+1)\ell^*(y^\vee)] \\
&+ \sum_{\dim y=p+2} [\ell^*(2 \cdot y) - (p+3)\ell^*(y)] \ell^*(y^\vee) \\
&- \sum_{\substack{\dim x=p \\ \dim y=p+1 \\ x < y}} \ell^*(x) \ell^*(y^\vee) - \sum_{\substack{\dim x=p+1 \\ \dim y=p+2 \\ x < y}} \ell^*(x) \ell^*(y^\vee),
\end{aligned}$$

where all sums run over faces of  $P$  of indicated dimensions. The expression for  $h_{st}^{n-3,1}(Y)$  is the same as for  $h_{st}^{1,1}(Y)$  with roles of  $P$  and  $P^*$  interchanged.

*Proof.* We have the following relation for the generating function:

$$(uv)^2 E_P(u, v) = \sum_{\emptyset \leq x \leq y \leq P} (-1)^{1+\dim x} u^{1+\dim y} S_x \left( \frac{v}{u} \right) S_{y^\vee}(uv) B_{[x,y]}(u^{-1}, v),$$

so  $h_{st}^{p,q}(Y)$  is equal (up to a sign) to the coefficient of  $u^{p+2}v^{q+2}$  in the right sum.

Our first step is to determine which of the terms in the sum may give contributions to monomials of the  $v$ -degree  $n - 1$  or higher. If  $[x, y] = [\emptyset, P]$ , then the  $v$ -degree is determined by the  $B$ -polynomial and it is less than  $n/2 + 1$  which is less than  $n - 1$ , since  $\text{rk}[\emptyset, P] = n + 2$  and  $n \geq 5$ . Now let  $\text{rk}[x, y] = d$  and note that  $\dim y^\vee = n - \dim y$ . If either  $x = \emptyset$  or  $y = P$ , the maximum possible  $v$ -degree of the corresponding term is less than  $n + 1 - d/2$ , so  $d$  can be at most 3. If both  $x$  and  $y$  are proper faces, then the maximum possible  $v$ -degree is less than  $n - d/2$  and  $d$  can be only 0 or 1. In [Table 3.1 on the following page](#) we list all terms of  $S_x(v/u)$ ,  $S_{y^\vee}(uv)$ , and  $B_{[x,y]}(u^{-1}, v)$  that can together give  $v^{n-1}$  or higher. We distribute  $u^{1+\dim y}$  in such a way that there are no negative powers and we use  $k(y)$  to denote the number of facets of  $y$ .

Now we can read off the coefficients of monomials with  $v^{n-1}$  or  $v^n$ . For  $h_{st}^{1,1}(Y) = h_{st}^{n-3, n-3}(Y)$  we need to take the coefficient of  $u^{n-1}v^{n-1}$ , which is

$$\begin{aligned}
h_{st}^{1,1}(Y) &= \ell(P^*) - n - 2 && - \sum_{\dim y=0} [\ell^*(2 \cdot y^\vee) - (n+1)\ell^*(y^\vee)] \\
&+ \sum_{\dim y=1} \ell^*(y^\vee) && - \sum_{\dim y=2} [k(y) - 3] \ell^*(y^\vee) \\
&+ \sum_{\dim y=1} \ell^*(y) [\ell^*(2 \cdot y^\vee) - n\ell^*(y^\vee)] && + \sum_{\dim y=3} [\ell^*(2 \cdot y) - 4\ell^*(y)] \ell^*(y^\vee) \\
&- \sum_{\substack{\dim x=1 \\ \dim y=2 \\ x < y}} \ell^*(x) \ell^*(y^\vee) && - \sum_{\substack{\dim x=2 \\ \dim y=3 \\ x < y}} \ell^*(x) \ell^*(y^\vee).
\end{aligned}$$

Observe that two sums with  $\dim y = 2$  can be naturally combined. For a fixed  $y$  the first sum contains the number of edges of  $y$ , which is the same as the number of vertices of  $y$ , while the second sum counts internal lattice points of all edges of  $y$ . Together these two sums count the number of boundary lattice points of  $y$  and their total contribution is

$$- \sum_{\dim y=2} [\ell(y) - \ell^*(y) - 3] \ell^*(y^\vee).$$

This leads us to the stated formula for  $h_{st}^{1,1}(Y)$ .

The expression for the ‘‘middle’’ stringy Hodge numbers follows from the table without any obvious simplifications.

$x$ and $y$	$\text{rk}[x, y]$	Terms of $(-u)^{1+\dim x} S_x(v/u)$	Terms of $S_{y^\vee}(uv)$	$u^{\text{rk}[x,y]} B_{[x,y]}(u^{-1}, v)$
$x = \emptyset$	0	1	$+[ \ell(P^*) - n - 2 ] (uv)^{n-1}$	1
	1		$+[ \ell^*(2y^\vee) - (n+1)\ell^*(y^\vee) ] (uv)^{n-1}$	$u - 1$
	2		$+[ \ell^*(2y^\vee) - n\ell^*(y^\vee) ] (uv)^{n-2}$	$u^2 - 2u + 1$
	3		$+[ \ell^*(2y^\vee) - (n-1)\ell^*(y^\vee) ] (uv)^{n-3}$	$u^3 - k(y)(u^2 - u) - 1$ $+ [k(y) - 3](u^2 - u)v$
$x \neq \emptyset,$ $\dim x = m,$ $y \neq P$	0	$(-1)^{m+1} \{ \ell^*(x) u v^m$ $+ [ \ell^*(2x) - (m+1)\ell^*(x) ] u^2 v^{m-1} \}$	$+[ \ell^*(2y^\vee) - (n-m+1)\ell^*(y^\vee) ] (uv)^{n-m-1}$	1
	1		$+[ \ell^*(2y^\vee) - (n-m)\ell^*(y^\vee) ] (uv)^{n-m-2}$	$u - 1$
	2		$+[ \ell^*(2y^\vee) - (n-m-1)\ell^*(y^\vee) ] (uv)^{n-m-3}$	$u^2 - 2u + 1$
	3		$+[ \ell^*(2y^\vee) - (n-m-2)\ell^*(y^\vee) ] (uv)^{n-m-4}$	$u^3 - k(y)(u^2 - u) - 1$ $+ [k(y) - 3](u^2 - u)v$
$y = P$	0	$(-1)^n \{ u^2 v^n$ $+ [ \ell(P) - n - 2 ] u^3 v^{n-1} \}$ $+[ \ell^*(2x) - (n+1)\ell^*(x) ] u^2 v^{n-1}$ $+ [ \ell^*(2x) - n\ell^*(x) ] u^2 v^{n-2}$ $+ [ \ell^*(2x) - (n-1)\ell^*(x) ] u^2 v^{n-3} \}$	1	1
	1			$u - 1$
	2			$u^2 - 2u + 1$
	3			$u^3 - k(y)(u^2 - u) - 1$ $+ [k(y) - 3](u^2 - u)v$

Table 3.1: Relevant terms of  $S$ - and  $B$ -polynomials

Finally, we know that  $h_{st}^{n-3,1}(Y) = h_{st}^{1,n-3}(Y)$  can be computed by dualizing the expression for  $h_{st}^{1,1}(Y)$  due to mirror-symmetric properties of the stringy  $E$ -function. One can also determine the coefficient of  $u^3v^{n-1}$  using the table — this way gives exactly the same expression.  $\square$

**Lemma 3.3.2.** *In the notation of Theorem 3.3.1, we have*

$$\begin{aligned} h_{st}^{0,0}(Y) &= 1 - \sum_{\dim y=0} \ell^*(y^\vee) + \sum_{\dim y=1} \ell^*(y)\ell^*(y^\vee), \\ h_{st}^{p,0}(Y) &= \sum_{\dim y=p+1} \ell^*(y)\ell^*(y^\vee), \quad \text{for } 1 \leq p \leq n-3, \\ h_{st}^{n-2,0}(Y) &= 1 - \sum_{\dim y=n} \ell^*(y) + \sum_{\dim y=n-1} \ell^*(y)\ell^*(y^\vee). \end{aligned}$$

*Proof.* Follows directly from Table 3.1 on the previous page using the same approach as in the proof of Theorem 3.3.1.  $\square$

**Corollary 3.3.3.** *In the notation of Theorem 3.3.1, the following relations hold, if the nef-partition is indecomposable:*

$$\sum_{\dim y=1} \ell^*(y)\ell^*(y^\vee) = \sum_{\dim y=0} \ell^*(y^\vee), \quad (3.3.1)$$

$$\sum_{\dim y=m} \ell^*(y)\ell^*(y^\vee) = 0, \quad \text{for } 2 \leq m \leq n-2, \quad (3.3.2)$$

$$\sum_{\dim y=n-1} \ell^*(y)\ell^*(y^\vee) = \sum_{\dim y=n} \ell^*(y). \quad (3.3.3)$$

*Proof.* Follows immediately from Lemma 3.3.2, since we know that  $h_{st}^{0,0}(Y) = 1 = h_{st}^{n-2,0}(Y)$  and  $h_{st}^{p,0}(Y) = 0$  for  $1 \leq p \leq n-3$ .  $\square$

Now we use this corollary to prove the following result.

**Lemma 3.3.4.** *Let  $\Delta$  be a reflexive polytope of dimension  $n \geq 5$ . Let  $P$  be the Cayley polytope of an indecomposable two part nef-partition of  $\Delta$ . Then  $\ell^*(y)\ell^*(y^\vee) = 0$  for any face  $y$  of  $P$ .*

*Proof.* First, let  $y$  be a vertex. Then  $\ell^*(y) = 1$  and we need to show that  $\ell^*(y^\vee) = 0$ . Note that  $y^\vee$  is an  $n$ -dimensional facet of  $P^*$ . Then either  $y^\vee$  is one of the polytopes  $\nabla_1$  or  $\nabla_2$  of the nef-partition and it does not have an interior point, since the nef-partition is indecomposable ([BN08], Corollary 6.12), or

$y^\vee$  has a non-empty intersection with both  $\nabla_1$  and  $\nabla_2$ . In the latter case consider the projection of  $N_{\mathbb{R}} \times \mathbb{R}^2 \supset P^*$  onto the second factor, which is a lattice morphism. Then the image of  $y^\vee$  is the line segment from  $(1, 0)$  to  $(0, 1)$ , which does not have interior lattice points. Therefore, in any case  $\ell^*(y^\vee) = 0$ , as desired.

Now that we know the result is true for  $m = 0$ , we conclude from (3.3.1) that it is true for  $m = 1$ . Then (3.3.2) and duality of  $P$  and  $P^*$  show that it is true for all  $m$ . (Including, obviously, non-proper faces as well.)  $\square$

**Lemma 3.3.5.** *In the notation of Theorem 3.3.1, we have<sup>2</sup>*

$$h_{st}^{0,1}(Y) = - \sum_{\dim y=2} [\ell(y) + 2\ell^*(y) - \ell^*(2 \cdot y) - 3] \ell^*(y^\vee).$$

*Proof.* Using again Table 3.1 on page 54, we get

$$\begin{aligned} -h_{st}^{0,1}(Y) &= \sum_{\dim y=0} [\ell^*(2 \cdot y^\vee) - (n+1)\ell^*(y^\vee)] - \sum_{\dim y=1} 2\ell^*(y^\vee) \\ &+ \sum_{\dim y=2} [k(y) - 3] \ell^*(y^\vee) - \sum_{\dim y=0} [\ell^*(2 \cdot y^\vee) - (n+1)\ell^*(y^\vee)] \\ &- \sum_{\dim y=2} [\ell^*(2 \cdot y) - 3\ell^*(y)] \ell^*(y^\vee) \\ &+ \sum_{\dim y=1} 2\ell^*(y^\vee) + \sum_{\substack{\dim x=1 \\ \dim y=2 \\ x < y}} \ell^*(x)\ell^*(y^\vee). \end{aligned}$$

Now cancelling the same terms and eliminating  $k(y)$  as it was done in the proof of Theorem 3.3.1 we obtain the stated result.  $\square$

**Corollary 3.3.6.** *In the notation of Theorem 3.3.1, the following relation holds, if the nef-partition is indecomposable:*

$$\sum_{\dim y=2} [\ell(y) - 3] \ell^*(y^\vee) = \sum_{\dim y=2} \ell^*(2 \cdot y)\ell^*(y^\vee).$$

*Proof.* Follows from Lemmas 3.3.4 and 3.3.5, since  $h_{st}^{0,1}(Y) = 0$ .

---

<sup>2</sup>There was a typo in the analogous formula for  $h^{3,2}(X)$  in Lemma 4.2 [DN10]: the coefficient of  $\ell^*(y)$  must be 2. Fortunately, this error did not propagate, for  $\ell^*(y)\ell^*(y^\vee)$  vanishes in the indecomposable case where this expression was used.

Alternatively, we can use Lemma 3.3.4 and Pick's formula. Indeed, let  $y$  be a face of  $P$  of dimension 2, such that  $\ell^*(y^\vee) \neq 0$ . Then  $\ell^*(y) = 0$ , the area of  $y$  is  $A(y) = \ell(y)/2 - 1$  and

$$A(2 \cdot y) = \ell^*(2 \cdot y) + \frac{\ell(2 \cdot y) - \ell^*(2 \cdot y)}{2} - 1 = 4A(y) = 2\ell(y) - 4,$$

but the number of boundary lattice points of  $2 \cdot y$  is  $2\ell(y)$ , thus  $\ell^*(2 \cdot y) = \ell(y) - 3$ .  $\square$

**Theorem 3.3.7.** *Let  $\Delta$  be a reflexive polytope of dimension  $n \geq 5$ . Let  $Y$  be a generic Calabi-Yau complete intersection in an MPCP-desingularization of  $X_\Delta$ , corresponding to a two-part indecomposable nef-partition with Cayley polytope  $P$ . Then*

$$\begin{aligned} h_{st}^{1,1}(Y) &= \ell(P^*) - n - 2 - \sum_{\dim y=0} \ell^*(2 \cdot y^\vee) + \sum_{\dim y=1} \ell^*(y^\vee) \\ &+ \sum_{\dim y=1} \ell^*(y)\ell^*(2 \cdot y^\vee) - \sum_{\dim y=2} \ell^*(2 \cdot y)\ell^*(y^\vee) \\ &+ \sum_{\dim y=3} \ell^*(2 \cdot y)\ell^*(y^\vee) - \sum_{\substack{\dim x=2 \\ \dim y=3 \\ x < y}} \ell^*(x)\ell^*(y^\vee) \end{aligned}$$

and for  $2 \leq p \leq n - 4$  we have

$$\begin{aligned} h_{st}^{p,1}(Y) &= \sum_{\dim y=p} \ell^*(y)\ell^*(2 \cdot y^\vee) + \sum_{\dim y=p+2} \ell^*(2 \cdot y)\ell^*(y^\vee) \\ &- \sum_{\substack{\dim x=p \\ \dim y=p+1 \\ x < y}} \ell^*(x)\ell^*(y^\vee) - \sum_{\substack{\dim x=p+1 \\ \dim y=p+2 \\ x < y}} \ell^*(x)\ell^*(y^\vee), \end{aligned}$$

where all sums run over faces of  $P$  of indicated dimensions. The expression for  $h_{st}^{n-3,1}(Y)$  is the same as for  $h_{st}^{1,1}(Y)$  with roles of  $P$  and  $P^*$  interchanged.

*Proof.* Follows from Theorem 3.3.1, Lemma 3.3.4, and Corollary 3.3.6.  $\square$

## 3.4 Examples

In this section we apply our results to compute Hodge numbers of several complete intersections corresponding to nef-partitions of five-dimensional poly-

topes. In this case MPCP-desingularizations actually completely resolve singularities of generic complete intersections and their Hodge numbers and stringy Hodge numbers coincide.

The reflexive polytopes considered here were selected from the data supplements to [KKRS05].<sup>3</sup> In each of the examples below we give the file name and the index of  $\Delta^\circ$  (starting with 0) in this database. We also explicitly give vertices of  $\Delta^\circ$  and their decomposition into a nef-partition. The expressions for Hodge numbers of the corresponding complete intersection are written as

$$h^{1,1}(Y) = s_0 + \cdots + s_6,$$

where  $s_0 = \ell(P^*) - 5 - 2$  and  $s_i$  for  $1 \leq i \leq 6$  is the  $i$ -th sum in the formula in Theorem 3.3.7. (In a few cases Hodge numbers do not coincide with the numbers in the file name. This is not an error, but an example of a reflexive polytope with several sets of Hodge numbers associated to its nef-partitions.)

First we give examples showing that for complete intersections there is no relation between conditions  $h^{1,1}(Y) = 1$  and “ $\Delta$  is a simplex”, i.e. an analogue of Corollary 3.2.3 is not obvious.

**Example 3.4.1** (0-th polytope from “H.1.25”, simplex,  $h^{1,1}(Y) = 1$ ). Let vertices of  $\Delta^\circ$  be given by columns of the matrix

$$\begin{pmatrix} -1 & 0 & 1 & 0 & 0 & 0 \\ -2 & 1 & 0 & 0 & 0 & 1 \\ -2 & 1 & 0 & 1 & 0 & 0 \\ -3 & 2 & 0 & 0 & 1 & 0 \\ -3 & 3 & 0 & 0 & 0 & 0 \end{pmatrix}$$

and consider the nef-partition with  $V_0 = \{0, 1, 3\}$  and  $V_1 = \{2, 4, 5\}$ . Then

$$\begin{aligned} h^{1,1}(Y) &= 1 - 0 + 0 + 0 - 0 + 0 - 0 = 1, \\ h^{2,1}(Y) &= 33 - 8 + 0 + 0 - 0 + 0 - 0 = 25. \end{aligned}$$

---

<sup>3</sup>Available at <http://hep.itp.tuwien.ac.at/~kreuzer/CY/hep-th/0410018.html>.

**Example 3.4.2** (1-st polytope from “H.1.37”, non-simplex,  $h^{1,1}(Y) = 1$ ). Let vertices of  $\Delta^\circ$  be given by columns of the matrix

$$\begin{pmatrix} 1 & 1 & -1 & 0 & 0 & 0 & 1 \\ 1 & -3 & 0 & 1 & 0 & 0 & 0 \\ 0 & -1 & 0 & 0 & 1 & 0 & 0 \\ 1 & -2 & 0 & 0 & 0 & 1 & 0 \\ 2 & -2 & 0 & 0 & 0 & 0 & 0 \end{pmatrix}$$

and consider the nef-partition with  $V_0 = \{0, 1, 4, 5\}$  and  $V_1 = \{2, 3, 6\}$ . Then

$$\begin{aligned} h^{1,1}(Y) &= 2 - 1 + 0 + 0 - 0 + 0 - 0 = 1, \\ h^{2,1}(Y) &= 47 - 14 + 0 + 5 - 1 + 0 - 0 = 37. \end{aligned}$$

**Example 3.4.3** (2-nd polytope from “H.1.73”, non-simplex,  $h^{1,1}(Y) \neq 1$ ). Let vertices of  $\Delta^\circ$  be given by columns of the matrix

$$\begin{pmatrix} 0 & 2 & -1 & 0 & 0 & 0 & 1 \\ 0 & -2 & 0 & 1 & 0 & 0 & 0 \\ 0 & -1 & 0 & 0 & 1 & 0 & 0 \\ 0 & -1 & 0 & 0 & 0 & 1 & 0 \\ 1 & -1 & 0 & 0 & 0 & 0 & 0 \end{pmatrix}$$

and consider the nef-partition with  $V_0 = \{0, 1, 2\}$  and  $V_1 = \{3, 4, 5, 6\}$ . Then

$$\begin{aligned} h^{1,1}(Y) &= 2 - 0 + 0 + 0 - 0 + 0 - 0 = 2, \\ h^{2,1}(Y) &= 107 - 35 + 0 + 0 - 0 + 0 - 0 = 72. \end{aligned}$$

**Example 3.4.4** (9-th polytope from “H.2.56”, simplex,  $h^{1,1}(Y) \neq 1$ ). Let vertices of  $\Delta^\circ$  be given by columns of the matrix

$$\begin{pmatrix} 0 & -2 & 1 & 0 & 0 & 0 \\ 1 & -3 & 0 & 0 & 0 & 1 \\ 0 & -1 & 0 & 1 & 0 & 0 \\ 0 & -1 & 0 & 0 & 1 & 0 \\ 2 & -2 & 0 & 0 & 0 & 0 \end{pmatrix}$$

and consider the nef-partition with  $V_0 = \{0, 1, 5\}$  and  $V_1 = \{2, 3, 4\}$ . Then

$$\begin{aligned} h^{1,1}(Y) &= 2 - 0 + 0 + 0 - 0 + 0 - 0 = 2, \\ h^{2,1}(Y) &= 61 - 18 + 0 + 13 - 0 + 0 - 0 = 56. \end{aligned}$$

In all of the examples above three terms were always zero:  $s_2$ ,  $s_5$ , and  $s_6$ . We give a few more examples showing that none of the terms in expressions for Hodge numbers for indecomposable nef-partitions vanishes identically, i.e. these expressions cannot be easily simplified further.

**Example 3.4.5** (1-st polytope from “H.1.73”). Let vertices of  $\Delta^\circ$  be given by columns of the matrix

$$\begin{pmatrix} 0 & -2 & 0 & 1 & 0 & 0 \\ 0 & -2 & 1 & 0 & 0 & 0 \\ 0 & -1 & 0 & 0 & 0 & 1 \\ 0 & -1 & 0 & 0 & 1 & 0 \\ 1 & -1 & 0 & 0 & 0 & 0 \end{pmatrix}$$

and consider the nef-partition with  $V_0 = \{0, 1, 2, 3\}$  and  $V_1 = \{4, 5\}$ . Then

$$\begin{aligned} h^{1,1}(Y) &= 1 - 0 + 0 + 0 - 0 + 0 - 0 = 1, \\ h^{2,1}(Y) &= 193 - 92 + 2 + 0 - 0 + 0 - 0 = 103. \end{aligned}$$

**Example 3.4.6** (0-th polytope from “H.6.20”). Let vertices of  $\Delta^\circ$  be given by columns of the matrix

$$\begin{pmatrix} 0 & -1 & 1 & 0 & 0 & 0 & -2 & 0 \\ 1 & -3 & 0 & 0 & 0 & -1 & 0 & 1 \\ 1 & -1 & 0 & 1 & 0 & 0 & -1 & 0 \\ 1 & -2 & 0 & 0 & 1 & 0 & 0 & 0 \\ 2 & -2 & 0 & 0 & 0 & 0 & 0 & 0 \end{pmatrix}$$

and consider the nef-partition with  $V_0 = \{0, 1, 5, 7\}$  and  $V_1 = \{2, 3, 4, 6\}$ . Then

$$\begin{aligned} h^{1,1}(Y) &= 4 - 2 + 0 + 0 - 0 + 7 - 3 = 6, \\ h^{2,1}(Y) &= 26 - 8 + 0 + 2 - 0 + 3 - 3 = 20. \end{aligned}$$

## 3.5 Relations with Other Results

It would be desirable to have a geometric interpretation for *each term* of the obtained expressions for stringy Hodge numbers and, in particular, to be able to identify the toric component of  $h_{st}^{1,1}(Y)$ , given by images of the torus-invariant divisors of the ambient space or, equivalently, the polynomial part of  $h_{st}^{n-3,1}(Y)$ , corresponding to polynomial deformations of the complete intersection in the ambient space. (In the hypersurface case this extra information follows “for free” from the proof of Batyrev’s formulas for the Hodge numbers.) While there is an algorithm for computing the toric part of the cohomology ring (see [BOKS07], for example), it does not give directly a “closed form” expression for its dimension. Also Borisov and Mavlyutov have constructed complete stringy cohomology spaces in [BM03] for semiample hypersurfaces in toric varieties and perhaps their techniques may be used in complete intersection case as well.

It would also be interesting to compare the result of Theorem 3.3.7 with the previously known formulas for Hodge numbers of complete intersections obtained by Batyrev and Borisov in [BB96b]. They have considered a special case when all divisors of the nef-partition in the non-resolved variety  $X_\Delta$  are ample. Doran and Morgan related formulas from [BB96b] to the mixed Hodge structure on the middle-dimensional cohomology of  $Y$  [DM07]. Our results could be useful for such applications, if we had a geometric interpretation for each term and identification of the toric contributions. Batyrev-Borisov formulas restricted to our case are given below, although we were not yet able to match all terms with ours.

**Definition 3.5.1.** A lattice polytope  $\Delta'$  is a Minkowski summand of another lattice polytope  $\Delta$  if there exist  $\mu \in \mathbb{Z}_{>0}$  and a lattice polytope  $\Delta''$  such that  $\mu\Delta = \Delta' + \Delta''$ .

If divisors  $E_i$  of a nef-partition are ample in  $X_\Delta$ , then  $\Delta$  is a Minkowski summand of  $\Delta_i$  for all  $i$ , all these polytopes are combinatorially equivalent, and each face  $\theta$  of  $\Delta$  decomposes into Minkowski sum  $\theta = \sum_i \theta_i$ , where  $\theta_i$  is a face of  $\Delta_i$  of the same dimension as  $\theta$ . In this case the nef-partition is necessarily irreducible and Theorem 3.3.7 is applicable, as well as the following result.

**Proposition 3.5.2.** *Let  $\Delta$  be a reflexive polytope of dimension  $n \geq 5$ . Let  $Y$  be a generic Calabi-Yau complete intersection in an MPCP-desingularization of  $X_\Delta$ , corresponding to a two-part nef-partition with ample divisors  $E_i$ . Then*

$$\begin{aligned}
h^{1,1}(Y) &= \ell(\Delta^\circ) - n - 1 - \sum_{\dim \theta=0} \ell^*(\theta^\vee) - \sum_{\dim \theta=1} \ell^*(\theta^\vee) \\
&\quad + \sum_{\dim \theta=2} [\ell^*(\theta) - \ell^*(\theta_0) - \ell^*(\theta_1)] \ell^*(\theta^\vee), \\
h^{p,1}(Y) &= \sum_{\dim \theta=p+1} [\ell^*(\theta) - \ell^*(\theta_0) - \ell^*(\theta_1)] \ell^*(\theta^\vee), \text{ for } 2 \leq p \leq n-4, \\
h^{n-3,1}(Y) &= [\ell^*(\Delta + \Delta_0) - \ell^*(2 \cdot \Delta_0) + \ell^*(\Delta + \Delta_1) - \ell^*(2 \cdot \Delta_1)] - n - 2 \\
&\quad - \sum_{\dim \theta=n-1} [\ell^*(\theta) - \ell^*(\theta_0) - \ell^*(\theta_1)] \\
&\quad + \sum_{\dim \theta=n-2} [\ell^*(\theta) - \ell^*(\theta_0) - \ell^*(\theta_1)] \ell^*(\theta^\vee),
\end{aligned}$$

where the sums are over faces of  $\Delta$  of indicated dimensions,  $\theta^\vee$  is the face of  $\Delta^\circ$  dual to  $\theta$ , and  $\theta = \theta_0 + \theta_1$  is the decomposition into Minkowski sum with  $\theta_i$  being a face of  $\Delta_i$ .

*Proof.* Follows from Corollary 8.4 in [BB96b], with the restriction to  $r = 2$ . Note that there was a typo in the expression for  $h^k(\Omega_V^1)$ : the sum should be taken over  $\dim \Theta = d - r - k$ , not  $d - r - k - 1$ . This is obvious if one compares this expression with the ‘‘corner’’ cases, since they include the same contribution with  $k = 1$  and  $k = d - r - 1$ . See also Corollary 8.5 in [BB96b], where all dimensions are correct.  $\square$

Our results presented in [DN10] have been recently used in [BJRR10], where the authors have observed some correspondence between their algorithm of computing Hodge numbers using line bundles and the following combinations of terms in the expression for  $h_{st}^{1,1}(Y)$  from Theorem 3.3.7 in the case  $n = 5$ :

$$\begin{aligned}
\mathfrak{h}_5^{1,1}(Y) &= \ell(P^*) - 7, \\
\mathfrak{h}_4^{1,1}(Y) &= - \sum_{\dim y=0} \ell^*(2 \cdot y^\vee) + \sum_{\dim y=1} \ell^*(y^\vee),
\end{aligned}$$

$$\begin{aligned} \mathfrak{h}_3^{1,1}(Y) &= \sum_{\dim y=1} \ell^*(y)\ell^*(2 \cdot y^\vee) - \sum_{\dim y=2} \ell^*(2 \cdot y)\ell^*(y^\vee), \\ \mathfrak{h}_2^{1,1}(Y) &= \sum_{\dim y=3} \ell^*(2 \cdot y)\ell^*(y^\vee) - \sum_{\substack{\dim x=2 \\ \dim y=3 \\ x < y}} \ell^*(x)\ell^*(y^\vee), \end{aligned}$$

see Equation (164) in [BJRR10]. These contributions  $\mathfrak{h}_i^{1,1}(Y)$  are described as

$$h^i(X; \mathcal{O}_X(m, n)) \rightsquigarrow \mathfrak{h}_i^{p,q}$$

in Equation (54) in [BJRR10]. Unfortunately, the authors of [BJRR10] do not explain exactly what do they mean by “contributions” and how the correspondence can be observed. As one can see from our examples in the previous section,  $\mathfrak{h}_4^{1,1}(Y) \leq 0$ , so it is not the dimension of any cohomology space. Of course, it can be such a dimension counted with negative sign. However,  $\mathfrak{h}_3^{1,1}(Y)$ -contributions may have different signs. In Example 3.4.6 it is positive for the dual nef-partition (since nef-partition duality exchanges  $h^{1,1}$  and  $h^{2,1}$ ), while in the following example it is negative (also for the dual nef-partition).

**Example 3.5.3** (4-th polytope from “H.1.101”). Let vertices of  $\Delta^\circ$  be given by columns of the matrix

$$\begin{pmatrix} 1 & 0 & 0 & 0 & 0 & 1 & -1 \\ 0 & 0 & 1 & 0 & 0 & 0 & -1 \\ 0 & 0 & 0 & 1 & 0 & 0 & -1 \\ 0 & 0 & 0 & 0 & 1 & 0 & -1 \\ -1 & 1 & 0 & 0 & 0 & 0 & 0 \end{pmatrix}$$

and consider the nef-partition with  $V_0 = \{0, 1, 5\}$  and  $V_1 = \{2, 3, 4, 6\}$ . Then

$$\begin{aligned} h^{1,1}(Y) &= 2 - 0 + 0 + 0 - 0 + 0 - 0 = 2, \\ h^{2,1}(Y) &= 130 - 43 + 0 + 0 - 1 + 0 - 0 = 86. \end{aligned}$$

Note that in this example terms without products of lattice point counts give an “overestimate” for  $h^{2,1}(Y)$ . Such examples prevented us from making a tempting conjecture that non-product terms correspond to the toric part of  $h^{1,1}(Y)$  and the polynomial part of  $h^{2,1}(Y)$ , as it is the case for hypersurfaces.

# Chapter 4

## Geometric Transitions Through Singular Subfamilies

In this chapter we present a detailed study of singularities of several subfamilies of Calabi-Yau threefolds realized either as anticanonical hypersurfaces or nef complete intersections in toric varieties. The considered subfamilies arose as potential representatives of the only class of variations of Hodge structure in Doran-Morgan classification [DM06] without known geometric realizations. In this analysis we rely on fibrations of the threefolds by polarized K3-surfaces, as these fibrations help us to establish a relation between the subfamilies.

### 4.1 Complete Intersection Model

In [DM06] Doran and Morgan have shown that there are 14 possible classes of variations of Hodge structure which can be associated to families of Calabi-Yau threefolds  $Y$  with  $h^{2,1} = 1$ . They have provided explicit examples for all but one of these classes and some suggestions on how one could construct an example for the last class. By analogy with other examples, one could hope to start with a complete intersection with  $h^{1,1} = 1$  in the weighted projective space  $\mathbb{WP}(1, 1, 1, 1, 4, 6)$ . Unfortunately, this ambient space is not Fano, so the Batyrev-Borisov mirror construction based on nef-partitions, described in Section 2.3, is not applicable to obtain a family with  $h^{2,1} = 1$ . Kreuzer and Sheidegger have suggested to work with a slightly different ambient space, a non-crepant blow-up of  $\mathbb{WP}(1, 1, 1, 1, 4, 6)$ , which is Fano and has a family of complete intersections corresponding to a suitable nef-partition, so the mirror

transition is possible. (See Section 8 and Appendix E.2 in [KKRS05] for some discussion of this example.) We construct and explore this mirror family below using Sage.<sup>1</sup>

Let  $\Delta \subset M_{\mathbb{R}}$  be a 5-dimensional reflexive polytope with its polar given by

```
sage: Delta5_polar = LatticePolytope([(1,-1,0,0,0), (-1,1,0,0,0),
(-1,-1,0,0,0), (-1,-1,2,0,0), (12,0,-1,-1,-1), (0,12,-1,-1,-1),
(0,0,-1,-1,-1), (0,0,11,-1,-1), (0,0,-1,2,-1), (0,0,-1,-1,1)])
```

i.e. vertices of  $\Delta^\circ$  are given by columns of the following matrix

$$\begin{pmatrix} 1 & -1 & -1 & -1 & 12 & 0 & 0 & 0 & 0 & 0 \\ -1 & 1 & -1 & -1 & 0 & 12 & 0 & 0 & 0 & 0 \\ 0 & 0 & 0 & 2 & -1 & -1 & -1 & 11 & -1 & -1 \\ 0 & 0 & 0 & 0 & -1 & -1 & -1 & -1 & 2 & -1 \\ 0 & 0 & 0 & 0 & -1 & -1 & -1 & -1 & -1 & 1 \end{pmatrix}. \quad (4.1.1)$$

The nef-partition we are interested in is “in agreement” with the block structure of this matrix: one part is formed by the first four vertices and the other by the last six.

```
sage: np = NefPartition([0]*4+[1]*6, Delta5_polar)
sage: np
Nef-partition {0, 1, 2, 3} U {4, 5, 6, 7, 8, 9}
```

Let  $\Sigma$  be a crepant subdivision of  $\Sigma_{\Delta}$  and  $X = X_{\Sigma}$  be the corresponding crepant partial resolution of  $X_{\Delta}$ . The choice of this resolution will depend on our needs, for the moment we only ensure that  $\Sigma$  is simplicial. We will use  $y_i$  as homogeneous coordinates on  $X$  with  $i$  being the index of the corresponding point of  $\Delta^\circ$ . For future use we introduce parameters  $c$ ,  $d$ , and  $e$  into the base field of  $X$ . Let  $Y \subset X$  be a generic member of the family of complete intersections corresponding to the nef-partition above.

```
sage: X5 = CPRFanoToricVariety(np.Delta(), make_simplicial=True,
coordinate_names="y+", base_field=QQ["c,d,e"].fraction_field())
sage: Y = X5.nef_complete_intersection(np)
```

<sup>1</sup>Computations shown in this section were performed using Sage 4.6.2 with several extra patches applied which are not yet included in the main code base. Therefore, these computations may not be reproducible in the current official releases of Sage, but all used patches will be submitted for inclusion in the near future and should become available shortly thereafter.

The defining polynomials of  $Y$  are<sup>2</sup>

$$g_0 = a_0 y_0^2 y_4^{12} + a_1 y_1^2 y_5^{12} + a_2 y_0 y_1 y_2 y_3, \quad (4.1.2)$$

$$g_1 = b_4 y_4^6 y_5^6 y_6^6 y_7^6 + b_5 y_4^4 y_5^4 y_6^4 y_7^4 y_8 + b_3 y_2^2 y_6^{12} + b_2 y_3^2 y_7^{12} \\ + b_7 y_4^3 y_5^3 y_6^3 y_7^3 y_9 + b_6 y_4^2 y_5^2 y_6^2 y_7^2 y_8^2 + b_8 y_4 y_5 y_6 y_7 y_8 y_9 + b_0 y_8^3 + b_1 y_9^2. \quad (4.1.3)$$

There are 12 parameters, but their number can be significantly reduced. First of all, we can set  $b_5 = b_6 = b_7 = 0$  using a change of variables. To see it easier, we switch to an affine chart.

```
sage: Yap = Y.affine_patch(3)
sage: g1 = Yap.defining_polynomials()[1]
```

In this chart  $g_1$  takes the form

$$g_1 = b_0 y_8^3 + b_3 y_2^2 + b_2 y_3^2 + b_6 y_8^2 + b_8 y_8 y_9 + b_1 y_9^2 + b_5 y_8 + b_7 y_9 + b_4$$

and making a substitution  $y_8 = y_8 + c$ ,  $y_9 = y_9 + d + e y_8$  does not lead to any new monomials.

```
sage: X5 = Y.ambient_space()
sage: X5.inject_coefficients();
sage: X5.inject_variables();
sage: g1s = g1.subs(y8=y8+c, y9=y9+d+e*y8)
sage: g1s.monomials()
[y8^3, y2^2, y3^2, y8^2, y8*y9, y9^2, y8, y9, 1]
sage: g1s.monomial_coefficient(y8^2)
e^2*b1 + 3*c*b0 + e*b8 + b6
sage: g1s.monomial_coefficient(y9)
2*d*b1 + c*b8 + b7
sage: g1s.monomial_coefficient(y8)
3*c^2*b0 + 2*d*e*b1 + c*e*b8 + 2*c*b6 + e*b7 + d*b8 + b5
```

We see that one can pick  $c$ ,  $d$ , and then  $e$  to make coefficients of these 3 monomials vanish, leaving only 9 parameters. Since we can also scale 2 polynomials

---

<sup>2</sup>Since we consider in this chapter “real life” examples rather than elementary ones as in [Chapter 1](#) and [Chapter 2](#), the command line output of Sage may take a lot of space and be hard to comprehend. Here  $g_i$  can be obtained as `Y.defining_polynomials()`, and that is exactly how they were obtained, but we present them in a typeset version (which can be used by default in Sage notebook interface).

and 5 variables, we can further reduce the number of parameters to 2. On the other hand, applying Theorem 3.3.7 to  $Y$ , we get

$$h_{st}^{1,1}(Y) = 754 - 557 + 46 + 0 - 0 + 0 - 0 = 243,$$

$$h_{st}^{2,1}(Y) = 5 - 3 + 0 + 0 - 0 + 1 - 0 = 3.$$

If we took  $X$  to be a MPCP-desingularization of  $X_\Delta$ ,  $Y$  would be generically smooth and stringy Hodge numbers would coincide with the regular ones, so the dimension of the space of complex deformations of  $Y$  is 3. Performed reduction of the number of parameters in defining polynomials of  $Y$  to 2 suggests that the dimension of the space of polynomial deformation of  $Y$  is  $h_{poly}^{2,1}(Y) = 2$ . To confirm this observation we compute the toric part of  $h_{st}^{1,1}(Y^\circ)$  for the Batyrev-Borisov mirror  $Y^\circ$  of  $Y$  inside a MPCP-desingularization  $X^\circ$  of  $X_\nabla$ . (It is easy to work with a maximal resolution in this case, since  $\nabla^\circ$  is much smaller than  $\Delta^\circ$ , i.e. it has only a few lattice points.)

```
sage: X5m = CPRFanoToricVariety(np.nabla(), make_simplicial=True,
    coordinate_points="all")
sage: X5m.is_smooth()
True
sage: Ym = X5m.nef_complete_intersection(np.dual(),
    monomial_points="vertices")
sage: H = Ym.ambient_space().cohomology_ring()
sage: H.gens()
([z5], [z5], [4*z5 + 2*z6 + z7 + z9], [6*z5 + 3*z6 + 2*z7 + z8 +
    z9], [z5], [z5], [z6], [z7], [z8], [z9])
```

Here we have restricted monomials used in the defining equations of  $Y^\circ$  to save some time, since nef divisors corresponding to it have hundreds of monomial sections and we need only its cohomology class. Note that  $X^\circ$  is smooth, so  $Y^\circ$  is (generically) smooth as well,  $h_{st}^{1,1}(Y^\circ) = h^{1,1}(Y^\circ)$  and to compute  $h_{tor}^{1,1}(Y^\circ)$ , the contribution of  $H^{1,1}(X^\circ)$  to  $H^{1,1}(Y^\circ)$ , we just need to consider intersections of the cohomology class of  $Y^\circ$  with generators of the cohomology ring of  $X^\circ$ . As it can be seen from the above output, this ring can be generated by the last five of “all generators”, each of which corresponds to a torus-invariant subvariety of codimension 1, e.g.  $[z5]$  corresponds to  $\{z_5 = 0\}$ , whose cohomology class is equivalent to  $\{z_0 = 0\}$ ,  $\{z_1 = 0\}$ , and  $\{z_4 = 0\}$ .

```

sage: Ym_c = Ym.cohomology_class()
sage: Ym_c
[24*z5^2 - 6*z6^2 + 8/3*z7*z8 - 2/3*z8^2 - 13*z6*z9 - 3/2*z9^2]
sage: [Ym_c * g for g in H.gens()[-5:]]
[[24*z5^3 + 3*z6^3 + 14/9*z7*z8^2 + 1/9*z8^3 + 19/2*z6^2*z9 +
  3/8*z9^3], [-z6^2*z9], [0], [0], [0]]

```

We conclude that  $h_{tor}^{1,1}(Y^\circ) = h_{poly}^{2,1}(Y) = 2$ .

As it was pointed out in [DM06], a certain subfamily of complete intersections  $Y$  corresponds to the desired hypergeometric series. To describe that subfamily precisely in our setting, we will compute the GKZ series of  $Y$  following the algorithm outlined in Section 5.5 of [CK99] and Appendix A of [KKRS05].

It is easy to check that monomials that can be eliminated in equations for  $Y$  correspond to all points of  $\Delta_i$  that are neither vertices of  $\Delta_i$  nor the origin. (This is true for our particular case, in general such information cannot be easily determined and one has to perform computations in the cohomology ring as above.) Let's use this information to reconstruct our varieties:

```

sage: X5 = CPRFanoToricVariety(np.Delta(), make_simplicial=True,
  coordinate_names="y+")
sage: Y = X5.nef_complete_intersection(np,
  monomial_points="vertices+origin")
sage: X5m = CPRFanoToricVariety(np.nabla())
sage: X5m.Mori_cone().rays()
((1, 1, 0, 0, 1, 1, -2, -2), (0, 0, 2, 3, 0, 0, 1, -6))

```

We now use the generators of the Mori cone of  $X^\circ$  to construct moduli parameters of  $Y$ . These generators are given as elements of the row span of the Gale transform of the fan of  $X^\circ$ , the  $i$ -th element of each generator corresponds to the  $i$ -th ray of this fan, except for the last one which corresponds to the origin and is equal to the negative sum of other entries. For complete intersections we need to take such sums for each part of the nef-partition separately. The following code adds them in a way compatible with the order of coefficients of  $Y$  in Sage with  $a_2$  and  $b_8$  corresponding to the origin (coefficient-monomial correspondence for the newly constructed  $Y$  is the same as in (4.1.2) and (4.1.3), since coefficient indices come from the internal enumeration of polytope lattice points).

```

sage: coefs = Y.ambient_space().base_ring().gens()
sage: coefs
(a0, a1, a2, b0, b1, b2, b3, b4, b8)
sage: degrees = [[[ray[i] for i in p] for p in np.dual().parts()]
for ray in X5m.Mori_cone()]
sage: degrees = [flatten([p + [-sum(p)] for p in degs]) for degs
in degrees]
sage: matrix(degrees)
[ 1  1 -2  0  0  1  1 -2  0]
[ 0  0  0  2  3  0  0  1 -6]
sage: B = [prod(c^d for c, d in zip(coefs, ds)) for ds in degrees]

```

The modular parameters of  $Y$  are

$$B_0 = \frac{a_0 a_1 b_2 b_3}{a_2^2 b_4^2}, \quad B_1 = \frac{b_0^2 b_1^3 b_4}{b_8^6},$$

and its GKZ series is

$$\sum_{m,n} \frac{(2m)!(6n)!}{(m!)^4 (2n)! (3n)! (n-2m)!} B_0^m B_1^n,$$

where the summation is over all integers  $m$  and  $n$  such that all arguments of factorials are non-negative. Making a substitution  $(n-2m) \rightarrow n$ , we can sum over all non-negative integers:

$$\sum_{m,n \in \mathbb{Z}_{\geq 0}} \frac{(2m)!(12m+6n)!}{(m!)^4 (4m+2n)! (6m+3n)! n!} B_0^m B_1^{2m+n}.$$

To simplify the description of  $Y$  further, we now scale its defining polynomials and coordinates to set all coefficients to 1 except for  $b_3 = \xi_0$  and  $b_4 = \xi_1$ .

```

sage: Y = X5.nef_complete_intersection(np, monomial_points=
"vertices+origin", coefficients=[[1,1,1],[1,1,1,"xi0","xi1",1]])

```

Now defining polynomials of  $Y$  are

$$g_0 = y_0^2 y_4^{12} + y_1^2 y_5^{12} + y_0 y_1 y_2 y_3, \quad (4.1.4)$$

$$g_1 = \xi_1 y_4^6 y_5^6 y_6^6 y_7^6 + \xi_0 y_2^2 y_6^{12} + y_3^2 y_7^{12} + y_4 y_5 y_6 y_7 y_8 y_9 + y_8^3 + y_9^2, \quad (4.1.5)$$

and the GKZ series takes the form

$$\sum_{m,n \in \mathbb{Z}_{\geq 0}} \frac{(2m)!(12m+6n)!}{(m!)^4(4m+2n)!(6m+3n)!n!} \xi_0^m \xi_1^n.$$

Comparing this series with the one given in the end of [DM06], we see that the subfamily of interest is  $\xi_1 = 0$ , leading to the series

$$\sum_{m \in \mathbb{Z}_{\geq 0}} \frac{(2m)!(12m)!}{(m!)^4(4m)!(6m)!} \xi_0^m.$$

We will come back to this subfamily in [Section 4.7](#).

Going back to the definition of  $\Delta^\circ$  in (4.1.1), we observe that in addition to its column decomposition into a nef-partition it has a “natural” row decomposition. Indeed, the projection onto the first two coordinates corresponds to a toric fibration  $\tilde{\alpha} : X \rightarrow B$  over a 2-dimensional toric variety  $B$ , as long as we pick a compatible resolution of  $X_\Delta$ . To get such a resolution, we start with the face fan of  $\Delta^\circ$ , take its minimal subdivision compatible with the projection, and then subdivide it to get a simplicial fan, so that  $X$  is an orbifold.

```
sage: m = matrix([(1,0), (0,1)] + [(0,0)]*3)
sage: Delta2_polar = LatticePolytope([(1,-1), (-1,1), (-1,-1),
(1,0), (0,1)])
sage: B2 = CPRFanoToricVariety(Delta_polar=Delta2_polar,
coordinate_names="u+")
sage: Sigma5 = FaceFan(Delta5_polar)
sage: Sigma5.nrays(), Sigma5.ngenerating_cones()
(10, 14)
sage: Sigma5 = FanMorphism(m, Sigma5, B2.fan(),
subdivide=True).domain_fan()
sage: Sigma5.nrays(), Sigma5.ngenerating_cones()
(10, 22)
sage: X5 = CPRFanoToricVariety(np.Delta(),
charts=[C.ambient_ray_indices() for C in Sigma5],
coordinate_names="y+", make_simplicial=True, check=False)
sage: alpha = FanMorphism(m, X5.fan(), B2.fan())
sage: alpha.is_fibration()
True
```

The command reconstructing X5 may look a little strange: at the moment Sage does not support constructing CPR-Fano toric varieties directly from a given fan, so we extracted the information about generating cones from the fan to explicitly specify `charts`. In this form the variety constructor performs compatibility checks and they may take quite a while, but we suppressed them via `check=False` option, since we know for sure that our input defines a crepant subdivision of  $\Sigma_\Delta$ .

In homogeneous coordinates

$$\tilde{\alpha} : [y_0 : \cdots : y_9] \mapsto [u_0 : \cdots : u_4] = [y_0 : y_1 : y_2 y_3 : y_4^{12} : y_5^{12}] .$$

Note that the hypersurface defined by the polynomial  $g_0$  in (4.1.4) depends only on the variables involved in the projection map. This means that we can interpret  $g_0 = 0$  as a defining equation of a *curve*  $C = \tilde{\alpha}(\{g_0 = 0\}) \subset B$  and  $g_1 = 0$  as a defining equation of a *surface* in each fiber of  $\tilde{\alpha}$ , in other words,  $\tilde{\alpha}$  induces a fibration of the complete intersection  $Y$  over  $C$ .

Generic fibers of  $\tilde{\alpha} : X \rightarrow B$  correspond to the fan whose rays are generated by the last four vertices of  $\Delta^\circ$ . The polytope spanned by these vertices is the last (the 4318-th) 3-dimensional reflexive polytope in the Kreuzer-Skarke list (included in Sage), with its normal fan corresponding to  $\mathbb{WP}(1, 1, 4, 6)$ :

```
sage: Sigma_0 = alpha.kernel_fan()
sage: vertices = Sigma_0.ray_matrix().matrix_from_rows([2,3,4])
sage: p = LatticePolytope(vertices)
sage: p.is_reflexive()
True
sage: p.index()
4318
sage: NormalFan(p).rays()
(N(1, 0, 0), N(0, 1, 0), N(0, 0, 1), N(-1, -4, -6))
```

## 4.2 Anticanonical Hypersurface Model

In the previous section we were able to represent the complete intersection  $Y$  as a fibration over a curve with fibers living in the space polar to  $\mathbb{WP}(1, 1, 4, 6)$ . This suggests that we can also look for a family realized as anticanonical

hypersurfaces in a four-dimensional space which can be fibered by the same toric varieties. We have searched for Fano varieties fibered by  $\mathbb{WP}(1, 1, 4, 6)$  among those whose anticanonical hypersurfaces have small  $h^{1,1}$  and with an extra condition that the torically induced fibration is “balanced” in the sense that the same 3-dimensional reflexive polytopes can play roles of both slices and projections, as it was described in [Section 2.4](#). The weighted projective space  $\mathbb{WP}(1, 1, 2, 8, 12)$  satisfies these requirements and below we consider the family of anticanonical hypersurfaces in its polar.

Let  $\Delta \subset M_{\mathbb{R}}$  be a 4-dimensional reflexive polytope given by

```
sage: Delta4 = LatticePolytope([(1,0,0,0), (0,1,0,0), (0,0,1,0),
(0,0,0,1), (-1,-2,-8,-12)])
```

i.e. vertices of  $\Delta$  and vertices of  $\Delta^\circ \subset N_{\mathbb{R}}$  are given by columns of the following matrices

$$\begin{pmatrix} 1 & 0 & 0 & 0 & -1 \\ 0 & 1 & 0 & 0 & -2 \\ 0 & 0 & 1 & 0 & -8 \\ 0 & 0 & 0 & 1 & -12 \end{pmatrix}, \quad \begin{pmatrix} 23 & -1 & -1 & -1 & -1 \\ -1 & -1 & 11 & -1 & -1 \\ -1 & 2 & -1 & -1 & -1 \\ -1 & -1 & -1 & -1 & 1 \end{pmatrix}.$$

Let  $\Sigma$  be a crepant subdivision of  $\Sigma_{\Delta}$  and  $X = X_{\Sigma}$  be the corresponding crepant partial resolution of  $X_{\Delta}$ . As before, the choice of this resolution will depend on our needs, for now we add only one extra ray in addition to the vertices of  $\Delta^\circ$ , namely the ray corresponding to the midpoint  $(11, -1, -1, -1)$  between the 0-th and the 3-rd vertices, which is the 16-th point in the internal enumeration in Sage:

```
sage: Delta4.polar().point(16)
(11, -1, -1, -1)
sage: X4 = CPRFanoToricVariety(Delta=Delta4,
coordinate_points=range(5)+[16])
sage: B1 = toric_varieties.P1("s,t")
sage: beta = FanMorphism(matrix([1,1,4,6]), X4.fan(), B1.fan())
sage: beta.is_fibration()
True
```

This extra ray is necessary to make  $\Sigma$  compatible with the projection onto the line in the direction  $(1, 1, 4, 6)$ . If  $B = \mathbb{P}^1$  with coordinates  $[s : t]$  corresponding

to the (unique) complete fan on this line and  $\tilde{\beta} : X \rightarrow B$  is the toric morphism associated to this projection, then

$$\tilde{\beta} : [z_0 : z_1 : z_2 : z_3 : z_4 : z_{16}] \mapsto [s : t] = [z_0^{12} : z_3^{12}]. \quad (4.2.1)$$

Let  $Z \subset X$  be a generic anticanonical hypersurface. Its defining polynomial is

$$\begin{aligned} h = & a_0 z_0^{24} z_{16}^{12} + a_5 z_0^{12} z_3^{12} z_{16}^{12} + a_4 z_3^{24} z_{16}^{12} + a_6 z_0^6 z_2^6 z_3^6 z_{16}^6 \\ & + a_1 z_2^{12} + a_{10} z_0 z_1 z_2 z_3 z_4 z_{16} + a_2 z_1^3 + a_3 z_4^2. \end{aligned}$$

Scaling the whole polynomial and four independent coordinates we can eliminate 5 out of 8 parameters. Using Batyrev's formulas for the Hodge numbers of anticanonical hypersurfaces, we check that  $h^{2,1}(Z) = h_{poly}^{2,1}(Z) = 3$ , so we should indeed have 3 independent parameters.

Anticanonical hypersurfaces inside the space polar to  $\mathbb{WP}(1, 1, 2, 8, 12)$  were extensively studied in [BDF<sup>+</sup>98] and in order to conveniently use their results we will match our toric description with theirs. (They have considered hypersurfaces in  $\mathbb{WP}(1, 1, 2, 8, 12)$  with extra symmetries, which allow taking the quotient under a certain group action. This is similar to the polar projective plane being  $\mathbb{P}^2/\mathbb{Z}_3$ , as it was shown in Section 2.1.)

First, we rewrite the polynomial of  $Z$  in its "fibered" form, thinking of it as a polynomial in  $z_1, z_2, z_4, z_{16}$  only and working in a chart with  $t = z_3 = 1$ :

$$[a_0 s^2 + a_5 s + a_4] z_{16}^{12} + [a_6 z_0^6] z_2^6 z_{16}^6 + a_1 z_2^{12} + [a_{10} z_0] z_1 z_2 z_4 z_{16} + a_2 z_1^3 + a_3 z_4^2.$$

Now we can compare our representation with (4.19) in [BDF<sup>+</sup>98]:

$$W^{(2)}(x; B', \psi_0, \psi_1) = \frac{1}{12}(B' x_0^{12} + x_3^{12}) + \frac{1}{3}x_4^3 + \frac{1}{2}x_5^2 - \psi_0 x_0 x_3 x_4 x_5 - \frac{1}{6}\psi_1 x_0^6 x_3^6.$$

We see that the matching of coordinates and coefficients is

$$\begin{aligned} z_1 &= x_4, & z_2 &= x_3, & z_4 &= x_5, & z_0 z_{16} &= x_0, \\ a_1 &= \frac{1}{12}, & a_2 &= \frac{1}{3}, & a_3 &= \frac{1}{2}, & a_6 &= -\frac{1}{6}\psi_1, & a_{10} &= -\psi_0, \end{aligned}$$

and

$$a_0s + \frac{a_4}{s} + a_5 = \frac{1}{12}B'.$$

To match these remaining parameters we use the definition of  $B'$  given in (3.18)[BDF+98]:

$$B' = \frac{1}{2} \left( B\zeta + \frac{B}{\zeta} - 2\psi_s \right),$$

where  $\zeta$  is an affine coordinate on the base of the fibration, so

$$s = \zeta, \quad a_0 = \frac{B}{24}, \quad a_4 = \frac{B}{24}, \quad a_5 = -\frac{\psi_s}{12}.$$

We can use these parameters in Sage as follows:

```
sage: var("B,psi0,psi1,psi_s");
sage: Z = X4.anticanonical_hypersurface(
coefficients=[B/24,1/12,1/3,1/2,B/24,-psi_s/12,-psi1/6,-psi0])
```

Now the defining polynomial of  $Z$  has the form

$$\begin{aligned} \frac{B}{24}z_0^{24}z_{16}^{12} - \frac{\psi_s}{12}z_0^{12}z_3^{12}z_{16}^{12} + \frac{B}{24}z_3^{24}z_{16}^{12} - \frac{\psi_1}{6}z_0^6z_2^6z_3^6z_{16}^6 \\ + \frac{1}{12}z_2^{12} - \psi_0z_0z_1z_2z_3z_4z_{16} + \frac{1}{3}z_1^3 + \frac{1}{2}z_4^2. \end{aligned}$$

One of the four parameters in this representation is redundant, e.g. we can set  $\psi_0 = 1$ .

### 4.3 Geometric Transitions

Both complete intersections and anticanonical hypersurfaces presented above have  $h^{2,1} = 3$ , while the original goal in their construction was to obtain families with  $h^{2,1} = 1$ . In fact, in the hypersurface case it was known in advance that we will “fail”, since it is known that there are only 5 reflexive polytopes yielding Calabi-Yau threefolds with  $h^{2,1} = 1$  and it was shown in [DM06] that they provide examples for other classes of Hodge structure variations.

However, we still can try to obtain desired families using subfamilies of

the constructed ones. Of course, just fixing some of the parameters does not change the Hodge numbers of the Calabi-Yau threefolds in question, but if these threefolds become singular, we may try to resolve the singularities and for the resolved family it is possible to have  $h^{2,1} = 1$ . So what we are looking for now are geometric transitions from the already constructed families to some new ones with, hopefully, “correct” Hodge numbers. We now give a precise definition and basic classification of geometric transitions following [Ros10].

**Definition 4.3.1.** Let  $Y$  and  $\tilde{Y}$  be smooth Calabi-Yau threefolds. They are connected by a **geometric transition** if there exist a normal variety  $\bar{Y}$ , a birational contraction  $\varphi : Y \rightarrow \bar{Y}$ , and a complex deformation (smoothing) of  $\bar{Y}$  to  $\tilde{Y}$ . It is a **primitive geometric transition** if  $\varphi$  cannot be factored into birational morphisms of normal varieties. It is a **conifold transition** if  $\bar{Y}$  has only conifold singularities (ordinary double points). It is a **trivial geometric transition** if  $\tilde{Y}$  is a deformation of  $Y$ .

**Theorem 4.3.2.** *Let  $\varphi : Y \rightarrow \bar{Y}$  be a primitive contraction of a smooth Calabi-Yau threefold  $Y$  to a normal variety  $\bar{Y}$ . Let  $E$  be the exceptional locus of  $\varphi$ . Then  $\varphi$  is of one of the following three types:*

***type I**  $\varphi$  is small,  $E$  may be reducible and is composed of finitely many rational curves;*

***type II**  $\varphi$  contracts a divisor to a point,  $E$  is irreducible and is a generalized del Pezzo surface;*

***type III**  $\varphi$  contracts a divisor to a smooth curve  $C$ ,  $E$  is irreducible and is a conic bundle over  $C$ .*

*Proof.* See [Wil92, Wil93], the given formulation is Theorem 1.9 in [Ros10].  $\square$

**Definition 4.3.3.** A primitive geometric transition is of type I, II, or III, if the corresponding birational contraction is of type I, II, or III, respectively.

It turns out, that our models are connected via a type III geometric transition. To see it explicitly, we first compare their fibration structures.

## 4.4 K3 Fibrations

Generic fibers of the fibrations induced by  $\tilde{\alpha}$  and  $\tilde{\beta}$  constructed earlier are anticanonical (“hyper”)surfaces inside the three-dimensional space polar to  $\mathbb{WP}(1, 1, 4, 6)$ , i.e. they are generically two-dimensional Calabi-Yau varieties — K3 surfaces. The choice of the toric ambient space for them induces a lattice polarization, in this case by the lattice  $M = H \oplus E_8 \oplus E_8$ , where  $H$  is the hyperbolic lattice of rank 2 and  $E_8$  is the unique even negative-definite unimodular lattice of rank 8. Such  $M$ -polarized K3 surfaces (the name “ $M$ -polarized” is a bit unfortunate in the toric context, but it should not cause too much confusion) were studied in [CD07] and [CDLW09], we start this section with some basic facts about them.

**Definition 4.4.1.** An  $M$ -polarization on a K3 surface  $X$  is a primitive lattice embedding  $i : M \hookrightarrow \text{NS}(X)$ , such that the image  $i(M)$  in the Néron-Severi lattice  $\text{NS}(X)$  contains a pseudo-ample class (corresponding to an effective nef divisor with positive self-intersection).

**Theorem 4.4.2.** *Let  $X$  be an  $M$ -polarized K3 surface. Then*

- 1)  $X$  is isomorphic to the minimal resolution of a quartic surface in  $\mathbb{P}^3$  given by

$$y^2zw - 4x^3z + 3axzw^2 + b zw^3 - \frac{1}{2}(dz^2w^2 + w^4) = 0;$$

- 2) parameters  $a$ ,  $b$ , and  $d$  in the above equation specify a unique point  $(a, b, d) \in \mathbb{WP}(2, 3, 6)$  with  $d \neq 0$ ;
- 3)  $X$  canonically corresponds to a pair of elliptic curves  $\{E_1, E_2\}$ ;
- 4) modular parameters of  $X$  and  $\{E_1, E_2\}$  are related by

$$\pi = j(E_1)j(E_2) = \frac{a^3}{d} \quad \text{and} \quad \sigma = j(E_1) + j(E_2) = \frac{a^3 - b^2 + d}{d};$$

- 5) there are exactly two isomorphism classes of elliptic fibrations with sections on  $X$ .

*Proof.* See Theorem 1.1, Corollary 1.3, and Section 3 in [CD07] and Theorems 3.1 and 3.2 in [CDLW09]. □

**Proposition 4.4.3.** *An anticanonical hypersurface in the space polar to the weighted projective  $\mathbb{WP}(1, 1, 4, 6)$  is an  $M$ -polarized  $K3$  surface defined by*

$$\lambda_0 x_0^{12} + \lambda_4 x_0^6 x_1^6 + \lambda_1 x_1^{12} + \lambda_5 x_0 x_3 x_1 x_2 + \lambda_3 x_3^3 + \lambda_2 x_2^2 = 0.$$

*It is related to the normal form given in Theorem 4.4.2 by*

$$a^3 = \frac{1}{12^6 \Lambda_0^2 \Lambda_1}, \quad b^2 = \frac{(6 \cdot 12^2 \Lambda_0 - 1)^2}{12^6 \Lambda_0^2 \Lambda_1}, \quad \text{where } \Lambda_0 = \frac{\lambda_2^3 \lambda_3^2 \lambda_4}{\lambda_5^6}, \quad \Lambda_1 = \frac{\lambda_0 \lambda_1}{\lambda_4^2}.$$

*Proof.* See Section 3.4 in [CDLW09]<sup>3</sup>. □

For the complete intersection model  $Y$  described in Section 4.1 the role of  $[x_0 : x_1 : x_2 : x_3]$  in Proposition 4.4.3 is played by  $[y_6 : y_7 : y_9 : y_8]$  and we obtain the following expressions for modular parameters of a fiber:

$$\pi_Y = \frac{y_4^{12} y_5^{12}}{12^6 \xi_0 y_2^2 y_3^2}, \quad \sigma_Y = 1 + (\xi_1 - 3 \cdot 12^2 \xi_1^2) \frac{y_4^{12} y_5^{12}}{12^3 \xi_0 y_2^2 y_3^2}.$$

For the anticanonical hypersurface model  $Z$  from Section 4.2  $[x_0 : x_1 : x_2 : x_3]$  correspond to  $[z_{16} : z_2 : z_4 : z_1]$  and we compute

$$\pi_Z = \frac{\psi_0^{12}}{2} \cdot \frac{z_0^{12} z_3^{12}}{B z_0^{24} - 2 \psi_s z_0^{12} z_3^{12} + B z_3^{24}},$$

$$\sigma_Z = 1 - 2(\psi_0^6 \psi_1 + \psi_1^2) \frac{z_0^{12} z_3^{12}}{B z_0^{24} - 2 \psi_s z_0^{12} z_3^{12} + B z_3^{24}}.$$

Next we switch to coordinates on bases  $B^2$  and  $B^1$  of fibrations  $\tilde{\alpha}$  and  $\tilde{\beta}$  respectively:<sup>4</sup>

$$\pi_Y = \frac{u_3 u_4}{12^6 \xi_0 u_2^2},$$

$$\sigma_Y = 1 + (\xi_1 - 3 \cdot 12^2 \xi_1^2) \frac{u_3 u_4}{12^3 \xi_0 u_2^2},$$

---

<sup>3</sup>There was a typo in the preprint version of [CDLW09] posted on arXiv: the numerator of the expression for  $b^2$  was not squared.

<sup>4</sup>We have used the same notation  $\Delta$ ,  $\Sigma$ ,  $X$ , and  $B$  in Section 4.1 and Section 4.2 to refer to different objects. When we need to consider them together and it is necessary to distinguish them, we will use their dimensions as superscripts. Names in Sage examples always include these dimensions to allow reusing of objects in later sections.

$$\pi_Z = \frac{\psi_0^{12}}{2} \cdot \frac{st}{Bs^2 - 2\psi_s st + Bt^2}, \quad (4.4.1)$$

$$\sigma_Z = 1 - 2(\psi_0^6 \psi_1 + \psi_1^2) \frac{st}{Bs^2 - 2\psi_s st + Bt^2}. \quad (4.4.2)$$

Finally, recall that  $Y$  is fibered not over  $B^2$ , but over a curve  $C \subset B^2$  corresponding to  $g_0$ . It is easy to see from (4.1.4), that  $g_0$  is the pullback of

$$u_0^2 u_3 + u_1^2 u_4 + u_0 u_1 u_2. \quad (4.4.3)$$

Using the fan of  $B^2$ , shown in Figure 4.1, we can see that  $C$  does not intersect divisors corresponding to  $u_0$  and  $u_1$ , e.g. if  $u_0 = 0$ , then  $u_1^2 u_4 \neq 0$  since there are no cones containing rays corresponding to  $u_0$  and  $u_1$  or  $u_4$ . This means that

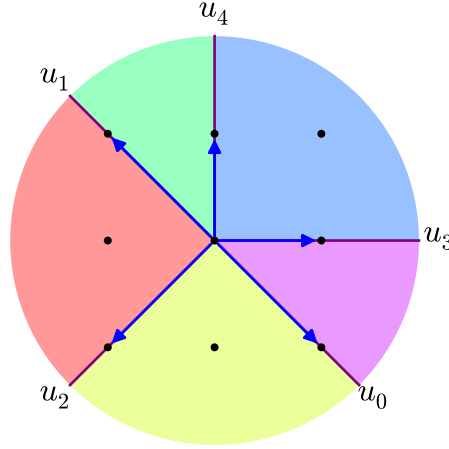


Figure 4.1: Base  $B^2$  of the fibration  $\tilde{\alpha}$

$C$  is isomorphic to the curve in  $\mathbb{P}^2$  with coordinates  $[u : v : w] = [u_3 : u_4 : u_2]$ , given by  $u + v + w = 0$ , i.e.  $C \simeq \mathbb{P}^1$  with coordinates  $[u : v]$ . In terms of these coordinates the modular parameters of a fiber are

$$\pi_Y = \frac{1}{12^6 \xi_0} \cdot \frac{uv}{(u+v)^2}, \quad (4.4.4)$$

$$\sigma_Y = 1 + \frac{\xi_1 - 3 \cdot 12^2 \xi_1^2}{12^3 \xi_0} \cdot \frac{uv}{(u+v)^2}. \quad (4.4.5)$$

Comparing expressions for  $\pi$  and  $\sigma$  for the complete intersection model, (4.4.4) and (4.4.5), with analogous expressions for the anticanonical hypersurface model, (4.4.1) and (4.4.2), we see that they are quite similar and this

similarity would be even more striking if we let  $\psi_s = -B$ :

$$\pi_Z = \frac{\psi_0^{12}}{2B} \cdot \frac{st}{(s+t)^2}, \quad (4.4.6)$$

$$\sigma_Z = 1 - \frac{2(\psi_0^6\psi_1 + \psi_1^2)}{B} \cdot \frac{st}{(s+t)^2}. \quad (4.4.7)$$

In fact, expressions (4.4.4) and (4.4.5) and expressions (4.4.6) and (4.4.7) would be exactly the same if we let  $[u : v] = [s : t]$  and

$$\xi_0 = \frac{2B}{(12\psi_0^2)^6}, \quad \xi_1 = -\frac{4\psi_1}{(12\psi_0^2)^3}. \quad (4.4.8)$$

Note also that with respect to the fiber modular parameters  $\pi_Y$  and  $\sigma_Y$  the subfamily of complete intersections with  $\xi_1 = 0$  is very special: in this case  $\sigma_Y \equiv 1$ , so all K3 fibers correspond to “complementary” elliptic curves with  $j(E_1) + j(E_2) = 1$ .

## 4.5 Ambient Space Morphism

Given such a perfect matching of modular parameters, we may try to construct a morphism between original varieties  $Y \rightarrow Z$ , perhaps by constructing a morphism (ideally — a fibration) between their ambient spaces  $X^5 \rightarrow X^4$ . Combining all correspondences used so far, we get

$$[y_0 : \cdots : y_9] \longleftrightarrow ([u : v], [x_0 : \cdots : x_3]) \longleftrightarrow [z_0 : \cdots : z_{16}],$$

or, more concretely,

$$[y_4 : y_8 : y_7 : y_5 : y_9 : y_6] \longleftrightarrow [z_0 : z_1 : z_2 : z_3 : z_4 : z_{16}].$$

This correspondence does not give us a morphism between toric varieties, since only some of the homogeneous coordinates on  $X^5$  are used and they are probably not well-defined due to relations involving the rest of coordinates as well. But we may look for a fan morphism that will map at least rays corresponding to these selected  $y_i$  to the rays corresponding to indicated  $z_j$ .

```

sage: m_y =
      Delta5_polar.vertices().matrix_from_columns([4,8,7,5,9,6])
sage: m_z =
      Delta4.polar().points().matrix_from_columns([0,1,2,3,4,16])
sage: m = m_y.solve_left(m_z)

```

This computation shows that if such a fan morphism exists, it must be given by the matrix  $m$

$$\begin{pmatrix} 1 & -1 & -1 & -4 & -6 \\ 0 & 0 & 1 & 0 & 0 \\ 0 & 0 & 0 & 1 & 0 \\ 0 & 0 & 0 & 0 & 1 \end{pmatrix},$$

which is unique since  $m_y$  has maximal rank. If this matrix defines a fibration, then rays of  $\Sigma^5$  must be mapped onto rays of  $\Sigma^4$  or the origin.

```

sage: rays = [m*r for r in Sigma5.rays() if not (m*r).is_zero()]
sage: from sage.geometry.cone import normalize_rays
sage: rays = set(normalize_rays(rays, None))
sage: points = sorted(Delta4.polar().points().columns().index(ray)
      for ray in rays)
sage: points
[0, 1, 2, 3, 4, 16, 331, 333, 334]

```

Since all necessary image rays can be generated by lattice points of  $(\Delta^4)^\circ$ , we can pick  $\Sigma^4$  as a crepant subdivision of  $\Sigma_{\Delta^4}$ . One can then subdivide the current  $\Sigma^5$  (the subdivision of  $\Sigma_{\Delta^5}$  compatible with the fibration  $\alpha$ ) and obtain indeed a fibration over  $X^4$ , but, unfortunately, this will not be a crepant subdivision of  $\Sigma_{\Delta^5}$ .

To fix this problem, we go back to the defining polynomial (4.4.3) of the curve  $C \subset B^2$  and the fan of  $B^2$ , shown in [Figure 4.1 on page 78](#). We have already established that  $C$  does not intersect divisors corresponding to  $u_0$  and  $u_1$ . Now we note that it also does not contain the point with  $u_3 = u_4 = 0$ , since this would imply that one of the other coordinates is zero, which is not possible. This means that  $C$  is completely contained within the part of  $B^2$  corresponding to the fan generated by rays of  $u_2$ ,  $u_3$ , and  $u_4$ . But then  $Y \subset X^5$  is completely contained within the toric variety corresponding to  $\Sigma^5$  *without* all cones that contain rays corresponding to either  $y_0$ , or  $y_1$ , or  $y_4$  and  $y_5$

together. Starting with such a subfan  $\Sigma_{\text{part}}^5$  of  $\Sigma^5$  we can find its subdivision leading to a fibration  $\tilde{\Phi} : X_{\text{part}}^5 \rightarrow X^4$  with affine lines as generic fibers.

```

sage: selected = []
sage: for sigma in flatten(Sigma5.cones()):
...     indices = sigma.ambient_ray_indices()
...     if (0 in indices or
...         1 in indices or
...         4 in indices and 5 in indices):
...         continue
...     selected.append(sigma)
sage: Sigma5_part = Fan(cones=selected, rays=Sigma5.rays())
sage: rays = [m*ray for ray in Sigma5_part.rays() if not
...            (m*ray).is_zero()]
sage: rays = set(normalize_rays(rays, None))
sage: points4 = sorted(Delta4.polar().points().columns().index(r)
...                    for r in rays)
sage: points4
[0, 1, 2, 3, 4, 16, 334]
sage: Delta4.polar().point(334)
(-1, 1, 0, 0)
sage: X4 = CPRFanoToricVariety(Delta4, coordinate_points=points4)
sage: Phi = FanMorphism(m.transpose(), Sigma5_part, X4.fan(),
...                    subdivide=True)
sage: Phi.is_fibration()
True
sage: Phi.kernel_fan().rays()
(N(-1, -1, 0, 0, 0),)
sage: all(ray in Delta5_polar.points().columns() for ray in
...        Phi.domain_fan().rays())
True
sage: points5 = [Delta5_polar.points().columns().index(ray) for
...              ray in Phi.domain_fan().rays()]
sage: points5
[2, 3, 4, 5, 6, 7, 8, 9, 752]
sage: Delta5_polar.point(752)
(0, 0, 1, 0, 0)
sage: Phi.domain_fan().is_simplicial()

```

**True**

```
sage: X5_part = ToricVariety(Phi.domain_fan(),
    coordinate_names="y+", coordinate_indices=points5)
```

Now not only all necessary rays in the codomain can be generated by lattice points of  $(\Delta^4)^\circ$ , but also all necessary rays in the domain can be generated by lattice points of  $(\Delta^5)^\circ$ , so we can think of  $X_{\text{part}}^5$  as an open subset of some crepant partial desingularization of  $X_{\Delta^5}$  and  $Y \subset X_{\text{part}}^5$  is still a Calabi-Yau variety.

From the computational point of view, we can no longer use the framework of CPR-Fano toric varieties in Sage to represent  $X_{\text{part}}^5$  and have to use generic toric varieties. We will however still use the same convention for naming coordinates: missing  $y_0$  and  $y_1$  now reflect the fact that we are interested only in charts where they are non-zero, in which case both can be set to 1 using relations between coordinates. In homogeneous coordinates we get

$$\begin{aligned}\tilde{\Phi} : [y_2 : \cdots : y_9 : y_{752}] &\mapsto [z_0 : z_1 : z_2 : z_3 : z_4 : z_{16} : z_{334}] \\ &= [y_4 : y_8 : y_7 : y_5 : y_9 : y_6 : y_3^2 y_{752}],\end{aligned}$$

which also does not involve  $y_2$ , since it corresponds to the only ray of the kernel fan. This map can be used to pullback  $Z$  and compare it with  $Y$ . We delay this comparison, however, since for analysis of singularities it is convenient to perform a few more subdivisions of underlying fans.

## 4.6 Singular Subfamilies: Hypersurfaces

Generically, complete intersections  $Y$  and anticanonical hypersurfaces  $Z$  in MPCP-desingularizations of their ambient spaces are smooth, since the singular locus in this case has codimension at least four. However, we are interested in the following subfamilies:

- 1) complete intersections  $Y$  with  $\xi_1 = 0$ , corresponding to the subfamily with the desired GKZ-series, we will denote a generic member of this subfamily as  $Y_1$  to emphasize dependence on a single parameter only;
- 2) hypersurfaces  $Z$  with  $\psi_s = -B$ , corresponding to the subfamily whose K3 fibration can be “perfectly matched” with the K3 fibration of complete intersections  $Y$ , we will denote a generic member of this subfamily as  $Z_2$ ;

- 3) hypersurfaces  $Z$  with  $\psi_s = -B$  and  $\psi_1 = 0$ , corresponding to the subfamily of the above subfamily with an analogue of  $\xi_1 = 0$  restriction, we will denote a generic member of this subfamily as  $Z_1$ .

Generic members of these subfamilies may be singular, we analyze them using results of [BDF<sup>+</sup>98] and computer software (Sage interfacing Magma [BCP97] for computing singular locus of affine varieties).

The singular locus in the moduli space of hypersurfaces  $Z$  is summarized in relations (4.39) of [BDF<sup>+</sup>98]:

$$\begin{aligned}
S_{a_1}^\pm & : & (\psi_0^6 + \psi_1)^2 + \psi_s & = \pm B, \\
S_{a_2}^\pm & : & \psi_1^2 + \psi_s & = \pm B, \\
S_b^\pm & : & \psi_s & = \pm B, \\
S_0^\pm & : & 0 & = B.
\end{aligned}$$

Relations  $S_{a_1}^\pm$  and  $S_{a_2}^\pm$  are actually the same in the sense that they are switched by an appropriate change of coordinates (there is a finite group action on the simplified polynomial moduli space of hypersurfaces). We see that hypersurfaces  $Z_2$  are singular (and, therefore, cannot be isomorphic to the full two-parameter family of complete intersections  $Y$ ), since the condition  $S_b^-$  is satisfied. Condition  $\psi_1 = 0$  makes relations  $S_{a_2}^\pm$  and  $S_b^\pm$  the same, but does not impose singularities on its own.

Explicit chart-by-chart check for singularities of  $Z_2$  using our current fan  $\Sigma^4$  and ignoring the orbifold structure of  $X^4$  (i.e. ignoring singularities of  $Z_2$  which are inevitable due to the ambient space structure) reveals a singular locus of dimension 1 in all charts involving  $z_{334}$ . To study this singular locus, it is convenient to put it into smooth charts of  $X^4$ , so we subdivide  $\Sigma^4$  further.

In fact, it is better to start fresh with  $\Sigma_{\Delta^4}$ . Recall that adding the ray corresponding to the 16-th point  $v_{16} = (11, -1, -1, -1)$  of  $(\Delta^4)^\circ$ , the midpoint between vertices  $v_0 = (23, -1, -1, -1)$  and  $v_3 = (-1, -1, -1, -1)$ , was necessary for compatibility with the fibration  $\tilde{\beta} : X^4 \rightarrow B^1 \simeq \mathbb{P}^1$ . We also had to add  $v_{334} = (-1, 1, 0, 0)$  to allow for a fibration  $\tilde{\Phi} : X_{\text{part}}^5 \rightarrow X^4$ . This is the only interior point of the triangle face on  $v_1 = (-1, -1, 2, -1)$ ,  $v_2 = (-1, 11, -1, -1)$ , and  $v_4 = (-1, -1, -1, 1)$ . The face fan of this triangle (in the spanned affine sublattice with  $v_{334}$  being the origin) is the fan of  $\text{WP}(1, 2, 3)$  used in Example 1.8.3. The three interior points of edges correspond to

$v_{251} = (-1, 7, 0, -1)$ ,  $v_{276} = (-1, 3, 1, -1)$ , and  $v_{325} = (-1, 5, -1, 0)$ . Adding all these rays is sufficient to resolve all singularities of the 3-dimensional cone on  $v_1$ ,  $v_2$ , and  $v_4$ , but the resulting subcones are still faces of singular 4-dimensional cones. This is also reflected in the homogeneous coordinate representation of  $\tilde{\beta}$  (4.2.1): coordinates on the base  $B^1$  correspond to the 12-th powers of coordinates on  $X^4$  (yet the defining equation of  $Z$  involves first powers of all variables as well). The problem is that  $v_0$  and  $v_3$  are “too far away” from the slice hyperplane defining the projection to  $B^1$ . We can remedy the situation by adding two more points right “above” and “below” the face on  $v_1$ ,  $v_2$ , and  $v_4$  (which is completely contained in the slice hyperplane), namely  $v_{168} = (-1, 10, -1, -1)$  and  $v_{170} = (1, 10, -1, -1)$ .

Using consecutive star-like subdivisions (which are used in Sage for automatic insertion of rays), it turns out that the best sequence is the following:

- 1) add  $v_{16}$  to allow fibration  $\tilde{\beta} : X^4 \rightarrow B^1$ ;
- 2) add  $v_{168}$  and  $v_{170}$  to “improve” this fibration;
- 3) add  $v_{334}$  to allow fibration  $\Phi : X_{\text{part}}^5 \rightarrow X^4$ ;
- 4) add  $v_{251}$ ,  $v_{276}$ , and  $v_{325}$  to cover the divisor of  $z_{334}$  by smooth charts.

```
sage: X4 = CPRFanoToricVariety(Delta4,
    coordinate_points=[0,1,2,3,4,16,168,170,334,251,276,325])
sage: beta = FanMorphism(matrix([1,1,4,6]), X4.fan(), B1.fan())
sage: beta.is_fibration()
True
sage: all(sigma.is_smooth() for sigma in X4.fan() if (-1,1,0,0) in
    sigma)
True
sage: Z = X4.anticanonical_hypersurface(
    coefficients=[B/24,1/12,1/3,1/2,B/24,-psi_s/12,-psi1/6,-psi0])
sage: X4 = Z.ambient_space()
sage: Z2 = X4.anticanonical_hypersurface(
    coefficients=[B/24,1/12,1/3,1/2,B/24,B/12,-psi1/6,-psi0])
sage: Z1 = X4.anticanonical_hypersurface(
    coefficients=[B/24,1/12,1/3,1/2,B/24,B/12,0,-psi0])
```

The ray matrix of the fan of  $X^4$  is now

$$\begin{pmatrix} 23 & -1 & -1 & -1 & -1 & 11 & -1 & 1 & -1 & -1 & -1 & -1 \\ -1 & -1 & 11 & -1 & -1 & -1 & 10 & 10 & 1 & 7 & 3 & 5 \\ -1 & 2 & -1 & -1 & -1 & -1 & -1 & -1 & 0 & 0 & 1 & -1 \\ -1 & -1 & -1 & -1 & 1 & -1 & -1 & -1 & 0 & -1 & -1 & 0 \end{pmatrix}$$

and the fibration  $\tilde{\beta} : X^4 \rightarrow B^1$  takes form

$$z \mapsto [s : t] = [z_0^{12} z_{170} : z_3^{12} z_{168}],$$

so working in affine charts we may treat, say,  $z_{170}$  as the K3 fiber parameter.

Since singularities of  $Z_2$  are located in charts involving  $z_{334}$ , it is natural to represent its defining polynomial as

$$h_2 = q_2 z_{334} + r_2, \tag{4.6.1}$$

where

$$\begin{aligned} q_2 = & \frac{1}{12} z_2^{12} z_{168}^{11} z_{170}^{11} z_{251}^8 z_{276}^4 z_{325}^6 z_{334} - \frac{\psi_1}{6} z_0^6 z_2^6 z_3^6 z_{16}^6 z_{168}^6 z_{170}^6 z_{251}^4 z_{276}^2 z_{325}^3 \\ & - \psi_0 z_0 z_1 z_2 z_3 z_4 z_{16} z_{168} z_{170} z_{251} z_{276} z_{325} + \frac{1}{3} z_1^3 z_{251} z_{276}^2 + \frac{1}{2} z_4^2 z_{325}, \end{aligned} \tag{4.6.2}$$

$$r_2 = \frac{B}{24} z_{16}^{12} (z_3^{12} z_{168} + z_0^{12} z_{170})^2. \tag{4.6.3}$$

In this form it is easy to see that the fiber of  $\tilde{\beta} : Z_2 \rightarrow B^1$  (which is generically a K3 surface) over  $[s : t] = [-1 : 1]$  splits into two components, corresponding to  $q_2 = 0$  and  $z_{334} = 0$ . The intersection of these components is a curve  $C_2$ , which is the singular locus of  $Z_2$ . In the affine chart  $(z_1, z_4, z_{170}, z_{334})$  the defining equations of  $C_2$  take the form

$$\frac{z_1^3}{3} + \psi_0 z_1 z_4 + \frac{z_4^2}{2} - \frac{\psi_1}{6} = 0, \quad z_{170} = -1, \quad z_{334} = 0,$$

which is (generically) a smooth elliptic curve. Hypersurfaces  $Z_2$  have compound Du Val  $A_1$  singularities along  $C_2$ .

If we now pass to the subfamily  $Z_1$ , the structure of the singularities remains mostly the same, except that the curve of singularities of  $Z_1$ , let's call

it  $C_1$  for this subfamily, develops a singularity of its own and becomes a nodal elliptic curve. In the same affine chart as before the position of the node is  $(0, 0, -1, 0)$ .

## 4.7 Singular Subfamilies: Desingularization

In this section we use the fibration  $\tilde{\Phi} : X_{\text{part}}^5 \rightarrow X^4$  to pullback families of hypersurfaces to  $X_{\text{part}}^5$  and compare them with complete intersections. We also determine singularities of the subfamily  $Y_1$ .

Since we have changed the resolution used for  $X^4$ , we need to reconstruct both  $X_{\text{part}}^5$  and  $\tilde{\Phi}$ . We do it using as a starting point  $\Sigma_{\text{part}}^5$ , constructed in [Section 4.5](#).

```
sage: Phi = FanMorphism(m.transpose(), Sigma5_part, X4.fan(),
    subdivide=True)
sage: [Delta5_polar.points().columns().index(ray) for ray in
    Phi.domain_fan().rays()]
[2, 3, 4, 5, 6, 7, 8, 9, 109, 469, 630, 32, 667, 752]
```

We see that  $X_{\text{part}}^5$  still can be realized as an open subset of a crepant partial desingularization of  $X_{\Delta^5}$ . In homogeneous coordinates

$$\begin{aligned} \tilde{\Phi} : y &\mapsto [z_0 : z_1 : z_2 : z_3 : z_4 : z_{16} : z_{168} : z_{170} : z_{334} : z_{251} : z_{276} : z_{325}] \\ &= [y_4 : y_8 : y_7 : y_5 : y_9 : y_6 : y_{109} : y_{32} : y_3^2 y_{752} : y_{469} : y_{630} : y_{667}]. \end{aligned}$$

Considering the subfamily of complete intersections  $Y_1 \subset X_{\text{part}}^5$ , it is possible to determine that there is a singular point  $(0, 0, 0, 0; -1)$  in the chart  $(y_2, y_3, y_8, y_9; y_{32})$ . (Recall that generating cones of  $\Sigma_{\text{part}}^5$  are 4-dimensional, so the corresponding affine charts have a torus factor without a canonical choice of coordinates. In such cases we will use the coordinate corresponding to some suitable ray of the total fan and separate it from the canonically chosen coordinates by “;”.) Note that this point is mapped by  $\tilde{\Phi}$  to the singular point of the curve of singularities  $C_1 \subset Z_1$ . It is also a singular point of  $X_{\text{part}}^5$  itself, since the cone on rays corresponding to  $y_2, y_3, y_8$ , and  $y_9$  is not smooth. To fix this we will perform one last subdivision by inserting the ray corresponding to the midpoint  $(-1, -1, 1, 0, 0)$  between ray generators of  $y_2$  and  $y_3$ . Sage

does not (yet) support automatic insertion of rays into fans generated by not full-dimensional cones, but since we are subdividing a simplicial fan it is not difficult to do it in this case.

```

sage: Sigma = Phi.domain_fan()
sage: sigma = Sigma.generating_cone(37)
sage: [Delta5_polar.points().columns().index(ray) for ray in
       sigma.rays()]
[2, 3, 8, 9]
sage: [Delta5_polar.points().columns().index(pt) for pt in
       sigma.lattice_polytope().points().columns() if not pt.is_zero()]
[2, 3, 8, 9, 745]
sage: Delta5_polar.point(745)
(-1, -1, 1, 0, 0)
sage: Sigma.is_simplicial()
True
sage: rays = Sigma.rays() + ((-1,-1,1,0,0),)
sage: last = len(rays) - 1
sage: cones = []
sage: for sigma in Sigma:
...     indices = sigma.ambient_ray_indices()
...     if 0 in indices and 1 in indices:
...         cones.append(indices[1:] + (last,))
...         cones.append((0,) + indices[2:] + (last,))
...     else:
...         cones.append(indices)
sage: Sigma_new = Fan(cones=cones, rays=rays, check=False)
sage: all(sigma.is_smooth() for sigma in Sigma_new if
       (-1,-1,1,0,0) in sigma)
True
sage: Phi = FanMorphism(m.transpose(), Sigma_new, X4.fan())
sage: Phi.is_fibration()
True
sage: points5 = [Delta5_polar.points().columns().index(ray) for
                 ray in Phi.domain_fan().rays()]
sage: points5
[2, 3, 4, 5, 6, 7, 8, 9, 109, 469, 630, 32, 667, 752, 745]

```

The ray matrix of the new fan is

$$\begin{pmatrix} -1 & -1 & 12 & 0 & 0 & 0 & 0 & 0 & 0 & 0 & 0 & 1 & 0 & 0 & -1 \\ -1 & -1 & 0 & 12 & 0 & 0 & 0 & 0 & 1 & 0 & 0 & 0 & 0 & 0 & -1 \\ 0 & 2 & -1 & -1 & -1 & 11 & -1 & -1 & 10 & 7 & 3 & 10 & 5 & 1 & 1 \\ 0 & 0 & -1 & -1 & -1 & -1 & 2 & -1 & -1 & 0 & 1 & -1 & -1 & 0 & 0 \\ 0 & 0 & -1 & -1 & -1 & -1 & -1 & 1 & -1 & -1 & -1 & -1 & 0 & 0 & 0 \end{pmatrix}$$

and  $\Phi$  is still a fibration with coordinate representation

$$\begin{aligned} \tilde{\Phi} : y &\mapsto [z_0 : z_1 : z_2 : z_3 : z_4 : z_{16} : z_{168} : z_{170} : z_{334} : z_{251} : z_{276} : z_{325}] \\ &= [y_4 : y_8 : y_7 : y_5 : y_9 : y_6 : y_{109} : y_{32} : y_3^2 y_{745} y_{752} : y_{469} : y_{630} : y_{667}]. \end{aligned} \quad (4.7.1)$$

To construct  $Y$  as a subvariety of  $X_{\text{part}}^5$  in Sage, we first construct  $Y$  in the full space  $X^5$  using the same coordinates as for  $X_{\text{part}}^5$  (plus  $y_0$  and  $y_1$ ), then we use its equations to obtain a subvariety of  $X_{\text{part}}^5$ . (In the code we refer to it as `Y_part`, but in the text we continue using  $Y$  only since mathematically these are the same varieties.)

```
sage: X5 = CPRFanoToricVariety(np.Delta(),
    coordinate_points=[0,1]+points5, coordinate_names="y+")
sage: Y = X5.nef_complete_intersection(np, monomial_points=
    "vertices+origin", coefficients=[[1,1,1],[1,1,1,"xi0","xi1",1]])
sage: X5_part = ToricVariety(Phi.domain_fan(), coordinate_names=
    "y+", coordinate_indices=points5, base_field=Y.base_ring())
sage: X5_part.inject_coefficients();
sage: X5_part.inject_variables();
sage: S = X5_part.coordinate_ring()
sage: Y_part = X5_part.subscheme([sum(S(g.monomial_coefficient(m))
    * S(m.subs(y0=1, y1=1)) for m in g.monomials()) for g in
    Y.defining_polynomials()]])
```

The defining polynomials of  $Y$  in the new  $X_{\text{part}}^5$  are

$$g_0 = y_5^{12} y_{109} + y_4^{12} y_{32} + y_2 y_3 y_{745}, \quad (4.7.2)$$

$$\begin{aligned}
g_1 &= y_3^2 y_7^{12} y_{109}^{11} y_{469}^8 y_{630}^4 y_{32}^{11} y_{667}^6 y_{752}^2 y_{745} \\
&+ \xi_1 y_4^6 y_5^6 y_6^6 y_7^6 y_{109}^4 y_{469}^2 y_{630}^6 y_{32}^3 y_{667}^3 y_{752} + \xi_0 y_2^2 y_6^{12} y_{745} \\
&+ y_4 y_5 y_6 y_7 y_8 y_9 y_{109} y_{469} y_{630} y_{32} y_{667} y_{752} + y_8^3 y_{469} y_{630}^2 y_{752} + y_9^2 y_{667} y_{752}.
\end{aligned} \tag{4.7.3}$$

Now computations show that there are *two* singular points on complete intersections  $Y_1$ :  $(\pm 1/\sqrt{\xi_0}, 0, 0, 0; -1)$  in the chart  $(y_2, y_8, y_9, y_{745}; y_{32})$ , which is smooth and does not induce any singularities on its subvarieties. Both points are conifold singularities on  $Y_1$ .

We finally turn our attention to the explicit comparison of  $Y$  and the pullback of  $Z$  under the fibration  $\tilde{\Phi}$ , combined with the first defining equation of  $Y$ . (Recall that the fibration map  $\alpha : X^5 \rightarrow B^2$  induces the K3 fibration of  $Y$  over the curve in  $B^2$  corresponding to  $g_0 = 0$ .) Since in [Section 4.4](#) we matched modular parameters of K3 fibers of  $Y$  and  $Z_2$ , we start with the subfamily  $Z_2$ .

It is clear that if we use  $\tilde{\Phi}$  (4.7.1) to pullback  $h_2$  (4.6.1), we will not get  $g_1$  (4.7.3), due to mismatch in the number of monomials and different coefficients, even taking into account the parameter correspondence (4.4.8). However, the pullback of  $r_2$  (4.6.3) is

$$\frac{B}{24} (y_5^{12} y_{109} + y_4^{12} y_{32})^2 y_6^{12} = \frac{B}{24} (y_2 y_3 y_{745})^2 y_6^{12},$$

where equality follows from vanishing of  $g_0$  (4.7.2). Now the number of monomials is not an issue anymore, but we can see that  $y_3^2 y_{745}$  is a factor of  $\tilde{\Phi}^*(h_2)$ . Further comparison of  $\tilde{\Phi}^*(h_2)$  and  $g_1$  reveals that, subject to  $g_0 = 0$ ,

$$\Psi^*(h_2) = \frac{y_3^2 y_{745}}{48} g_1,$$

where  $\Psi$  is  $\tilde{\Phi}$  precomposed with the following coordinate scaling (which cannot be realized as a toric morphism):

$$y_6 = \frac{y_6}{\psi_0 \sqrt{12}}, \quad y_8 = \frac{y_8}{2}, \quad y_9 = -\frac{y_9}{\sqrt{12}}, \quad y_{752} = \frac{y_{752}}{2}.$$

Using  $\Psi$  to pullback the defining polynomial  $h_3$  of a generic member  $Z$  of the full 3-parameter family of hypersurfaces, we obtain an isomorphism of  $Z$

with the complete intersection defined by  $\Psi^*(h_3)$  and  $g_0$ . Indeed,

$$\begin{aligned}\Psi^*(h_3) &= \Psi^* \left( h_2 - \frac{\psi_s + B}{12} (z_0 z_3 z_{16})^{12} z_{168} z_{170} \right) \\ &= \frac{y_3^2 y_{745}}{48} g_1 - \frac{\psi_s + B}{127 \psi_0^{12}} (y_4 y_5 y_6)^{12} y_{32} y_{109},\end{aligned}$$

and  $\Psi^*(h_3) = 0$  implies that  $y_3 y_{745} \neq 0$ , since otherwise it would be necessary to have  $y_4 y_5 y_6 y_{32} y_{109} = 0$ , but these sets of variables do not appear together in any of the covering charts of  $X_{\text{part}}^5$ , as can be checked via the following computation.

```
sage: charts = [set(S.gen(j) for j in sigma.ambient_ray_indices())
for sigma in X5_part.fan()]
sage: any(chart.intersection([y3, y745]) and
chart.intersection([y4, y5, y6, y32, y109]) for chart in charts)
False
```

Then  $g_0 = 0$  can be solved for  $y_2$ , which is the only fiber variable. This 3-parameter family of complete intersections does not correspond to a nef-partition of  $\Delta^5$ , the easiest way to see this is to note that it shares one of the equations with  $Y$  and in the case of two-part nef-partitions (and corresponding nef complete intersections) each part completely determines the other.

Coming back to the subfamily  $Z_2$ , we see that these singular hypersurfaces are pulled back to the union of  $Y$  (which is generically smooth) and two toric divisors intersected with  $\{g_0 = 0\}$ . Both of these intersections are mapped to  $[s : t] = [-1 : 1]$  by the composition  $\tilde{\beta} \circ \Psi$ . Let's also look at the preimage of the curve of singularities  $C_2$  of  $Z_2$  inside of  $Y$ . This means imposing the following conditions:

$$g_0 = g_1 = \Psi^*(z_{334}) = \Psi^*(r_2) = \Psi^*(q_2) = 0.$$

Conditions  $g_0 = \Psi^*(r) = 0$  imply  $y_2 y_3 y_{745} = 0$ , while  $\Psi^*(z_{334}) = 0$  means  $y_3 y_{745} y_{752} = 0$ . But  $y_2$  and  $y_{752}$  cannot vanish simultaneously (we check it below), thus  $y_3 y_{745} = 0$ . We also have  $g_1 - 24 y_{752} \Psi^*(q_2) = \xi_0 y_2^2 y_6^{12} y_{745}$  and  $y_3$  cannot vanish simultaneously with  $y_2$  or  $y_6$ , thus  $y_{745} = 0$ . Finally,  $y_{745}$  and

$y_{752}$  cannot vanish simultaneously, so the above conditions are equivalent to

$$g_0 = g_1 = y_{745} = 0$$

and the preimage of  $C_2$  in  $Y$  is a (generically smooth) surface  $S_2$ . Therefore, we have obtained a geometric transition from  $Y$  to  $Z$  through a singular subfamily  $Z_2$ ! In fact,  $S_2 \simeq C_2 \times \mathbb{P}^1$  and we have obtained a primitive geometric transition of type III in terms of Definition 4.3.3. We now verify assertions made about simultaneous vanishing of coordinates:

```
sage: any(chart.issuperset([y2, y752]) for chart in charts)
False
sage: any(chart.issuperset([y2, y3]) for chart in charts)
False
sage: any(chart.issuperset([y3, y6]) for chart in charts)
False
sage: any(chart.issuperset([y745, y752]) for chart in charts)
False
```

Our last pair of subfamilies to compare using the map  $\Psi$  is  $Z_1$  and  $Y_1$ . We have already determined that hypersurfaces  $Z_1$  have a curve of singularities  $C_1$  which itself has a singular point  $(0, 0, -1, 0)$  in the chart  $(z_1, z_4, z_{170}, z_{334})$ . Let  $S_1 \subset Y_1$  be the preimage of  $C_1$  (defined by the same equations as  $S_2 \subset Y_2$ ). If we consider the preimage of the singular point in  $Y_1$ , then in addition to the defining equations of  $S_1$  we need to impose  $y_8 = y_9 = 0$ . This leads to

$$y_8 = y_9 = y_{745} = y_5^{12} y_{109} + y_4^{12} y_{32} = 0,$$

which defines a projective line, containing both nodes of  $Y_1$ . The surface  $S_1$  also becomes singular with the singular locus being precisely this line, which is  $(*, 0, 0, 0; -1)$  in charts  $(y_2 \text{ or } 3, y_8, y_9, y_{745}; y_{32})$ .

## 4.8 Involutions

There are several involutions acting on complete intersections  $Y$ . One of them is easily visible from the vertices of  $(\Delta^5)^\circ$  or rays of  $\Sigma^5$ : it is the exchange of

the first two affine coordinates. In homogeneous coordinates it is realized by

$$y_4 \leftrightarrow y_5, \quad y_{32} \leftrightarrow y_{109},$$

with other  $y_i$  unchanged, and in terms of the K3 fibration of  $Y$  over  $\mathbb{P}^1$  induced by  $\tilde{\alpha}$ , as discussed in Section 4.4, it corresponds to  $[u : v] \leftrightarrow [v : u]$ .

Another involution is given in homogeneous coordinates by

$$y_9 \mapsto -y_9 - y_4 y_5 y_6 y_7 y_8 y_{109} y_{469} y_{630} y_{32},$$

with other  $y_i$  unchanged. It comes from either of the two elliptic fibrations of  $M$ -polarized K3 surfaces as the  $y \mapsto -y$  involution in the coordinates of the Weierstrass normal form. This is also the same involution as the one described in Section 4.2.1 of [BDF<sup>+</sup>98].<sup>5</sup>

It is, of course, possible to take a composition of these two involutions and it is easy to see from their representations in homogeneous coordinates that they commute with each other, so this gives us yet another involution.

Of particular interest is the action of these involutions on the singular locus of  $Y_1$  and its related subvarieties. In the chart  $(y_2, y_8, y_9, y_{745}; y_{32})$ , used before, the second involution is  $y_9 \mapsto -y_9 - y_8 y_{32}$ . On the exceptional K3 fiber containing the nodes  $y_{32} = -1$  and we are left with  $y_9 \mapsto y_8 - y_9$ . The line passing through the nodes with  $y_8 = y_9 = 0$  is a part of the fixed point locus.

In order to get a chart representation of the first involution we need to know the relation between  $y_{109}$  and the variables of the chosen chart.

```
sage: Delta5_polar.points().matrix_from_columns(
      [2,8,9,745,32,109]).transpose().kernel()
Free module of degree 6 and rank 1 over Integer Ring
Echelon basis matrix:
[ 11  4  6 -10  1  1]
```

This shows that there is a  $\mathbb{C}^*$  scaling action on homogeneous coordinates  $y$

---

<sup>5</sup>There it is realized as  $x_5 \mapsto -x_5$  in the “alternative gauge”. One can convert it to the gauge used in Section 4.2 via formulas (4.13) and (4.15) in [BDF<sup>+</sup>98]. (Those formulas contain a typo in the expression for  $\tilde{\psi}_4$ : the term  $-4b_4 \lambda_4'^2 \lambda_4 \psi_0$  should not contain  $\psi_0$ , while the term  $4\lambda_5' \lambda_4' \lambda_{03}$  should.)

given by

$$[\lambda^{11}y_2 : \lambda^4y_8 : \lambda^6y_9 : \lambda^{-10}y_{745} : \lambda y_{32} : \lambda y_{109}] .$$

Using it to eliminate  $y_{109}$ , we get

$$[y_{109}^{-11}y_2 : y_{109}^{-4}y_8 : y_{109}^{-6}y_9 : y_{109}^{10}y_{745} : y_{109}^{-1}y_{32} : 1] ,$$

so a chart representation of the first involution is

$$(y_2, y_8, y_9, y_{745}; y_{32}) \mapsto (y_{32}^{-11}y_2, y_{32}^{-4}y_8, y_{32}^{-6}y_9, y_{32}^{10}y_{745}; y_{32}^{-1}) ,$$

which reduces to

$$(y_2, y_8, y_9, y_{745}; -1) \mapsto (-y_2, y_8, y_9, y_{745}; -1) , \text{ i.e. } y_2 \mapsto -y_2 ,$$

on the exceptional K3 fiber containing the singular locus. Note that this action exchanges the nodes of  $Y_1$ .

## 4.9 Open Questions

A number of questions are raised by the above analysis of our families of complete intersections and anticanonical hypersurfaces.

First of all, we have not constructed complete resolutions for 1-parameter subfamilies. However, we have identified the singular locus of  $Y_1$ , classified the singularities, and found a transitive action on the nodes by a group of automorphisms of  $Y_1$ . This may lead to a proof of existence of a small projective resolution of nodes via generalizing arguments of [Wer87], where hypersurfaces in projective spaces were considered.

Alternatively, one can try to construct such a resolution directly using suitable blow up/down maps. The shortest path would be to blow up a smooth surface passing through the nodes of  $Y_1$ , but we were not able to find such a surface. Blowing up  $Y_1$  along the line of singularities  $L$  of  $S_1$  replaces  $S_1$  with the union of four smooth surfaces:  $Q \simeq \mathbb{P}^1 \times \mathbb{P}^1$ ,  $R \simeq \mathbb{P}^1 \times \mathbb{P}^1$ , and  $P_{\pm} \simeq \mathbb{P}^2$ , where  $P_{\pm}$  contract to two nodes,  $R$  contracts to  $L$ , and  $Q$  is the strict transform of  $S_1$ . The strict transform of  $Y_1$  has four nodes located at

the triple intersections  $Q \cap R \cap P_{\pm}$ , which are actually the same as double intersections  $Q \cap P_{\pm}$ . Having smooth surfaces passing through the nodes, it is possible to resolve them by one more blow up introducing a copy of  $\mathbb{P}^1$  at each node. This will not be a small resolution of  $Y_1$  and it is likely to be discrepant, but it may be possible to blow down “extraneous” surfaces on the resolution without reintroducing singularities. We have made some progress in this direction, but more work has to be done to obtain conclusive results.

Assuming that a suitable resolution  $X$  of  $Y_1$  exists, the next step would be to compute its Hodge numbers. This can be done using results in [Ros10], relating Hodge numbers of varieties involved in a geometric transition. If  $h^{2,1}(X) \neq 1$ , one can also consider (resolutions of) quotients of  $X$  by lifts of involutions on  $Y_1$ .

Finally, two natural questions for further exploration are construction of mirror families for these resolutions and generalization of the geometric transition  $Y \rightarrow Z_2 \rightsquigarrow Z$  to other singular subfamilies of Calabi-Yau subvarieties of toric varieties, that can be (partially) desingularized in the toric setting.

# Bibliography

- [Bat94] Victor V. Batyrev. Dual polyhedra and mirror symmetry for Calabi-Yau hypersurfaces in toric varieties. *J. Algebraic Geom.*, 3(3):493–535, 1994. [arXiv:alg-geom/9310003v1](#).
- [Bat98] Victor V. Batyrev. Stringy Hodge numbers of varieties with Gorenstein canonical singularities. In *Integrable systems and algebraic geometry (Kobe/Kyoto, 1997)*, pages 1–32. World Sci. Publ., River Edge, NJ, 1998. [arXiv:alg-geom/9711008v2](#).
- [BB96a] Victor V. Batyrev and Lev A. Borisov. Mirror duality and string-theoretic Hodge numbers. *Invent. Math.*, 126(1):183–203, 1996.
- [BB96b] Victor V. Batyrev and Lev A. Borisov. On Calabi-Yau complete intersections in toric varieties. In *Higher-dimensional complex varieties (Trento, 1994)*, pages 39–65. de Gruyter, Berlin, 1996. [arXiv:alg-geom/9412017v1](#).
- [BCP97] Wieb Bosma, John Cannon, and Catherine Playoust. The Magma algebra system. I. The user language. *J. Symbolic Comput.*, 24(3–4):235–265, 1997. Computational algebra and number theory (London, 1993).
- [BD96] Victor V. Batyrev and Dimitrios I. Dais. Strong McKay correspondence, string-theoretic Hodge numbers and mirror symmetry. *Topology*, 35(4):901–929, 1996.
- [BDF<sup>+</sup>98] Marco Billó, Frederik Denef, Pietro Frè, Igor Pesando, Walter Troost, Antoine Van Proeyen, and Daniela Zanon. The rigid limit in special Kähler geometry — from  $K3$ -fibrations to spe-

- cial Riemann surfaces: a detailed case study. *Classical Quantum Gravity*, 15(8):2083–2152, 1998.
- [BH11] Volker Braun and Marshall Hampton. *polyhedra module of Sage*. The Sage Development Team, 2011. <http://www.sagemath.org/doc/reference/sage/geometry/polyhedra.html>.
- [BJRR10] Ralph Blumenhagen, Benjamin Jurke, Thorsten Rahn, and Helmut Roschy. Cohomology of line bundles: Applications. [arXiv:1010.3717v1](https://arxiv.org/abs/1010.3717v1), 2010.
- [BM03] Lev A. Borisov and Anvar R. Mavlyutov. String cohomology of Calabi-Yau hypersurfaces via mirror symmetry. *Adv. Math.*, 180(1):355–390, 2003.
- [BN08] Victor V. Batyrev and Benjamin Nill. Combinatorial aspects of mirror symmetry. In *Integer points in polyhedra—geometry, number theory, representation theory, algebra, optimization, statistics*, volume 452 of *Contemp. Math.*, pages 35–66. Amer. Math. Soc., Providence, RI, 2008. [arXiv:math/0703456v2](https://arxiv.org/abs/math/0703456v2) [[math.CO](https://arxiv.org/abs/math/0703456v2)].
- [BN11] Volker Braun and Andrey Y. Novoseltsev. *Toric varieties framework for Sage*. The Sage Development Team, 2011. [http://www.sagemath.org/doc/reference/sage/schemes/generic/toric\\_variety.html](http://www.sagemath.org/doc/reference/sage/schemes/generic/toric_variety.html).
- [BOKS07] Volker Braun, Burt A. Ovrut, Maximilian Kreuzer, and Emanuel Scheidegger. Worldsheet instantons and torsion curves. B. Mirror symmetry. *J. High Energy Phys.*, (10):023, 53, 2007.
- [Bor93] Lev A. Borisov. Towards the mirror symmetry for Calabi-Yau complete intersections in Gorenstein toric Fano varieties. [arXiv:alg-geom/9310001v1](https://arxiv.org/abs/alg-geom/9310001v1), 1993.
- [CD07] Adrian Clingher and Charles F. Doran. Modular invariants for lattice polarized  $K3$  surfaces. *Michigan Math. J.*, 55(2):355–393, 2007.

- [CdI0HS08] Philip Candelas, Xenia de la Ossa, Yang-Hui He, and Balázs Szendrői. Triadophilia: a special corner in the landscape. *Adv. Theor. Math. Phys.*, 12(2):429–473, 2008.
- [CDLS88] P. Candelas, A. M. Dale, C. A. Lütken, and R. Schimmrigk. Complete intersection Calabi-Yau manifolds. *Nuclear Phys. B*, 298(3):493–525, 1988.
- [CDLW09] Adrian Clingher, Charles F. Doran, Jacob Lewis, and Ursula Whitcher. Normal forms,  $K3$  surface moduli, and modular parametrizations. In *Groups and symmetries*, volume 47 of *CRM Proc. Lecture Notes*, pages 81–98. Amer. Math. Soc., Providence, RI, 2009. [arXiv:0712.1880v1](https://arxiv.org/abs/0712.1880v1) [math.AG].
- [CHSW85] P. Candelas, Gary T. Horowitz, Andrew Strominger, and Edward Witten. Vacuum configurations for superstrings. *Nuclear Phys. B*, 258(1):46–74, 1985.
- [CK99] David A. Cox and Sheldon Katz. *Mirror symmetry and algebraic geometry*, volume 68 of *Mathematical Surveys and Monographs*. American Mathematical Society, Providence, RI, 1999.
- [CLS88] P. Candelas, C. A. Lütken, and R. Schimmrigk. Complete intersection Calabi-Yau manifolds. II. Three generation manifolds. *Nuclear Phys. B*, 306(1):113–136, 1988.
- [CLS90] P. Candelas, M. Lynker, and R. Schimmrigk. Calabi-Yau manifolds in weighted  $\mathbf{P}_4$ . *Nuclear Phys. B*, 341(2):383–402, 1990.
- [CLS11] David A. Cox, John Little, and Hal Schenck. *Toric Varieties*, volume 124 of *Graduate Studies in Mathematics*. American Mathematical Society, Providence, RI, 2011.  
Pre-publication version will be available until publication at <http://www.cs.amherst.edu/~dac/toric.html>.
- [D<sup>+</sup>10] Dan Drake et al. *SageTeX package for L<sup>A</sup>T<sub>E</sub>X (Version 2.3)*, 2010. <https://bitbucket.org/ddrake/sagetex>.
- [Dix88] Lance J. Dixon. Some world-sheet properties of superstring compactifications, on orbifolds and otherwise. In *Superstrings, unified*

- theories and cosmology 1987 (Trieste, 1987)*, volume 4 of *ICTP Ser. Theoret. Phys.*, pages 67–126. World Sci. Publ., Teaneck, NJ, 1988.
- [DM06] Charles F. Doran and John W. Morgan. Mirror symmetry and integral variations of Hodge structure underlying one-parameter families of Calabi-Yau threefolds. In *Mirror symmetry. V*, volume 38 of *AMS/IP Stud. Adv. Math.*, pages 517–537. Amer. Math. Soc., Providence, RI, 2006.  
**arXiv:math/0505272v1 [math.AG]**.
- [DM07] Charles F. Doran and John W. Morgan. Algebraic topology of Calabi-Yau threefolds in toric varieties. *Geom. Topol.*, 11:597–642, 2007.
- [DN10] Charles F. Doran and Andrey Y. Novoseltsev. Closed form expressions for Hodge numbers of complete intersection Calabi-Yau threefolds in toric varieties. In *Mirror Symmetry and Tropical Geometry*, volume 527 of *Contemporary Mathematics*, pages 1–14. Amer. Math. Soc., Providence, RI, 2010.  
**arXiv:0907.2701v2 [math.CO]**.
- [EBB<sup>+</sup>10] Greg Ewing, Robert W. Bradshaw, Stefan Behnel, Dag S. Seljebotn, et al. *Cython compiler (Version 0.13)*, 2010.  
<http://www.cython.org>.
- [Ful93] William Fulton. *Introduction to toric varieties*, volume 131 of *Annals of Mathematics Studies*. Princeton University Press, Princeton, NJ, 1993. The William H. Roever Lectures in Geometry.
- [GP90] B. R. Greene and M. R. Plesser. Duality in Calabi-Yau moduli space. *Nuclear Phys. B*, 338(1):15–37, 1990.
- [GS06] Mark Gross and Bernd Siebert. Mirror symmetry via logarithmic degeneration data. I. *J. Differential Geom.*, 72(2):169–338, 2006.
- [GS<sup>+</sup>10a] Daniel R. Grayson, Michael E. Stillman, et al. *Macaulay2, a software system for research in algebraic geometry (Version 1.4)*, 2010. <http://www.math.uiuc.edu/Macaulay2/>.

- [GS10b] Mark Gross and Bernd Siebert. Mirror symmetry via logarithmic degeneration data, II. *J. Algebraic Geom.*, 19(4):679–780, 2010.
- [HKK<sup>+</sup>03] Kentaro Hori, Sheldon Katz, Albrecht Klemm, Rahul Pandharipande, Richard Thomas, Cumrun Vafa, Ravi Vakil, and Eric Zaslow. *Mirror symmetry*, volume 1 of *Clay Mathematics Monographs*. American Mathematical Society, Providence, RI, 2003. With a preface by Vafa.
- [HLY02] Yi Hu, Chien-Hao Liu, and Shing-Tung Yau. Toric morphisms and fibrations of toric Calabi-Yau hypersurfaces. *Adv. Theor. Math. Phys.*, 6(3):457–506, 2002.  
arXiv:math/0010082v2 [math.AG].
- [KKRS05] Albrecht Klemm, Maximilian Kreuzer, Erwin Riegler, and Emanuel Scheidegger. Topological string amplitudes, complete intersection Calabi-Yau spaces and threshold corrections. *J. High Energy Phys.*, (5):023, 116 pp. (electronic), 2005.  
arXiv:hep-th/0410018v2.
- [Kre08] Maximilian Kreuzer. On the statistics of lattice polytopes. arXiv:0809.1188v1 [math.AG], 2008.
- [KRS03] Maximilian Kreuzer, Erwin Riegler, and David A. Sahakyan. Toric complete intersections and weighted projective space. *J. Geom. Phys.*, 46(2):159–173, 2003.  
arXiv:math/0103214v3 [math.AG].
- [KS97] Maximilian Kreuzer and Harald Skarke. On the classification of reflexive polyhedra. *Comm. Math. Phys.*, 185(2):495–508, 1997.  
arXiv:hep-th/9512204v2.
- [KS98] Maximilian Kreuzer and Harald Skarke. Classification of reflexive polyhedra in three dimensions. *Adv. Theor. Math. Phys.*, 2(4):853–871, 1998. arXiv:hep-th/9805190v1.
- [KS02] Maximilian Kreuzer and Harald Skarke. Complete classification of reflexive polyhedra in four dimensions. *Adv. Theor. Math. Phys.*, 4(6):1209–1230, 2002. arXiv:hep-th/0002240v1.

- [KS04] Maximilian Kreuzer and Harald Skarke. PALP: a package for analysing lattice polytopes with applications to toric geometry. *Comput. Phys. Comm.*, 157(1):87–106, 2004. [arXiv:math/0204356v1 \[math.NA\]](#).
- [LVW89] Wolfgang Lerche, Cumrun Vafa, and Nicholas P. Warner. Chiral rings in  $N = 2$  superconformal theories. *Nuclear Phys. B*, 324(2):427–474, 1989.
- [Mav00] Anvar R. Mavlyutov. *Toric geometry and mirror symmetry*. ProQuest LLC, Ann Arbor, MI, 2000. Thesis (Ph.D.)—University of Massachusetts Amherst.
- [Mer10] Zeeya Merali. Computational science: Error. *Nature*, 467(7317):775–777, October 2010. <http://www.nature.com/doi/10.1038/467775a>.
- [MG04] Frank Mittelbach and Michel Goossens. *The L<sup>A</sup>T<sub>E</sub>X Companion*. Tools and Techniques for Computer Typesetting. Addison-Wesley, Boston, Massachusetts, 2 edition, 2004. With Johannes Braams, David Carlisle, and Chris Rowley.
- [Nov11] Andrey Y. Novoseltsev. `lattice_polytope` module of Sage. The Sage Development Team, 2011. [http://www.sagemath.org/doc/reference/sage/geometry/lattice\\_polytope](http://www.sagemath.org/doc/reference/sage/geometry/lattice_polytope).
- [NS10] Benjamin Nill and Jan Schepers. Gorenstein polytopes and their stringy e-functions. [arXiv:1005.5158v1 \[math.CO\]](#), 2010.
- [Oda88] Tadao Oda. *Convex bodies and algebraic geometry*, volume 15 of *Ergebnisse der Mathematik und ihrer Grenzgebiete (3) [Results in Mathematics and Related Areas (3)]*. Springer-Verlag, Berlin, 1988. An introduction to the theory of toric varieties, Translated from Japanese.
- [PS97] Eugene Perevalov and Harald Skarke. Enhanced gauge symmetry in type II and F-theory compactifications: Dynkin diagrams from polyhedra. *Nuclear Phys. B*, 505(3):679–700, 1997. [arXiv:hep-th/9704129v2](#).

- [Roh04] Falk Rohsiepe. Lattice polarized toric K3 surfaces. [arXiv:hep-th/0409290v1](https://arxiv.org/abs/hep-th/0409290v1), 2004.
- [Ros10] Michele Rossi. Homological type of geometric transitions. [arXiv:1001.0457v3](https://arxiv.org/abs/1001.0457v3) [math.AG], 2010.
- [S<sup>+</sup>11] William A. Stein et al. *Sage Mathematics Software (Version 4.6.2)*. The Sage Development Team, 2011. <http://www.sagemath.org>.
- [vR<sup>+</sup>10] Guido van Rossum et al. *Python programming language (Version 2.7.1)*. Python Software Foundation, 2010. <http://www.python.org>.
- [Wer87] Jürgen Werner. *Kleine Auflösungen spezieller dreidimensionaler Varietäten*. Bonner Mathematische Schriften [Bonn Mathematical Publications], 186. Universität Bonn Mathematisches Institut, Bonn, 1987. Dissertation, Rheinische Friedrich-Wilhelms-Universität, Bonn, 1987.
- [Wil92] P. M. H. Wilson. The Kähler cone on Calabi-Yau threefolds. *Invent. Math.*, 107(3):561–583, 1992.
- [Wil93] P. M. H. Wilson. Erratum: “The Kähler cone on Calabi-Yau threefolds” [*Invent. Math.* **107** (1992), no. 3, 561–583; MR1150602 (93a:14037)]. *Invent. Math.*, 114(1):231–233, 1993.